Technische Universität München

TUM School of Engineering and Design

Model-Based Determination of the Residual Stress State in the Sub-Surface changed by Peripheral Milling of Ti-6Al-4V

Matthias Johann Wimmer

Vollständiger Abdruck der von der TUM School of Engineering and Design der Technischen Universität München zur Erlangung des akademischen Grades eines

Doktors der Ingenieurwissenschaften (Dr.-Ing.)

genehmigten Dissertation.

Vorsitz: Prof. Dr.-Ing. Veit Senner

Prüfende der Dissertation:
1. Prof. Dr.-Ing. Michael F. Zäh
2. Assoc. Prof. Julius M. Schoop, Ph.D.

Die Dissertation wurde am 06.06.2025 bei der Technischen Universität München eingereicht und durch die TUM School of Engineering and Design am 06.10.2025 angenommen.

Preface

This dissertation was elaborated during my employment as a research associate at the Institute for Machine Tools and Industrial Management (*iwb*) of the Technical University of Munich (TUM).

First of all, I would like to thank Prof. Dr.-Ing. Michael F. Zaeh, full professor of the Chair of Machine Tools and Manufacturing Technology, for the opportunity to pursue a doctorate and for his valuable supervision. During my work at the *iwb*, he provided me with the necessary scientific skills and excellently promoted my abilities and talents. Furthermore, I would like to thank the second examiner and the examination board chairman.

A special thanks goes to my colleagues at the institute, especially to the Machine Tools Department members. The creative and motivating mindset at the institute has facilitated the elaboration of this thesis. I have a close friendship with many of them, which has left a permanent impression on my life through shared ups and downs. Let us not forget the good times we were able to enjoy with each other outside of our work, which contributed to a well-balanced experience at the institute. It is my wish to preserve and cherish this friendship in the future. I would like to particularly mention my colleagues Christian Schieber, and Christioph Woelfle. You all gave me valuable advice on my scientific work and contributed to a successful result. Furthermore, I would like to thank all my students and co-authors of the publications for the exciting and inspiring discussions during our scientific work.

I would like to extend a heartfelt thank you to my family. My parents, Christine Wimmer and Johann Wimmer, my sister, Sandra Wimmer, and my stepfather, Wolfgang Nadelstumpf, have all encouraged me since my childhood. They have made me understand the value of education on my life's path. Thank you for your enduring support and for teaching me the values of solidarity and integrity.

Finally, I would like to thank my girlfriend, Josefa Korisanski, for supporting me in every situation and for always motivating me.

Matthias Wimmer

Table of Contents

List of Abbreviations

Acronym	Description
2D	Two-dimensional
3D	Three-dimensional
Al	Aluminum
ASM	American Society for Metals
B	Boron
bbc	Body centered cubic structure
blisk	Blade integrated disk
C	Carbon
cf.	confer (Engl.: compare)
CFRP	Carbon fiber reinforced plastics
CIRP	International Academy for Production Engineering (Fr.: Collège International pour la Récherche en Productique)
CMMO	Conference on Modeling of Machining Operations
Co	Cobalt
Cr	Chromium
Cu	Copper
DIC	Digital image correlation
DIN	German Institute for Standardization (Ger.: Deutsches Institut für Normung)
DoE	Design of experiments
EDX	Energy dispersive X-Ray analysis
E-Modulus	Elastic modulus (Young's modulus)

et al.	et alii (Engl.: and others)
e.g.	exempli gratia (Engl.: for example)
Fe	Iron
FEM	Finite Element Method
hcp	Hexagonal closed-packed
HSM	High Speed Machining
i.e.	id est (Engl.: that is)
ISO	International Organization for Standardization
iwb	Institute for Machine Tools and Industrial Management of TU Munich
L-BFGS	Limited-memory Broyden–Fletcher–Goldfarb–Shanno
LED	Light Emitting Diode
ML	Machine Learning
MLP	Multilayer Perceptron
Mn	Manganese
Mo	Molybdenum
N	Nitrogen
NC	Numerial control
Nb	Niobium
Ni	Nickel
O	Oxygen
P	Publication
pCBN	Polycrystalline Cubic Boron Nitride
PCD	Polycrystalline Diamond
RS	Residual stress
Si	Silicon
SO	Sub-objective

Ta	Tantalum
Ti	Titanium
TUM	Technical University of Munich
V	Vanadium
W	Tungsten
XRD	X-ray diffraction

List of Symbols

Latin variables

Variable	Unit	Description
a	µm	Half width of contact
a_e	mm	Radial depth of cut
a_p	mm	Axial depth of cut
D	mm	Diameter of the tool
d_{RS}	µm	Residual stress depth
F	N	Resultant force
F_a	N	Active force component
F_c	N	Cutting force component
F_{ch}	N	Chip forming force component
F_{cN}	N	Cutting normal force component
F_f	N	Feed force component
F_p	N	Passive force component
F_{pl}	N	Ploughing force component
F_x	N	Cutting force component in x-direction
F_y	N	Cutting force component in y-direction
$F_{y,norm}$	-	Normalized cutting force component in y-direction
F_z	N	Cutting force component in z-direction
f_z	mm	Feed per tooth
h	mm	Uncut chip thickness
h_{eff}	mm	Effective uncut chip thickness

h_{max}	mm	Maximum uncut chip thickness
h_{min}	mm	Minimum uncut chip thickness
i	s	Time
k_{ie}	N/mm²	Edge force coefficient
L_1	mm	Total length of the tool
L_2	mm	Cutting length of the tool
l_c	mm	Chip lenght
L_t	mm	Lenght of the cutting edge
M_{max}	Nm	Maximum spindle torque
n	min^{-1}	Spindle speed
n_{max}	min^{-1}	Maximum spindle speed
p_0	N/mm²	Contact pressure
P_{max}	kW	Maximum spindle power
R_m	MPa	Ultimate tensile strength
R_p	MPa	Yield strength
r_β	µm	Cutting-edge radius
S	-	Intersection point
v_c	m/min	Cutting speed
v_e	mm/min	Effective velocity
v_f	mm/min	Feed velocity
v_{sp}	m/min	Chip velocity
x, y, z	-	Tool coordinate system
z	-	Number of teeth

Greek variables

Variable	Unit	Description
α	°	Clearance angle
β	°	Helix angle of the cutting edge
β_w	°	Wedge angle
γ	°	Rake angle
$\Delta\tau$	°	Tooth pitch angle
η	°	Effective direction angle
μ_e	-	Friction coefficient
$\boldsymbol{\sigma}$	Pa	Cauchy stress tensor
σ_1	MPa	First principal stress
σ_2	MPa	Second principal stress
σ_{a}	MPa	Residual stress perpendicular to the feed direction
σ_{f}	MPa	Residual stress in the feed direction
σ_{ij}	MPa	Normal stress components (i,j =1, 2, 3)
$\sigma_{\mathrm{mechanical}}$	MPa	Mechanical stresses
σ_{RS}	MPa	Residual stress
$\sigma_{\mathrm{thermal}}$	MPa	Thermal stresses
τ_{ij}	MPa	Shear stress components
Φ	°	Feed direction angle
φ	°	Tool rotation angle
φ_c	°	Contact angle
φ_{ex}	°	Tool exit angle
$\varphi_{\mathrm{h,max}}$	°	Tool rotation angle at the maximum uncut chip thickness
φ_{i}	°	Tool rotation angle at the time i

φ_{st}	°	Tool entry angle

1 Introduction

1.1 Motivation and objective

Global warming is expected to increase temperatures on the planet Earth by 4 to 5 °C (Kelvin) by the end of the 21st century compared to the pre-industrial era. This will lead to increasing weather extremes, an elevation in sea level, and growing drought zones. The rise in the average temperature is due to an anthropogenic increase in the concentration of greenhouse gases in the Earth's atmosphere. Greenhouse gases are released, for example, from the combustion of fossil fuels and the associated emission of carbon dioxide. Accordingly, German energy and climate policy has defined targets for reducing the temperature rise, which include the reduction of greenhouse gas emissions by at least 55 % by 2030 compared to the 1990 amounts (BMU 2019). Therefore, it is essential to focus on the effective utilization of resources across all sectors of industry. The consistent use of lightweight materials in the transport sector in particular offers great potential for saving fossil fuels (FRIEDRICH 2017). Using lightweight materials can reduce the total mass to be transported which in turn leads to a reduction in fuel consumption. This results in the emission of less carbon dioxide into the Earth's atmosphere. Particularly in the aerospace sector, mass reduction contributes considerably to increasing fuel efficiency (KROLL 2019). In this industry, the use of carbon fibre reinforced plastics (CFRP) and lightweight metals, such as aluminum and titanium, is becoming increasingly important. Titanium in the aviation industry has been increasingly used since 1958 (Figure 1-1). At that time, the mass proportion of titanium in a Boeing 707 was still less than 1 %. In modern passenger aircraft, such as the Boeing 787 or the Airbus A350, the proportion of titanium components used is up to 15 %. The increasing use of titanium in the aerospace industry has, on the one hand, been consistently pursued as a lightweight construction approach. On the other hand, the demand for airplanes has been constantly growing due to the continuous increase in passenger numbers. In commercial aircraft, titanium and its alloys are used in the structural components of the airframe, the engine components, the suspension parts for the wings, and the landing gear components. For the production of aircraft turbines, the titanium alloy Ti-6Al-4V has been used due to its high temperature resistance to increase the maximum temperatures in the turbine and thus, the efficiency. In addition, Ti-6Al-4V is used for the production of structural components due to its high strength and low density (ROTELLA ET AL. 2014, ABBOUD 2015). This decreases the total weight while guaranteeing high durability of the components.

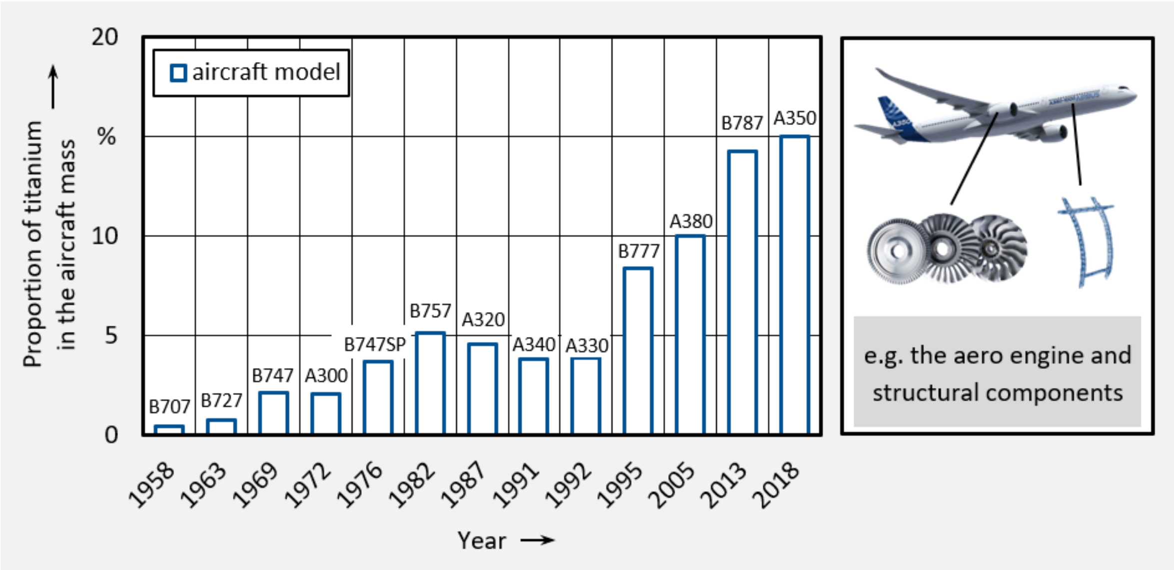

Figure 1-1: Proportion of titanium in the total mass of aircraft models from Airbus and Boeing from 1958 (Boeing 707) to 2015 (Airbus A350) based on FROES (2015)

The final geometry of these components is usually produced by machining. During this manufacturing process, the relative metal-removal rate is particularly high, as pockets are often machined out of the solid raw parts. One example is the process chain for the production of a blisk (blade integrated disk) and a door carrier made of Ti-6Al-4V, which are used in aircraft turbines and aircraft bodies, respectively (Figure 1-1). The raw parts are pre-machined, followed by a rough finishing to produce a near-net-shape geometry. In the last step, the workpiece is finished by peripheral milling, which is considered in this work, with a small depth of cut. The final geometry of the part is achieved through these processes. The resulting surface integrity of the part, through finish machining, considerably affects the quality and functional performance of the component in use.

In particular, the residual stress state in the sub-surface is an important influencing factor that determines the service life of a component after machining (BRINKSMEIER ET AL. 1982). Metal cutting changes the residual stresses as a result of mechanical and thermal loads and, to a lesser extent, phase transformations. For the example of an aircraft engine, the residual stresses in the components influence the fatigue strength. This is especially important for compressor components, which are predominantly made of titanium alloys. Therefore, the residual stress state is the most important sub-surface property for this type of component (Figure 1-2).

The interrelationships leading to a change in the residual stress state during Ti-6Al-4V machining are almost unknown. The resulting residual stresses in the sub-surface are determined by the choice of the process parameters, the tool geometry, and the occuring thermo-mechanical workpiece load.

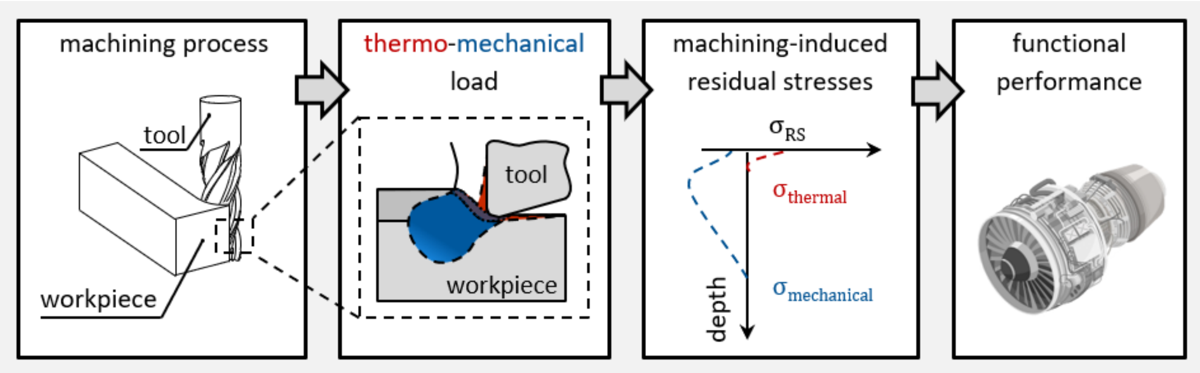

Figure 1-2: The influence of the machining process on the machining-induced residual stresses and the functional performance of components

In the scope of this thesis, a model describing the interrelationships between the peripheral milling process and the machining-induced residual stresses in the sub-surface of Ti-6Al-4V is to be developed. The focus is placed on analyzing the interactions between the process parameters, the tool microgeometry, and the thermo-mechanical loads acting on the workpiece, as well as their effects on the residual stress change. The process parameters and cutting-edge microgeometry are systematically examined to quantify their impact on the resulting residual stresses. The research incorporates a sensory tool holder for the in-process measurement of the process forces, capturing changes caused by tool wear. Machine Learning methods are employed to quantify the variations in the cutting-edge microgeometry resulting from tool wear, based on the collected in-process data. The combination of the experimental investigations, including in-situ characterization techniques, with a semi-analytical modeling approach provides the basis to establish a comprehensive understanding of the mechanisms driving residual stress formation. The semi-analytical model calculates the machining-induced residual stress state and is validated through experimental data. It considers the effects of changes in the process parameters and the tool microgeometry, providing a framework for optimizing the residual stress state in the sub-surface. By coupling experiments with validated models, the research establishes process optimization strategies aimed at achieving residual stress-optimized machining. These strategies are intended to improve the service life and the functional performance of Ti-6Al-4V components while reducing resource consumption and emissions. The findings are intended to be applicable in industrial production, offering sustainable manufacturing solutions that contribute to improved product quality and ecological impact mitigation.

1.2 Structure of the thesis

This thesis is divided into seven chapters. After the introduction in Chapter 1, Chapter 2 presents the fundamental properties of the titanium alloy Ti-6Al-4V, the basics of metal cutting, the kinematics of the peripheral milling process, the process variables during metal cutting, the sub-surface influences of machining processes, and the methods for residual stress modeling. Chapter 3 presents the state of the art. In this context, the emphasis is placed on existing research results on the residual stresses after the metal cutting of titanium. In addition, alternative approaches for the modeling of residual stresses in milling processes are included. Chapter 4 outlines the research approach of this thesis, including the definition of scientific objectives as well as the refinement of the pursued methodology. Chapter 5 explains the experimental procedure. Chapter 6 presents the publication-based part of this dissertation and briefly summarizes the core research findings. The publications comprise process investigations on the peripheral milling of Ti-6Al-4V, experimental analyses on machining-induced residual stress states, and the work on modeling the relationships between the process parameters, the microgeometry of the cutting edge, and the residual stress state during peripheral milling. Chapter 6 discusses the results, classifies the findings with reference to the state of the art, and reflects on the scientific objectives defined in Chapter 4. Finally, the thesis concludes in Chapter 7 with a summary and an outlook on prospective research and industrial activities.

2 Fundamentals

2.1 Chapter Overview

This chapter, dedicated to the fundamentals, is divided into six sections. Section 2.2 provides the relevant background on the properties of titanium alloy Ti-6Al-4V, focusing on its mechanical behavior and relevance in machining applications. Section 2.3. begins with the basic principles of metal cutting, including the chip formation and the kinematics of the cutting process, before addressing the specifics of the milling process and the role of the tool geometry. Section 2.4 describes the examination of the thermal loads generated in milling processes, the process forces during machining, and the influence of rounded cutting edges on these forces. Section 2.5 investigates the effect of the thermo-mechanical loads generated during the machining process on the sub-surface properties, particularly the residual stresses. Afterwards, Section 2.6 outlines the fundamental principles behind various methods for modeling residual stresses induced by machining, emphasizing empirical, analytical, numerical, and hybrid approaches.

Sub-section 2.2.2 is dedicated to the properties and the machinability of the titanium alloy Ti-6Al-4V, building upon its classification and microstructure outlined in Sub-section 2.2.1. The fundamental mechanisms of chip formation are detailed in Sub-section 2.3.1, whereas Sub-section 2.3.2 provides an in-depth explanation of the milling process.. These concepts form the basis for understanding the effects of the milling process on the resulting residual stress state in the sub-surface. Sub-section 2.3.3 addresses the process kinematics, the engagement conditions, and the generation of the final component surface during peripheral milling, which are influenced by the selection of the process parameters. In this regard, this sub-section also introduces both the macroscopic and the microscopic descriptions of the tool geometry. Thermal loads during milling are analyzed in Sub-section 2.4.1, which are related to the process forces in Sub-section 2.4.2. The influence of rounded cutting edges on the mechanical load is described in Sub-section 2.4.3. Furthermore, the sub-surface and its properties are depicted in Sub-section 2.5.1 to elucidate the physical properties of a surface and its functional behavior, which depends on the resulting microstructure and the deformation of the sub-surface described in Sub-section 2.5.2. The interaction between the tool and the workpiece, along with the description of residual stresses and their variation due to the thermo-mechanical workpiece load during milling, are presented in Sub-sections 2.5.3 and 2.5.4. Finally, Sub-section 2.6.1 provides an overview of different modeling methods for the calculation of residual stresses, with detailed descriptions provided in Sub-sections 2.6.2 to 2.6.5.

2.2 Properties of Ti-6Al-4V titanium alloy

2.2.1 Classification and material microstructure of Ti-6Al-4V

William Gregor discovered titanium in 1791 in the mineral ilmenite, followed by Heinrich Klaproth in 1795, who found titanium in rutile ore (LÜTJERING & WILLIAMS 2007). However, an industrial application was not possible until 1940, after William Justin Kroll patented a process for obtaining pure titanium. Therefore, titanium is a young construction material. In subsequent decades, MCQUILLAN ET AL. (1956), GRIEST & FROST (1957), ADENSTEDT & WHITMORE (1955), and KORNILOV & BORSIKINA (1965) systematically intensified the development of titanium alloys. Titanium is allotropic and has a hexagonal close-packed structure (hcp, α-titanium) below 882 °C. Above this temperature, the lattice structure becomes hexagonal-dense, and a body-centered cubic lattice structure (bcc, β-titanium) is present. Alloying elements can be added to change the transformation temperature or the respective area in the phase diagram, which are classified as α- or β-stabilizing. These allow a wide variation in microstructural types. In this context, aluminum is considered the most important α-stabilizing alloying element for titanium alloys (WAGNER & GREGORY 1994). For the classification of titanium alloys into α, α + β, and β alloys, the pseudo-binary, isomorphic phase diagram is mostly used, as shown in Figure 2-1 (LÜTJERING & WILLIAMS 2007).

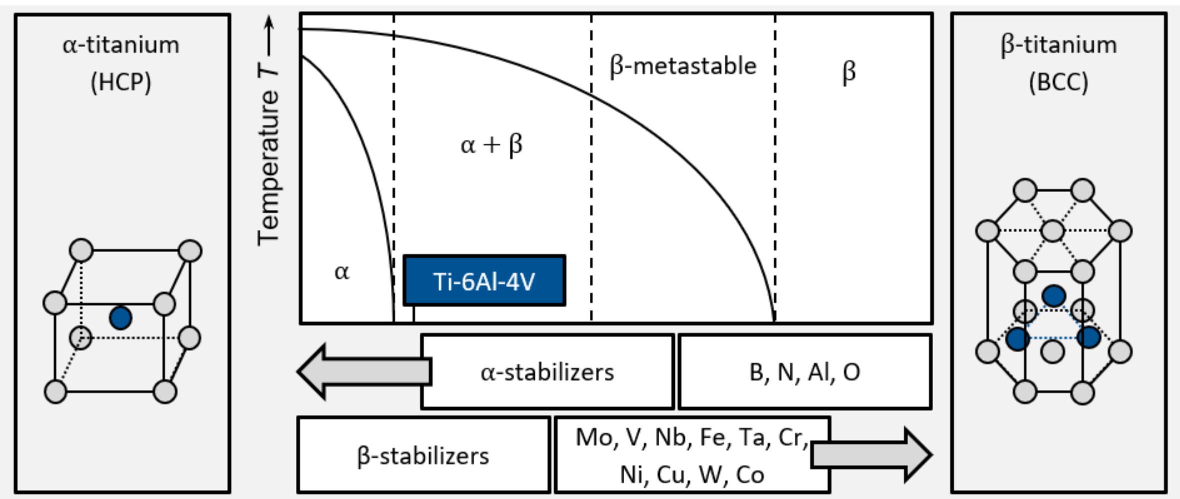

Figure 2-1: Schematic of the alloying elements and their influence on the two-phase diagram according to LÜTJERING & WILLIAMS (2007)

PETERS & LEYENS (2002) and DONACHIE (2000) further subdivided titanium alloys into α-near and metastable β-alloys. Notably, α-alloys exhibit a single-phase hcp structure, and the atoms are more densely packed. Therefore, the diffusion rate in the crystal lattice is considerably lower in β-alloys (bcc), which makes them unsuitable for heat treatment (PETERS & CLEMENS 2010). However, the grain size can be adjusted by altering the cooling rate (WAGNER & GREGORY 1994). Therefore, these alloys, which include pure titanium, are mainly used in the chemical industry and biomedical engineering because of their good formability and corrosion resistance. However, the strength is lower than that of α + β and β-alloys (PETERS & LEYENS 2002). If vanadium, molybdenum, or niobium are added as β-stabilizing elements, α-near alloys can be produced, which have a higher strength and are used in the high-temperature range up to 600 °C, where good creep properties are required (WAGNER & GREGORY 1994). The widest application in industry is found in the two-phase α + β alloys, which include Ti-6Al-4V. These types of alloys exhibit lower high-temperature strength but have higher strength and ductility than α and α-near alloys. In addition, phase transformations in α + β alloys allow the use of heat treatment processes (DONACHIE 2000). Currently available β-alloys are, strictly speaking, metastable β-alloys, as the quenching process passes through the α + β phase. The transformation is not martensitic (LÜTJERING & WILLIAMS 2007), which leads to strengths of more than 1,400 MPa, and good formability can be achieved by downstream heat treatment (PETERS & LEYENS 2002). However, metastable β-alloys exhibit a high density, poor weldability, and high acquisition costs.

Currently, more than 100 titanium alloys exist, of which 30 to 40 are used in industry for the production of goods (ROOS ET AL. 2017). With a total market share of over 50 %, Ti-6Al-4V is by far the most commonly used titanium alloy. The microstructural states of Ti-6Al-4V can be lamellar, globular, or bimodal, depending on the heat treatment (GROVE 2015). The classification of the microstructural states of the titanium alloy Ti-6Al-4V is shown in Figure 2-2.

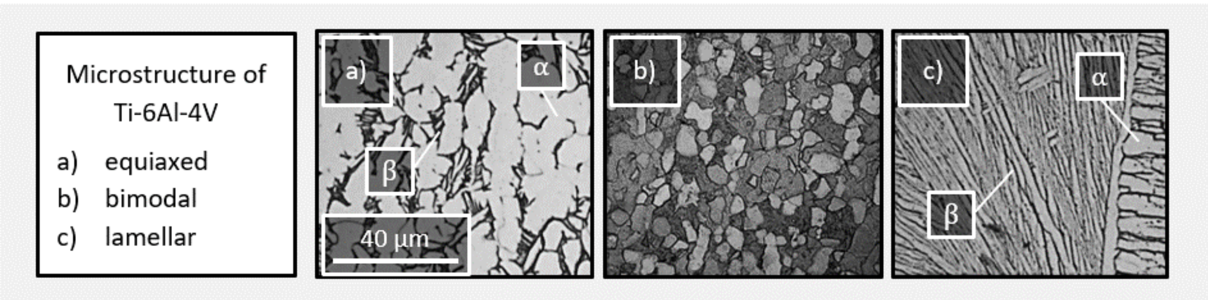

Figure 2-2: Classification of the microstructural states of Ti-6Al-4V based on WAGNER & GREGORY (1994)

Lamellar microstructures are produced in the Ti-6Al-4V alloy by slow cooling above the β-transus temperature, which is approximately 995 °C. These become finer and eventually martensitic as the cooling decreases. Unlike steel, titanium martensite offers no strength advantages and is therefore rarely used in industry (WAGNER & GREGORY 1994, GROVE 2015). To produce globular and bimodal structures, a previous hot forming step and subsequent recrystallization below the β-transus temperature are required. The microstructure types are determined here by the cooling rate and temperature. Ti-6Al-4V quickly forms a chemically stable titanium oxide layer during contact with air due to its high gas affinity, which leads to embrittlement of the material. Therefore, heat treatments have to be conducted under vacuum.

2.2.2 Properties and Machinability of Ti-6Al-4V

Material properties

The microstructures, described in Sub-section 2.2.1, define the properties of the material. The lamellar microstructure exhibits good fatigue strength at high load cycles (high-cycle fatigue). However, at low load cycles (low-cycle fatigue), the material fails earlier than the equiaxed and bimodal microstructures due to the lower fracture strain and ductility (WAGNER & GREGORY 1994). The globular microstructure exhibits opposite effects. The bimodal structure can be classified as one of the two types of microstructure and is therefore the most frequently used in industry (DONACHIE 2000, GROVE 2015).

Machinability

This sub-section deals with the machinability of the Ti-6Al-4V titanium alloy based on the described material properties of titanium. According to DIN 6583, machinability is defined as "[...] the property of a workpiece or material to be machinable under given conditions." Ti-6Al-4V is classified as difficult to machine due to its outstanding material properties, namely high ductility and reactivity, low thermal conductivity and modulus of elasticity, and high strength. Shaw, Cook, and Bosten conducted the first studies on titanium machining in the 1950s (KOMANDURI 1982). The material properties severely limit the productivity of machining titanium. Compared to aluminum alloys, the achievable metal-removal rate during milling of Ti-6Al-4V is lower by a factor of 20 (NIKNAM ET AL. 2014). In addition, KREIS (1973), ALTMÜLLER (2001), GEY (2003), ZANGER (2013), and GROVE (2015) investigated the machinability of Ti-6Al-4V for different metal-cutting manufacturing processes. Furthermore, the keynote papers by MACHADO & WALLBANK (1990), EZUGWU & WANG (1997), ULUTAN & ÖZEL (2011), and books by KLOCKE & KÖNIG (2008) and DONACHIE (2000) summarized the findings on the machinability of Ti-6Al-4V.

According to DENKENA & TÖNSHOFF (2011), the four evaluation criteria for quantifying machinability are

- the chip formation,
- tool wear,
- the process forces, and
- the workpiece quality.

Therefore, the mechanical, thermal, and chemical processes, and the resulting effects on the chip formation, the cutting forces, and the tool wear during Ti-6Al-4V machining are described below. The following description is based on the explanations of GEY (2003), SCHLENKER (2014), WESSELS (2007), and GROVE (2015).

Chip formation: The material properties of titanium considerably influence the chip formation. In this process, sliding bands and segmented chips with a high degree of segmentation are formed, as Ti-6Al-4V tends to shear locally due to its low thermal conductivity, sharp strength reduction with increasing temperature, and low formability (PUERTA VELÁSQUEZ 2007). In addition, the different material microstructures and vibrations influence the formation of segmented chips (KLOCKE & KÖNIG 2008). Considering the interaction between the tool and the workpiece at the beginning of the cutting process, a part of the material is initially compressed and elastoplastically deformed. This process continues until a critical stress in the material is exceeded, and local shear occurs in the primary shear zone. The resulting chip segment then slides along the shear plane, and the process is repeated (ARRAZOLA ET AL. 2009, CALAMAZ ET AL. 2011).

Cutting force: During the formation of segmented chips, sliding and compression constantly alternate. This subjects the tool to a pulsating load, which results in a high-pressure swell and thermally alternating stress in the cutting edge, which is directly correlated with the formation of chip segments. This results in a cyclic variation in the process forces, which is influenced by the grain size of the material (GROVE 2015). Here, the dynamic force component can amount to 20–35 % of the static cutting force load (KLOCKE & KÖNIG 2008, KREIS 1973). Therefore, the main load on the tool cannot be described purely by the average process forces, which are approximately at the level of steel alloys with comparable strengths (DONACHIE 2000). Another negative effect results from segmented chip formation, as this mechanism reduces the contact area between the cutting edge and the chip. Therefore, the load is concentrated on a small area of the tool's cutting edge, which induces high local mechanical and thermal stresses. According to MACHADO & WALLBANK (1990), the contact area between the tool and the chip during titanium machining is approximately

70 % smaller than that of steel, and the resulting stresses at the cutting edge are thus considerably higher.

Tool wear: During milling, the low thermal conductivity and specific heat capacity of titanium lead to an increased thermal load on the cutting edge. Energy is converted during chip formation into heat predominantly. Only a small proportion of the heat can be dissipated via the workpiece and the chips. This increases the local temperature at the cutting edge of the tool (KREIS 1973). During titanium machining, 60–80 % of the generated heat energy is transferred into the tool (KREIS 1973). In comparison, when machining steel materials, 40–60 % of the heat is dissipated to the tool, which means that the maximum temperature increase during titanium machining is approximately twice as high as that during steel machining (ABELE & FRÖHLICH 2008, ALTMÜLLER 2001). The thermo-physical properties of the cutting material and the cutting speed determine the temperature reached during titanium machining. According to ALTMÜLLER (2001), the temperature in the contact zone can reach a value ranging from 200 °C to 900 °C. In this case, the maximum temperatures occur on the bottom side of the chip shortly before the chip separates from the cutting surface of the tool (KOMANDURI & HOU 2000, KOMANDURI & HOU 2001a, 2001b). This promotes the subsequent melting of the material on the cutting edge and the associated adhesive wear. Thus, the high thermal load on the tool is an important influencing factor on tool wear. In addition, the effects already mentioned are intensified by the high chemical affinity of titanium to carbon, oxygen, and nitrogen. Moreover, the interrupted cut during milling leads to a transient thermo-mechanical load on the tool. This results in thermally induced stresses on the cutting edge, which can lead to the formation of cracks in the cutting material and thus reduce the service life of the tool. During Ti-6Al-4V machining, in addition to the high thermal stress, high mechanical stresses occur on the cutting edge of the tool because of the high deformation resistance of titanium alloys, which persist even at higher temperatures. According to KREIS (1973), the mechanical stress on the cutting edge during the machining of titanium is considerably higher than that for steel because Ti-6Al-4V retains its deformation resistance even at temperatures far above 200 °C. In addition, only a small amount of plasticity is required for the cutting edge. Moreover, Ti-6Al-4V is capable of only small deformation, as this material has a high yield strength ratio (yield strength R_p/ ultimate tensile strength R_m). Combined with the low Young's modulus, the material tends to plastically deform when mechanically loaded by the cutting edge and elastically spring back when unloaded. This leads to an increase in friction under the flank face of the cutting edge and thus to increased abrasive wear and an additional increase in temperature. For this reason, flank wear and micro-chipping of the cutting edge due to thermal and adhesive stress are the most common wear mechanisms in the milling of Ti-6Al-4V. In the choice of cutting material, tools made of cemented carbide are mostly used for cutting Ti-6Al-4V. Ceramics and cermets are unsuitable for machining due to their high chemical affinity for titanium. In some cases, cutting materials made of polycrystalline diamond (PCD) and polycrystalline cubic boron nitride (pCBN) are used for finishing operations due to their high thermal conductivity (KLOCKE & KÖNIG 2008).

2.3 Basics of metal cutting

2.3.1 Mechanisms in the Chip-Formation Process

During chip formation, the cutting edge of the tool engages the workpiece material with a cutting speed v_c and depth of the uncut chip thickness h. Moreover, the material undergoes elastic and plastic deformation (MILBERG 1992). Chip formation and the resulting shear and friction zones are shown in Figure 2-3. During this process, the shear plane starts to form in the primary shear zone (I) after the material-specific maximum permissible shear stress has been exceeded. The deformed workpiece material forms a chip, which flows off over the rake face of the tool with the chip velocity v_{ch}. The friction zone between the chip and the rake face is called the secondary deformation zone (II). The friction between the flank face of the tool and the generated workpiece surface forms the tertiary deformation zone (III). During chip formation, a continuous, discontinuous, or segmented chip is produced depending on the deformation capability of the material. Continuous sliding of the chip over the rake face leads to continuous chips. If the shear strength of the material is periodically exceeded, discontinuous chip formation follows, resulting in discontinuous and segmented chips. Chipping occurs in brittle materials when the chip separates from the workpiece without significant deformation due to cracks preceding the cutting edge (HOPPE 2003). During machining, mechanical work is performed, which is largely converted into thermal energy and, to a lesser extent, into latent energy in the workpiece, chip, and tool. The latent energy is primarily composed of residual stresses that remain in the sub-surface of the material and kinetic energy in the form of chip acceleration (SCHWARZ 2010). Heat is generated during chip formation due to the following mechanisms (KLOCKE & KÖNIG 2008):

- Plastic deformation work in the primary, secondary, and tertiary deformation zones
- external friction between the rake face of the tool and the flowing chip
- extern friction between the flank face of the tool and the workpiece
- separation work before the cutting edge, and
- internal and external friction of the outflowing chip.

If machining is performed without a coolant, the generated heat is primarily dissipated via the chip, the tool, and the workpiece. For workpiece materials with good thermal conductivity, the largest proportion of the heat passes into the chip, while only a small proportion flows away via the tool. Regarding materials with poor thermal conductivity, only a small proportion of the heat flows into the chip, which means that more heat has to be removed via the tool (VICTOR ET AL. 1983, MÜLLER 2004).

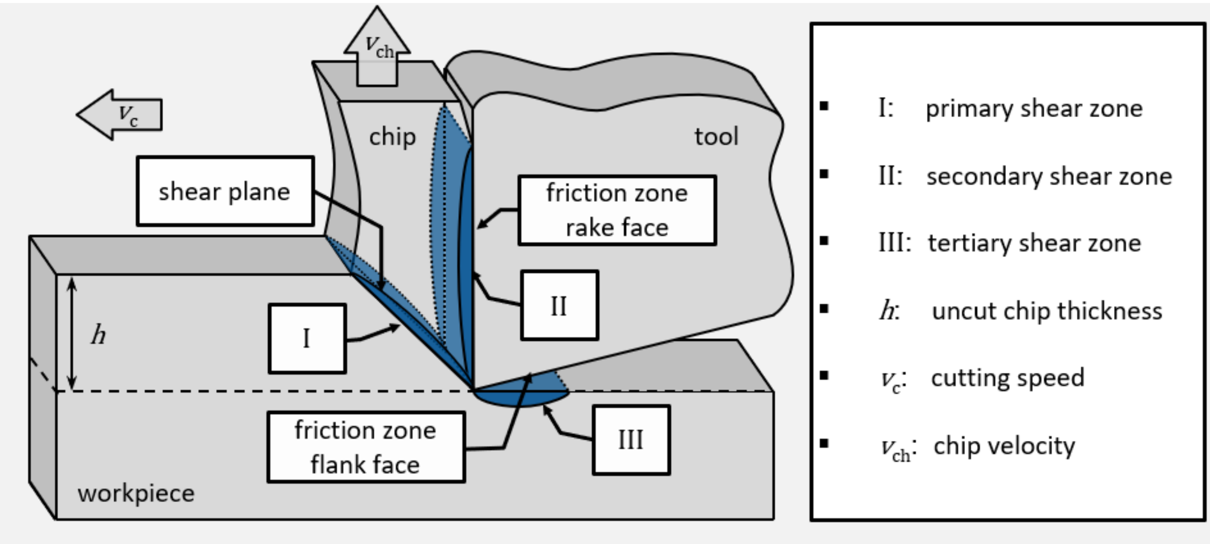

Figure 2-3: The chip formation in the (I) primary, (II) secondary, and (III) tertiary shear zone during metal cutting according to KLOCKE & KÖNIG (2018)

2.3.2 Process fundamentals of milling

Milling is a machining process performed using a geometrically defined cutting edge. The relative movement between the workpiece and the tool is realized by a circular cutting motion of the tool and a linear feed motion that is perpendicular or oblique to its rotational axis (KLOCKE & KÖNIG 2018). This kinematics causes an interrupted cut as the cutting edge loses contact with the workpiece at least once during each tool rotation (KRONENBERG 1969). Depending on the tool geometry and the process kinematics, milling processes can be divided into face, circular, screw, profile, shape milling, and gear hobbing, according to DIN 8589-3 (Figure 2-4).

Face milling is the most common milling process, which is used to produce flat surfaces through a linear feed motion. It can be further divided into peripheral milling and front peripheral milling depending on the areas of the tool in engagement (DENKENA & TÖNSHOFF 2011). When the angle of contact between the milling tool and the workpiece during face milling is 180°, the process is referred to as slot milling. Other special processes are screw milling to produce helix-shaped workpiece surfaces; gear hobbing, which is mainly used in the machining of gears; and circular milling, which produces circular–cylindrical inner or outer surfaces.

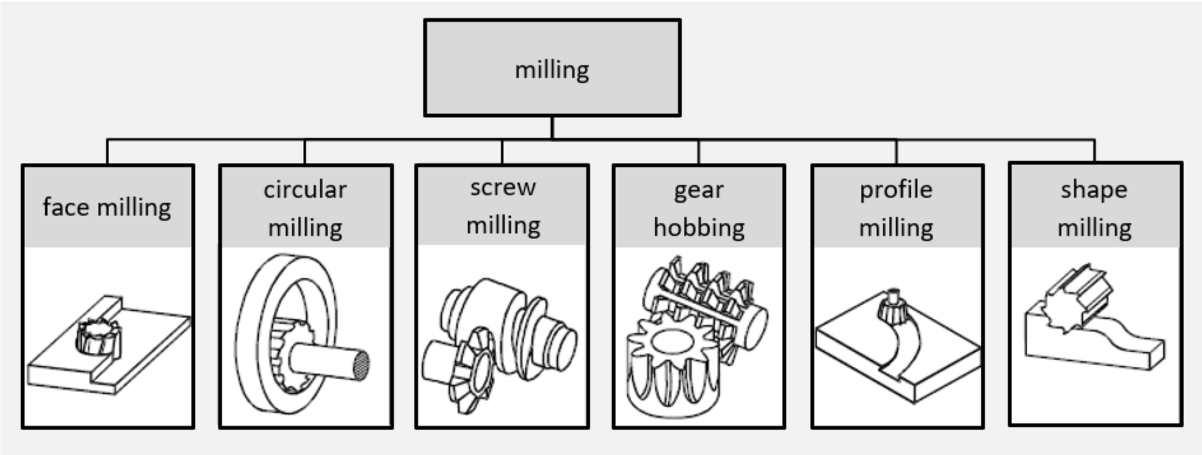

Figure 2-4: Classification of milling operations according to DIN 8589-3

Profile milling is used to produce special contours, such as T-slots, by mapping the profile of the tool directly onto the workpiece. During shape milling, free-form surfaces can be produced by using up to five controlled feed axes; thus, it is among the most important milling processes in tool and mold production (FRITZ & SCHULZE 2015). In this work, the peripheral milling process was applied; therefore, the following sections focus on this type of milling operation.

2.3.3 Tool geometry, process kinematics, and engagement conditions

Tool geometry: Milling tools are available in various designs. The classification is based on different factors such as the shape, area of application, and helix angle. The geometry, cutting material, and coating of the tool depend on the specific application. Solid milling cutters are among the most commonly used tools in multi-axis milling operations. Their tool geometry can be characterized by the macroscopic and the cutting-edge geometry. This distinction is important for process modeling, as not all models can consider both geometries or geometry scales (ZABEL 2010).

Macroscopic tool geometry: Spiral-shaped solid carbide cutters (end mills) with a cylindrical shank are generally used for peripheral milling. Depending on the machining task, the shape of the milling tool can be cylindrical, tapered, or customized. The geometric dimensions diameter D, cutting-edge length L_t, and the helix angle β of the main cutting edge are used to describe the macroscopic geometry of an end mill, as defined in DIN 6528 as shown in Figure 2-5.

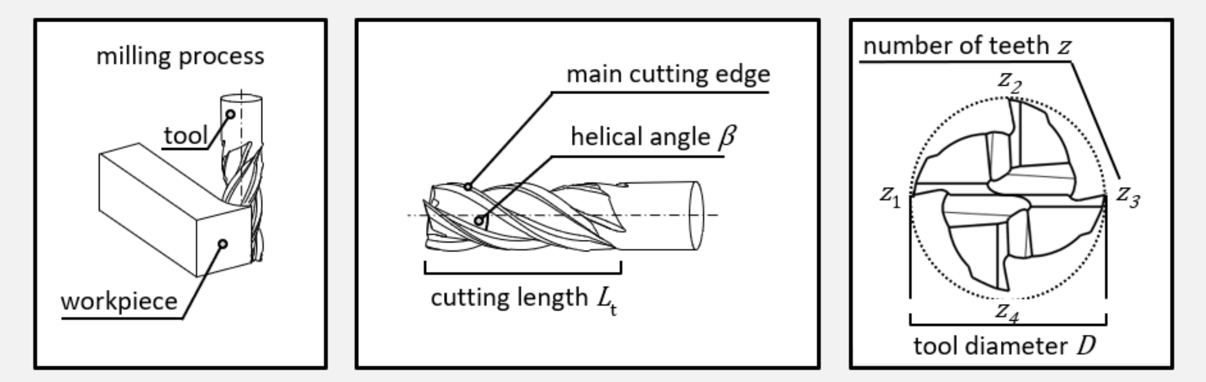

Figure 2-5: Solid carbide end mills with continuous cylindrical shank according to DIN 6528

The helix angle, which is defined by the angle between the tool axis and the cutting edge, significantly influences the mechanical load on the cutting edges during the milling process (KRONENBERG 1969). With a helix angle $\beta > 0$, the cutting edge continuously enters the workpiece during peripheral milling, resulting in a smooth increase in force. Furthermore, end mills differ based on the number of teeth z, which determines the tooth pitch angle $\Delta\tau$ of the tool in evenly spaced tools according to

$$\Delta\tau = \frac{360°}{z} \tag{2-1}$$

Using milling tools with multiple teeth enables simultaneous engagement of individual tool cutting edges due to the contact length and the tool pitch angle, which reduces the load on the milling tool. In this work, cylindrical, right-twisted end mills were used. Therefore, the following description of the kinematics is adapted to them.

Microscopic cutting-edge geometry: The cutting edge is defined according to the DIN 6581 standard. It is the part of the tool that effectively generates the machined surface. The variables specifying the geometry of the cutting edge are shown in Figure 2-6. The rake face of the tool is the area over which the chip flows until it leaves the workpiece. The flank face is the area of the tool adjacent to the final machined surface. The wedge angle β_w to be selected, which is formed between the rake and flank face, depends on the physical resistance that the workpiece exhibits when the cutting edge enters the workpiece material. Smaller wedge angles result in lower resistance. A cutting edge with a larger wedge angle is more stable and can better absorb the generated heat (AWISZUS 2002).

The clearance angle α is the angle between the flank face and the machined surface. A compromise must be considered when selecting the clearance angle α because high values lead to heat buildup in the cutting edge, which increases tool wear and the probability of tool breakage. Values close to zero, however, can affect the quality of the machined surface and significantly increase wear on the flank due to pressure welding. In addition, ploughing forces increase when the clearance angle decreases.

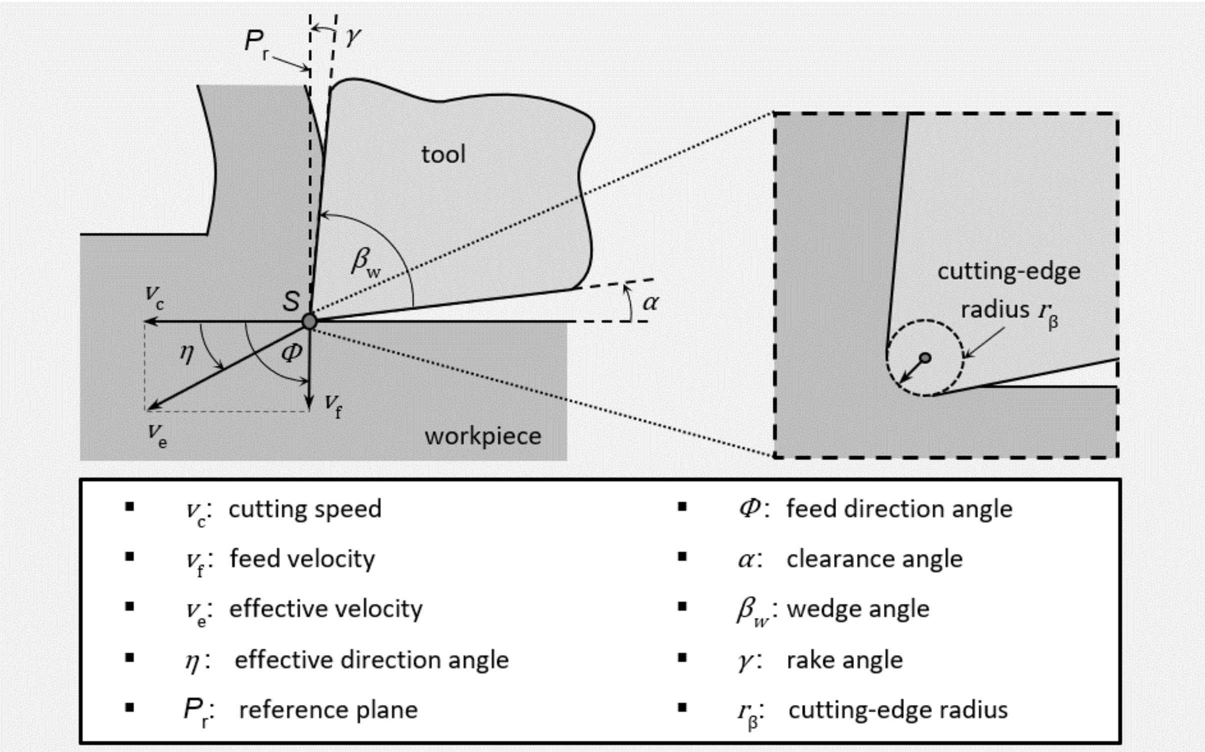

Figure 2-6: Depiction of the idealized cutting edge and cutting-edge geometry according to DIN 6581

Another important angle is the rake angle γ, which is formed between the rake face of the cutting edge and the reference plane P_r. The rake angle has a distinct influence on the chip formation. As shown in Figure 2-6, γ assumes a positive value in this depiction. However, zero and negative values can also be used. In the positive range, the rake angle causes a reduction in the tangential and the feed forces (ALTINTAS 2012). Using a large positive rake angle, on the other hand, leads to higher stress on the cutting edge. In the negative range, the rake angle stabilizes the process and improves the chip breaking. However, in this case, the forces and thermal loads to which the cutting edge is subjected are higher. This leads to an increase in wear on the rake face and reduces the tool life (KLOCKE & KÖNIG 2008).

In practice, no tools have ideal sharpness. In this context, a cutting-edge radius is considered, as illustrated in Figure 2-6 (KLOCKE & KÖNIG 2008). The flank and the rake face are almost always rounded in the transition. This rounding is defined by the cutting-edge radius r_β. While the characterization of the cutting-edge macro-geometry is internationally standardized (DIN 6581, ISO 3002), no standard exists to describe the cutting-edge micro-geometry, which is the actual shape of the intersection of the flank and the rake face of a tool (WYEN ET AL. 2012). The cutting-edge shapes are described in the DIN 6582 standard. Cutting-edge profiles can be chamfered, sharp, or rounded. A rounded cutting edge is formed by a rounded transition between the rake face of the tool and the flank face. The nominal radius r_β of a rounded cutting edge is measured in the cutting normal plane. The cutting-edge radius r_β is an important variable in milling, especially when its size is in the same order of magnitude as the uncut chip thickness h (ALBRECHT 1960, WYEN ET AL. 2012).

The cutting-edge geometry plays a key role in the milling of titanium alloys from the perspective of tool wear. Results from research and industrial practice demonstrate that the stabilization of the cutting edge by a defined radius in the range of 5–20 μm leads to a considerable increase in the tool life (KLOCKE & KÖNIG 2008).

Process kinematics and engagement conditions

These terms clearly indicate that the cutting edge (tool) must always be considered in relation to the workpiece, which means that the process kinematics are of considerable importance.

The model of the selected cutting point is often used to simplify the description of the process kinematics between the cutting edge and the workpiece material (cf. Figure 2-6). Therefore, the real kinematics are described by summarizing the spatial velocity fields in the selected cutting point S. At the selected intersection point, the velocity fields can be summarized by vectors. The resulting vectors can be combined into an overall vector by addition. In most cases, the workpiece is assumed to be stationary and all movements are performed by the tool. The resulting velocity vector is called the effective velocity v_e. It can be decomposed into two components; the cutting speed v_c in the cutting direction and the feed velocity v_f in the feed direction. Two angles are defined to uniquely locate the components of the effective velocity:

- the direction of action angle η as the angle between the direction of action and the direction of intersection, cf. Figure 2-6, and
- the feed direction angle Φ as the angle between the feed direction and the cutting direction, cf. Figure 2-6.

The investigation of the kinematics and geometry of peripheral milling processes has already been the subject of numerous research works. SALOMON (1924) conducted the first scientific studies on milling using cylindrical milling tools. He found a transient load on the cutting edge resulting from the discontinuous interaction between the tool and the workpiece. Due to the helix angle β, this occurs with a time offset and is the same for each cutting edge. In this context, the comprehensive analysis of the process kinematics requires specific knowledge of the contact conditions between the workpiece and the tool. A distinction is made between the macroscopic and microscopic contact conditions (WITTY 2014). The macroscopic contact conditions can be described using the feed velocity v_f, the axial depth of cut a_p, and the radial depth of cut a_e, which are depicted in Figure 2-7.

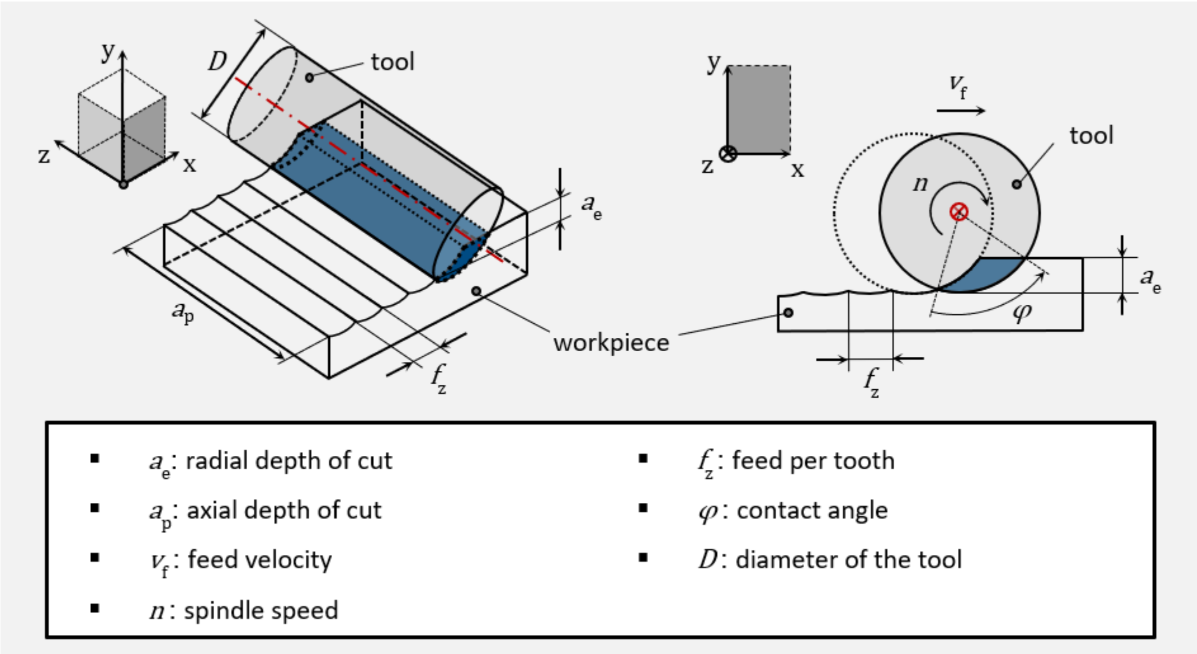

Figure 2-7: Macroscopic engagement conditions for peripheral milling

Based on these process parameters, the contact angle φ can be calculated, which indicates the angular section of the tool as being in contact with the workpiece:

$$\varphi = \cos^{-1}\left(1 - \left(2 \cdot \frac{a_e}{D}\right)\right) \tag{2-2}$$

The chip length l_c can be derived from the contact angle. It describes the length of the contact angle arc on the tool circumference:

$$l_c = \frac{D}{2} \cdot \varphi \cdot \frac{\pi}{180°} = \frac{\pi \cdot D}{360°} \cdot \varphi \tag{2-3}$$

The chip length can also be expressed as the product of the cutting speed v_c and the contact duration between a cutting edge and the workpiece. A high contact duration results in a higher thermal load on the tool cutting edge. The chip length thus has a direct influence on the resulting tool wear (MEINECKE 2009).

The effective motion of the tool can be described by superimposing the rotational movement of the tool and the translational feed velocity. The resulting cutting speed v_c at the tool circumference can be calculated based on the rotation of the tool.

$$v_c = \pi \cdot D \cdot n, \quad (2\text{-}4)$$

where

D: diameter of the tool, and

n: spindle speed of the tool.

The translational feed velocity v_f is calculated as the product of the spindle speed n, the number of teeth of the tool z, and the feed per tooth f_z:

$$v_f = n \cdot z \cdot f_z \quad (2\text{-}5)$$

Depending on the orientation of the cutting direction of the cutting edge and the feed direction of the workpiece, a distinction is made for the peripheral milling process in up- and down-milling. During up-milling, the cutting edge moves in the engagement area against the feed direction of the workpiece. The chip thickness is minimal at the tool entry angle φ_{st} and peaks at the tool exit angle φ_{ex}. Because the minimum uncut chip thickness h_{min} is not reached at the cutting-edge entry, squeezing and friction processes occur before the chip formation in this case. This results in an increase in the flank wear of the tool and a higher heat input into the workpiece. When using up-milling, tensile residual stresses can occur at the cutting edge at large chip thicknesses, which can lead to the formation of cracks and, ultimately, the breakage of the tool. In addition, the low modulus of elasticity of titanium in up-milling causes a long friction phase between the tool and the workpiece before chip formation is defined (PEKELHARING 1978). Therefore, up-milling is generally not economical, as it reduces tool life (RÖSCH 2015). In contrast, during down-milling (Figure 2-8), the cutting edge rotates in the engagement area in the direction of the feed direction of the tool.

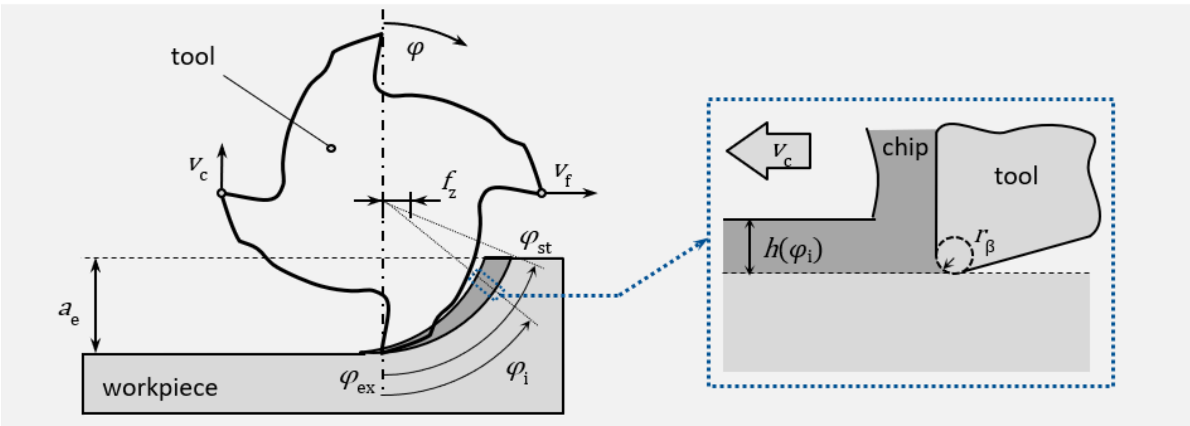

Figure 2-8: Tool–workpiece–interaction during down-milling

This results in a maximum uncut chip thickness at the entry angle φ_{st} of the tool cutting edge, which becomes zero at the exit angle φ_{ex}. In contrast to up-milling, tool wear can be reduced and the surface quality improved by down-milling. Consequently, the down-milling process is particularly suitable for milling of titanium alloys, which are difficult to machine. The position of a tool cutting edge can be determined based on the tool rotation angle φ, starting perpendicular to the feed direction on the side facing away from the workpiece. The tool entry angle φ_{st} and the tool exit angle φ_{ex} describe the positions at which the cutting edge contacts and exits the workpiece.

As the cutting speed is considerably higher than the feed velocity ($v_c >> v_f$), the cutting-edge movement can be approximated by a circular path. The superposition of the rotational and translational motion of the cutting edge is neglected, as it would result in a cycloidal path. Under this assumption, MARTELOTTI (1941) derived an equation for calculating the instantaneous uncut chip thickness $h(\varphi)$, which is the distance between two circumferences of the rotating tool. In the range ($\varphi_{st} < \varphi < \varphi_{ex}$), the uncut chip thickness can be approximated linearly from h_{max} to zero, leading to the following relationship (MEYER 2009):

$$h(\varphi) = h_{max} \cdot \frac{\varphi - \varphi_{st}}{\varphi_{h,max} - \varphi_{st}} \tag{2-6}$$

where $\varphi_{h,max}$ represents the angular position at the maximum uncut chip thickness, which can be calculated as follows:

$$\varphi_{h,max} = 180° - arctan\left(\frac{D \cdot \sin\varphi - 2f_z}{D - 2a_e}\right) \tag{2-7}$$

In a simplified form, for processes where the feed velocity v_f is much smaller than the cutting speed v_c, and the feed per tooth is much smaller than the tool radius ($f_z << D/2$). The uncut chip thickness $h(\varphi)$ can be expressed as follows (ALTINTAS 2012, KÖNIG ET AL. 1982):

$$h(\varphi) = f_z \cdot \sin\varphi \tag{2-8}$$

Neglecting the cycloidal shape of the tool path curve results in an error of less than 1% compared to the exact formulation; therefore, the uncut chip thickness h is calculated according to equation 2-6. It is defined as the thickness of the undeformed chip. This provides a phenomenological explanation of the chip formation and the wear mechanisms. In addition, the uncut chip thickness forms the basis for most approaches for modeling the occurring cutting forces, as it directly correlates with the local cutting-edge load (MEINECKE 2009).

Surface generation during peripheral milling

Regarding peripheral milling a new workpiece surface is always generated during the engagement of the cutting edge in the range $\varphi_{st} < \varphi < \varphi_{ex}$ (Figure 2-9a). However, this new surface does not necessarily have to correspond to the final workpiece surface. During the following tool rotation, a large part of the generated surface is removed, and only a small part of the previously formed surface represents the final surface ($\varphi_2 < \varphi < \varphi_{ex}$), as illustrated in Figure 2-9b. NESPOR (2015) defined this relationship in ball-end milling as surface generation, where a surface is technically generated at any time, but the term surface generation always refers to the final surface.

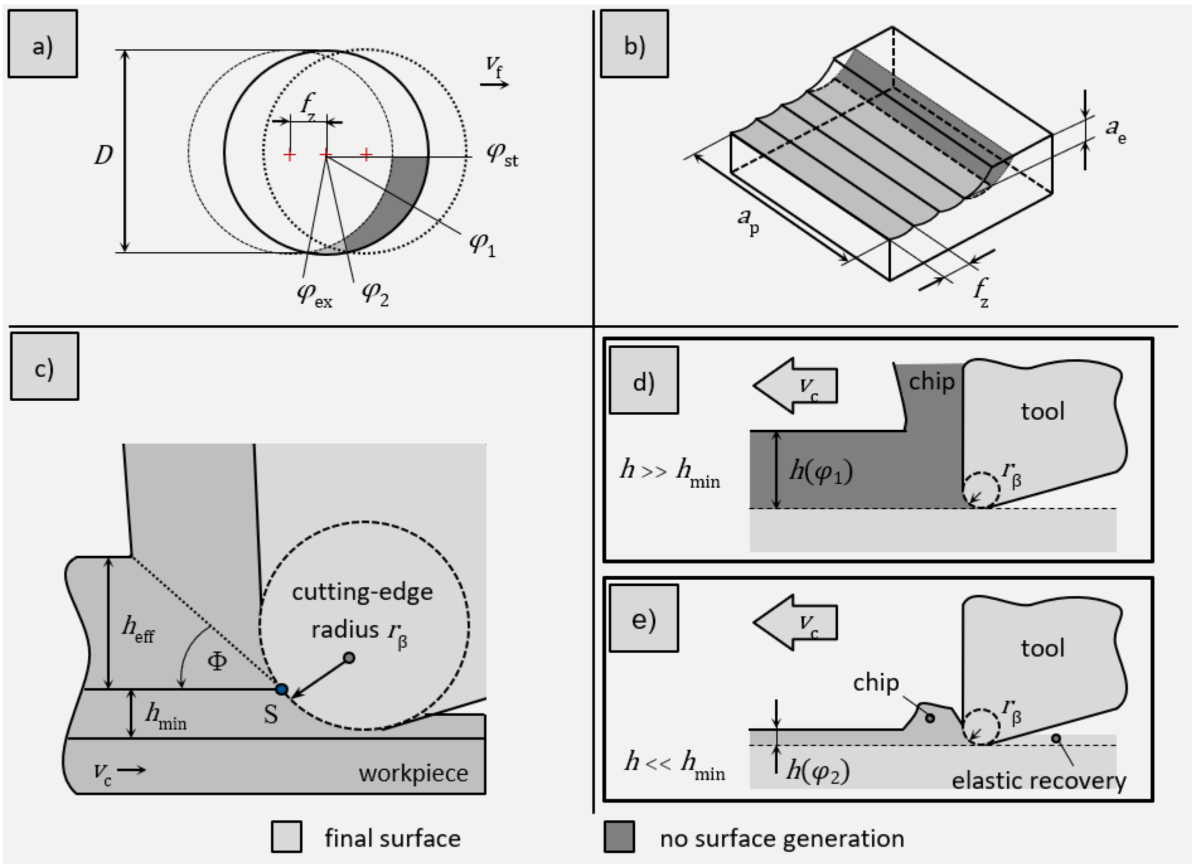

Figure 2-9: The surface generation during peripheral milling and the size effect in the chip formation according to ARAMCHAROEN & MATIVENGA (2009)

During the generation of the final surface, the plasto-mechanical processes in front of the cutting edge must be considered, which are influenced by the uncut chip thickness and the size of the cutting-edge radius (WARNECKE 1974). During chip formation, a part of the material flows under the cutting edge. The separation point of the material on the cutting-edge radius is called stagnation point S, as shown in Figure 2-9c. At this point, the flow velocity of the chip is at its minimum. The position of the stagnation point determines the proportion of the chip thickness that flows into the chip h_{eff} and under the cutting edge. This characterizes the so-called size effect, as illustrated in Figure 2-9d and Figure 2-9e (ARAMCHAROEN & MATIVENGA 2009). The uncut chip thickness h that is forced to flow under the cutting edge is called the minimum uncut chip thickness h_{min}. This is mainly determined by the rounding of the cutting edge (WARNECKE 1974, WALDORF ET AL. 1998). If the uncut chip thickness h is equal to or smaller than the minimum uncut chip thickness h_{min}, the material flowing under the cutting edge is ploughed instead of removed (Figure 2-9e). Subsequently, it undergoes elastic recovery and consequently presses on the flank face. Under these conditions, the specific cutting energy increases nonlinearly as the rake angle becomes negative.

2.4 Process variables during machining

2.4.1 Thermal load in milling processes

During milling, which is one of the manufacturing processes with a geometrically defined cutting edge, most of the mechanical power introduced to the spindle is converted into thermal energy. Heat is transferred through the primary, secondary, and tertiary shear zones. The respective averaged share of the heat sources in the total heat is summarized according to KUMAR & AJAY (2012), KOMANDURI & HOU (2000), and PABST (2008) as follows. The majority of the heat (approx. 70–90 %) generated in the primary shear zone is dissipated via the chip (KUMAR & AJAY 2012, SCHMIDT 1949, SHAW 1996). The specific distribution of the heat depends on the selected process parameters, the manufacturing process, and the tool-workpiece combination and can therefore not be generalized (VIEREGGE 1953). Titanium alloys, such as Ti-6Al-4V, have a low thermal conductivity, which means that more heat is dissipated through the tool and less into the chip or the workpiece (LOEWEN & SHAW 1954, KOMANDURI 1982). ARMENDIA ET AL. (2010) demonstrated this experimentally for the orthogonal cut using a thermographic camera. They investigated the machining of Ti-6Al-4V and 42CrMoS4. This confirms the calorimetric measurements conducted by SCHMIDT (1949), which showed that the heat distribution between the tool, the chip, and the workpiece is significantly dependent on the thermal conductivity of the material combination as well as the cutting speed.

2.4.2 Process forces during machining

During machining, the tool is under mechanical load, which is referred to as the cutting force F. The cutting force can be divided into the cutting force components active force F_a and passive force F_p. The active force is located in the working plane formed by the cutting vector and the feed vector, and it significantly determines the power converted during cutting. The active force can be further subdivided into the cutting force F_c and the cutting normal force F_{cN}, which act in the cutting direction and perpendicularly to it, respectively:

$$\overrightarrow{F_a} = \overrightarrow{F_c} + \overrightarrow{F_{cN}} \tag{2-9}$$

The passive force F_p is perpendicular to the active force F_a, and consequently, the following equation applies:

$$\vec{F} = \overrightarrow{F_a} + \overrightarrow{F_p}. \tag{2-10}$$

The passive force has no contribution to the power that is converted during the milling process (HEISEL ET AL. 2014). Figure 2-10 shows the relationships between the individual force components in the peripheral milling process considered in this work. The components of the cutting force depend on the contact angle φ and can be determined as follows:

$$F_c(\varphi) = F_{c,x}(\varphi) + F_{c,y}(\varphi) \tag{2-11}$$

$$F_{cN}(\varphi) = F_{cN,x}(\varphi) + F_{cN,y}(\varphi) \tag{2-12}$$

$$F_p(\varphi) = F_{p,z}(\varphi) \tag{2-13}$$

The forces acting on the tool were measured with respect to a Cartesian coordinate system as part of this work. In the following, the forces F_x, F_y, and F_z will therefore be referred to as the cutting-force-components, where

$$F_x(\varphi) = F_{c,x}(\varphi) + F_{cN,x}(\varphi) \tag{2-14}$$

$$F_y(\varphi) = F_{c,y}(\varphi) + F_{cN,y}(\varphi) \tag{2-15}$$

$$F_z(\varphi) = F_{p,z}(\varphi) \tag{2-16}$$

Depending on the selected process parameters, multiple cutting edges may be simultaneously engaged in milling tools with multiple teeth. In this case, the respective cutting force components F_x, F_y, and F_z of the cutting edges in engagement can be summed up to a total force.

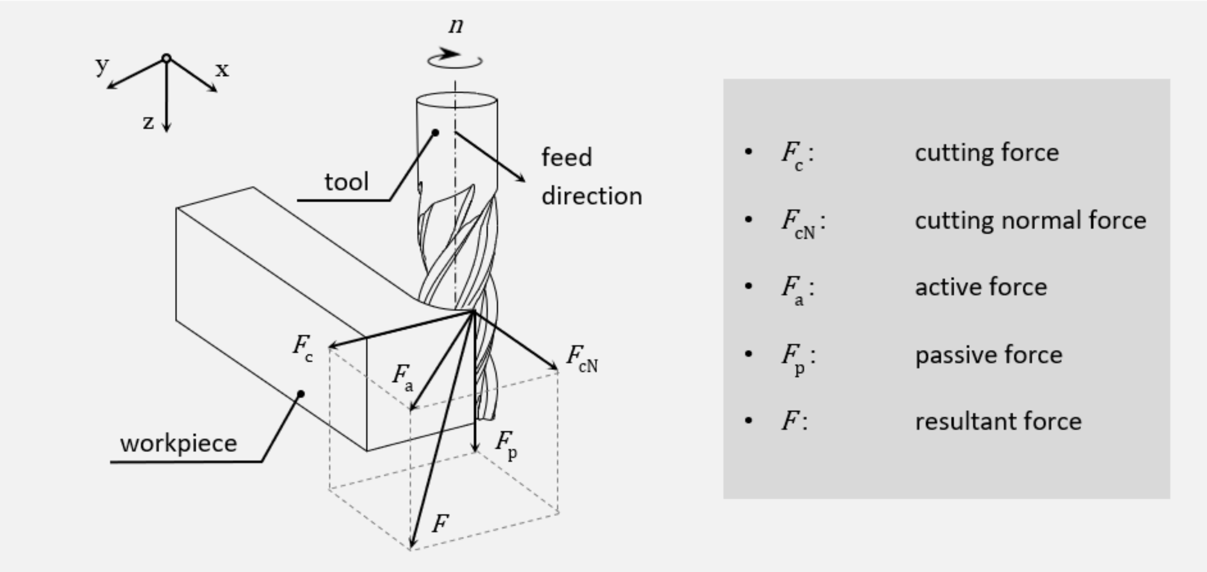

Figure 2-10: Cutting force components during peripheral milling following DIN 6584 and DIN 6580

2.4.3 Influence of rounded cutting edges on the process forces

Taylor investigated the influence of rounded cutting edges on the process forces. He observed an increase in the process forces over the tool life, which is not purely due to tool wear but the result of the cutting edge becoming blunt and rounded after a certain cutting length (TAYLOR 1907). MASUKO (1953) and ALBRECHT (1960) independently demonstrated the relevance of the cutting-edge rounding for the machining process using essentially the identical explanatory model for the occurring phenomena depending on the cutting-edge radius. In addition to the chip forming force component F_{Ch}, which is responsible for chip formation, ALBRECHT (1960) considered the ploughing effect. He defined the ploughing force F_{pl} as the pressure on the rounded area of the cutting edge. This leads to a force loading, where the material in front of the cutting edge is pressed into both the chip and the material surface (WYEN 2011). The material pressed into the newly formed surface leads to residual compressive stresses, which in turn can lead to shape defects due to deformation if the workpiece shape is not sufficiently rigid (ALBRECHT 1960). ALBRECHT (1960) presented an adaptation of the force diagrams proposed by MERCHANT (1945), which is shown in Figure 2-11.

ALBRECHT (1960) determined that the amount of the ploughed material depends on the size of the cutting-edge radius r_β and that the total force increases linearly with the feed per tooth f_z as soon as the surface of the cutting edge is fully engaged. However, the ploughing force F_{pl} remains constant with increasing feed per tooth and the friction angle is independent of the uncut chip thickness h (ALBRECHT 1960). The ploughing force F_{pl} can thus be determined by extrapolating the forces to an uncut chip thickness h of zero. For this purpose, the model resembles the method proposed by ALTINTAS (2012). The ploughing forces are consequently related to the edge force coefficient k_{ie}.

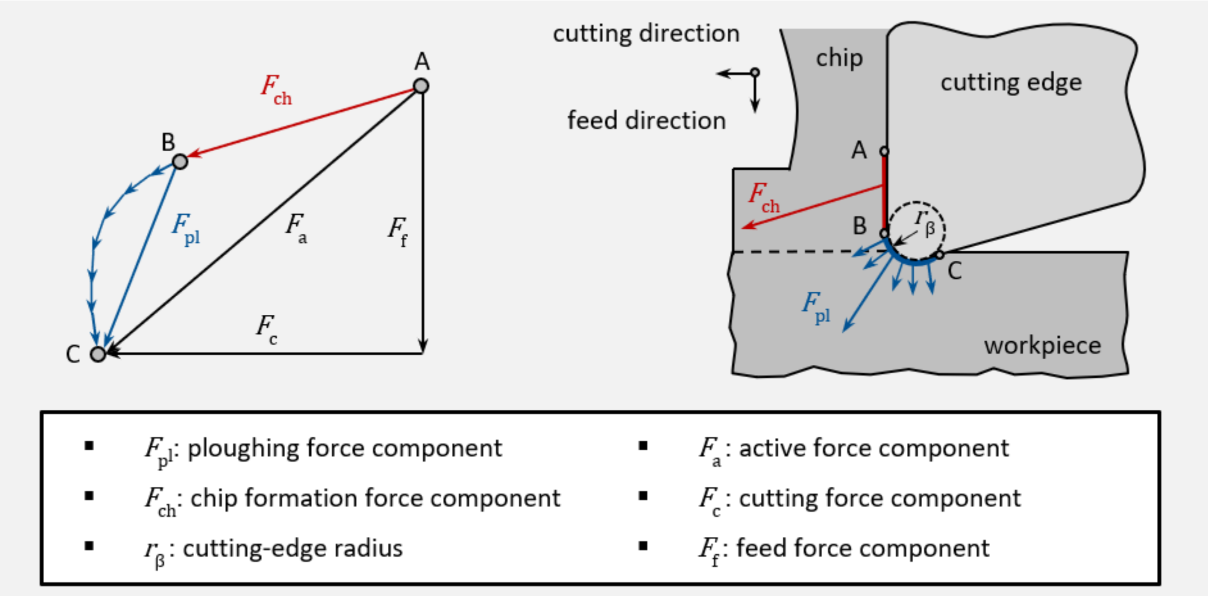

Figure 2-11: Force diagram according to MERCHANT (1945) and ALBRECHT (1960)

WYEN (2011) used a modified Kienzle model to determine the influences of the cutting-edge radius for titanium machining. He described the linear and exponential coefficients k_i and m_i derived from the Kienzle model (equation 2-17) as a function of the cutting-edge radius r_β, the rake angle γ, and the clearance angle α:

$$F_i = k_{i1.1} \cdot b \cdot h^{(1-m_i)} = k^*_{i1.1} \cdot \gamma^{n_{\gamma'}} \cdot \alpha^{n_{\alpha'}} \cdot r_\beta^{n_{r\beta'}} \cdot b \cdot h^{(c \cdot \gamma^{m_{\gamma'}} \cdot \alpha^{m_{\alpha'}} \cdot r_\beta^{m_{r\beta'}})} \qquad (2\text{-}17)$$

The values of the coefficients $k^*_{i1.1}$, $n_{\gamma'}$, $n_{\alpha'}$, $n_{r\beta'}$, $m_{\gamma'}$, $m_{\alpha'}$, $m_{r\beta'}$, and c are obtained by regressing the results of orthogonal experiments. Thus, they are valid only within the investigated range. The model error increases for values of uncut chip thicknesses outside the investigated range. However, this model is only applicable in determining the cutting force F_c and the cutting normal force F_{cN} but not the axial force F_a in multi-axis milling operations, which require the calculation of the passive force component F_p.

2.5 Sub-surface influence by machining processes

2.5.1 Sub-surface and sub-surface properties

The sub-surface critically affects numerous functions and the service life of the machined part (LINSLER ET AL. 2016, BREIDENSTEIN ET AL. 2020). For this reason, individual properties are examined within the scope of downstream material testing, especially in the automotive and aerospace industries, as well as in mechanical engineering.

The term sub-surface properties was first defined by FIELD & KAHLES (1964) as “inherent and extended properties of a surface produced by machining or other surface generating processes.” As shown in Section 2.4, during machining, the material is affected by the thermo-mechanical load, which is dependent on the process variables and the tool geometry. This causes a change in the sub-surface properties. The functionality of a component is significantly dependent on the quality and reliability of the generated surface and thus on the topography, as well as the metallurgical and mechanical condition of the sub-surface (M'SAOUBI ET AL. 2008). Consequently, investigating the interrelationships between the process parameters, their influence on the workpiece sub-surface, and the resulting effects on the component function is becoming increasingly important. FIELD & KAHLES (1971) defined the relationship between the physical properties of a surface and its functional behavior as surface integrity. In machining, the surface integrity depends on thermal, mechanical, and chemical interactions between the tool and the workpiece (BRINKSMEIER ET AL. 1982). The influence of the machining process on the surface integrity includes characteristic phenomena, such as the plastic deformation of the microstructure, the formation of microcracks, phase transformations, hardness variations, and the alteration of residual stresses, as illustrated in Figure 2-12 (JAWAHIR ET AL. 2011).

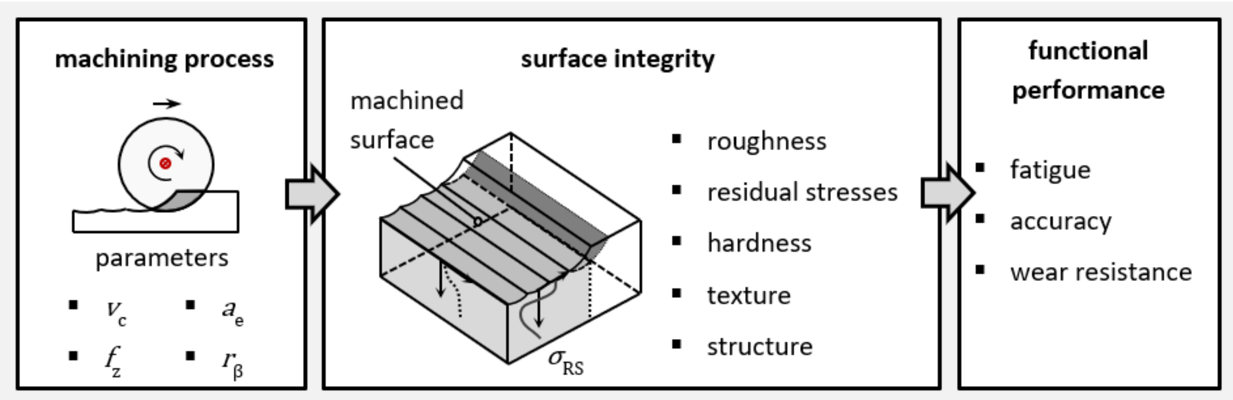

Figure 2-12: The influence of the machining process on the surface integrity and functional performance

Within this work, the microstructure and residual stresses in the material Ti-6Al-4V after the milling process were investigated in detail within the framework of the sub-surface analysis. Consequently, the sub-surface properties are briefly explained below.

2.5.2 Microstructure and deformation of the sub-surface

Metallic materials consist of small grains, which are referred to as the microstructure. This is characterized by the grain size, grain orientation, grain shape, and present phase. Mechanical processing can lead to a change in the microstructure. Changes with regard to the microstructural properties in the sub-surface can be observed during machining, where plastic deformation and the resultant temperatures cause alterations in the residual stress state (BREIDENSTEIN 2011).

2.5.3 Residual stresses

By definition, residual stresses (RS) are mechanical stresses in a solid body where no external forces or moments act, and thus, the internal forces or moments are in equilibrium. Compressive and tensile residual stresses, which are distinct, compensate for each other in a body, and therefore, their sum is zero. In principle, no completely residual stress-free solids exist according to SCHOLTES (1991). Residual stresses occur due to the inhomogeneous distribution of elastic or elastic–plastic deformations, which is called deformation incompatibility. These can be caused by thermal or mechanical workpiece loads or phase transformations. In this context, thermo-mechanical loading can lead to both an increase and a decrease in residual stresses. The mathematical proof of REIßNER (1931) demonstrated that residual stresses can be described by an infinite number of stress sources. Therefore, the residual stresses of multi-crystalline metallic materials are not classified by stress sources but according to related objects in a material volume into 1st (Type I), 2nd (Type II), and 3rd (Type III) order type residual stresses (MACHERAUCH ET AL. 1973). These are shown in Figure 2-13a for the example of a two-phase structure, such as Ti-6Al-4V.

The residual stresses σ_{RS} of the 1st type, which are the cause of macroscopic shape-changes, are obtained by averaging a suitable number of grains. They are therefore referred to as macro-residual stresses. The 2nd type residual stresses involve individual grains in the crystal, whereas 3rd type residual stresses are the result of lattice defects. The last two are called micro-residual stresses. For the evaluation of technical components, the residual stresses of the 1st type are relevant, as they significantly influence the component properties.

In the following, the residual stresses of the 1st type will be considered in more detail. These can be described mathematically as a vector in 3-dimensional space in relation to a surface and are described in the uniaxial case by dividing the applied force by the surface. However, this simplified mathematical description does not apply to every point in the body. If the stress vector and the surface are not perpendicular to each other, normal and tangential components result (shown in Figure 2-13b).

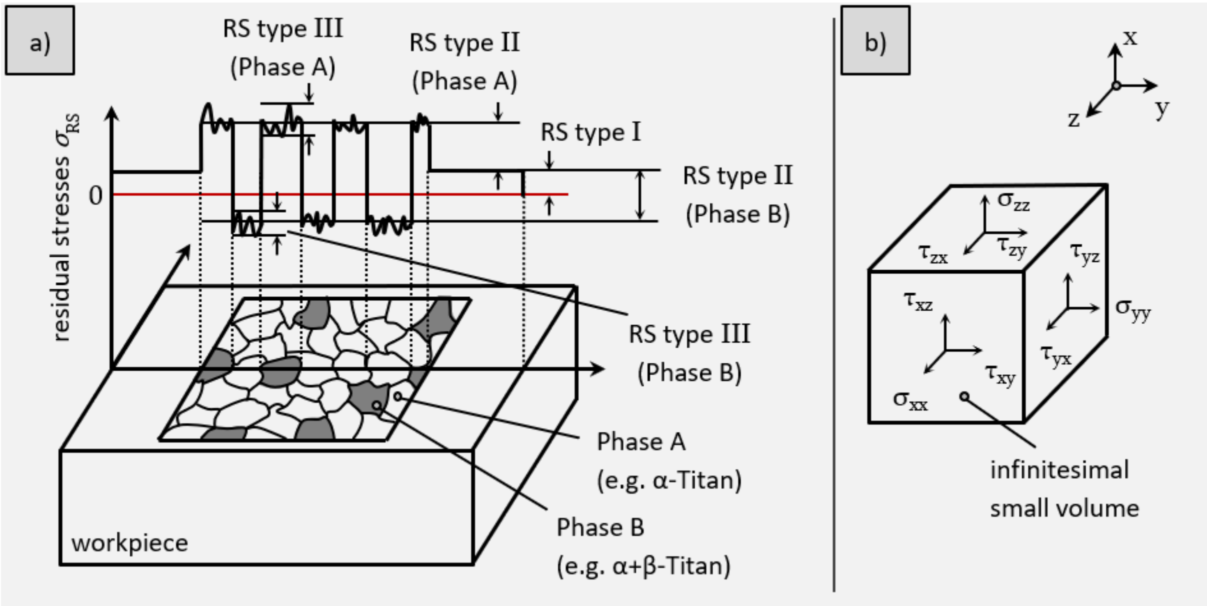

Figure 2-13: Schematic of the residual stresses of the 1st, 2nd and 3rd type in a two-phase material according to SCHOLTES (1991)

Therefore, it is necessary to divide the stresses into normal and tangential components, depending on the selected reference system. An unambiguous description of the stress state in any point of a body is possible with the stress tensor $\boldsymbol{\sigma}$, which consists of the shear stress components τ_{ij} and the normal stress components σ_{ij}:

$$\boldsymbol{\sigma} = \sigma_{ij} = \begin{bmatrix} \sigma_{xx} & \tau_{xy} & \tau_{xz} \\ \tau_{yx} & \sigma_{yy} & \tau_{yz} \\ \tau_{zx} & \tau_{zy} & \sigma_{zz} \end{bmatrix} \tag{2-18}$$

Due to the rigid body condition, the matrix is symmetric ($\tau_{ij} = \tau_{ji}$), which uniquely describes the stress tensor $\boldsymbol{\sigma}$ by using only six independent components. The mathematical object tensor can be interpreted here as an operator for linking any two vectors in space so that a force vector is spatially completely described by $\vec{F} = \sigma \cdot \vec{A}$.

The residual stress state is often considered as one of the essential parameters in the evaluation of surface integrity related to machining processes, as it has a direct effect on the fatigue life of a machined component (MOHAMMADPOUR ET AL. 2010). This has been demonstrated in numerous studies (KOSTER ET AL. 1970, MATSUMOTO ET AL. 1991, LIU & MITTAL 1998, YANG & LIU 2002b, YANG & LIU 2002a, YANG ET AL. 2002, KLEIN & EIFLER 2010, M. KLEIN ET AL. 2011). The residual stresses present in the sub-surface have a decisive role in the use of a component, as they determine the average service life and its fluctuations. Tensile residual stresses at the surface of the component have a prominent negative effect on the service life. Knowledge of the residual stress development is therefore important for correctly predicting the fatigue life.

2.5.4 Residual stress change due to thermo-mechanical loading

During cutting, the generated surface is affected by both mechanical and thermal loads, which leads to a change in the residual stress state of the component sub-surface. The magnitude and depth of the effect depend to a large extent on the process parameters. The thermal and mechanical workpiece loads occur simultaneously during machining. Due to the complex superposition, the two mechanisms cannot be separated (BREIDENSTEIN 2011). To characterize the resulting residual stresses, JACOBUS ET AL. (2000) introduced a mathematical model that describes the general shape of a residual stress depth curve. Here, the sub-surface of the workpiece is divided into regions where direct mechanical effects act deeper in the workpiece than the direct thermal effects near the surface.

SCHOOP ET AL. (2022) adopted this schematic model and explained the thermo-mechanical workpiece load acting during the cutting process in the contact zone between the cutting edge and the workpiece by a separate representation of the effects. Here, the thermal and mechanical effects are present simultaneously in a machined component but act on different length scales and lead to different domains, as schematized in Figure 2-14.

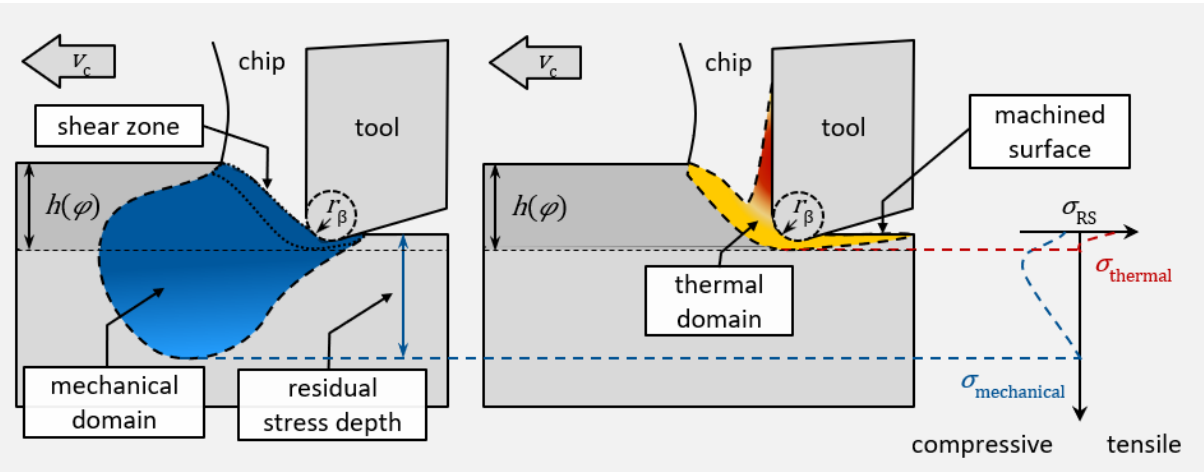

Figure 2-14: Schematic of the mechanical and thermal effects on the residual stress formation and the relative extent of the mechanical and the thermal domain residual stress contributions according to SCHOOP ET AL. (2022)

Mechanical effects

Purely mechanically induced residual stresses $\sigma_{mechanical}$ result from direct mechanical effects that plastically deform the material microstructure. During machining, the material is stretched due to the contact between the tool cutting edge and the material. This results in three different deformation zones (cf. Figure 2-3) (IMBROGNO ET AL. 2018, WAN ET AL. 2019). The highest shear strains occur in the primary shear zone. The severe deformation in the primary shear zone, in combination with friction and ploughing effects in the tertiary shear zone, leads to a strongly plastically deformed layer. The plastic deformation of the material structure results in residual stress curves in the compressive residual stress range. These can be slightly shifted in the tensile direction by indirect thermal effects. An example of a process incorporating the mechanical effect is shot peening, which induces purely mechanical residual stresses (SCHULZE 2003). Direct thermal effects at the surface are negligible in this case.

Thermal effects

In addition to the mechanically induced load, cutting temperatures increase during machining. These result from the plastic deformation of the material in the primary shear zone and the friction at the secondary and tertiary shear zone (LIAO ET AL. 2019, KRYZHANIVSKYY ET AL. 2019). The local or global heating of the workpiece with subsequent cooling can lead to direct thermal effects. These cause local material expansion and resulting deformation compatibilities and generate thermally induced residual stresses σ_{thermal} in the tensile region.

Thermo-mechanical workpiece load

During machining, a combination of thermal and mechanical effects occurs. As a result of this, both compressive and tensile residual stresses are present. The thermal effects usually occur in the layers closer to the surface, whereas the mechanical effects reach deeper into the material. When the maximum residual stresses from thermal mechanisms are larger than those from the mechanical effects, the residual stress depth curve exhibits more positive values at the machined surface. Subsequently, in the depth direction, a global minimum is reached, which corresponds to the peak compressive residual stresses, followed by a decreasing tendency toward the initial residual stress value of the bulk material. As a result, the residual stress value at the surface is either in the tensile or compressive range, depending on the machining process, the workpiece material, the tool geometry, and the cutting parameters selected. Tensile residual stresses in this case provoke the formation and propagation of fatigue cracks and are therefore disadvantageous. However, if the amount of compressive residual stresses is higher than the tensile residual stresses, purely compressive residual stresses are induced.

Consequently, residual stresses are always a result of the superposition of mechanical and thermal effects. These can be dominant or negligible, which tends to be dependent on the resulting residual stress curve after the machining process (BREIDENSTEIN 2011).

2.6 Methods for modeling residual stresses

2.6.1 Overview

In the last 20 years, the modeling of the residual stress state in the sub-surface has garnered increasing scientific attention This is due to the prominent influence of residual stresses on the component service life and the increased need for virtual optimization of machining processes. Numerous modeling methods are available for determining residual stresses, which are summarized and evaluated in the following. In this context, it is possible to distinguish between

- empirical models,
- analytical models,
- numerical model, and
- hybrid models.

2.6.2 Empirical models

Empirical models representing the correlation of input variables, such as the process parameters, with the machining-induced residual stresses, are used to describe cause–effect relationships. In most cases, the physical effects are not considered. This modeling method is suitable for a fast and reliable prediction of complex interrelationships. However, the results are only valid within the investigated parameter range and are usually not transferable to other processes. For a suitable regression, statistical methods for the choice of the experimental space are used, which are summarized under the term Design of Experiments (DoE), and subsequent evaluation is carried out. This type of modeling was used, for example, by AXINTE & DEWES (2002) for ball-end milling of X40CrMoV5-1, by EL-KHABEERY & FATTOUH (1989) for face milling, and by EL-AXIR (2002) for orthogonal turning of different materials.

2.6.3 Analytical models

Analytical models use physical input variables, such as process forces and temperatures, to mathematically describe the generation of residual stresses and thus reduce the experimental effort. Due to the high number of variables in the machining process, the analytical formulation is usually simplified by setting boundary conditions. One simplification is, for example, the consideration of an orthogonal process. An example for this is the modeling of residual stresses by using the Hertz equations for mechanical loads or moving heat sources according to, for instance, JAEGER (1943), whose respective input variables were formulated based on the machining process. For the orthogonal process, JACOBUS ET AL. (2000), LAZOGLU ET AL. (2008), and LIANG & SU (2007), among others, were able to predict the residual stress depth curves after machining of different materials. For milling operations, the analytical determination of residual stresses has been limited so far. This is shown, for example, by the approach of SU (2006) for orthogonal grooving, which was later transferred to flank or face milling of Ti-6Al-4V by SU ET AL. (2013). However, the predictions by SU ET AL. (2013) agreed only qualitatively with the measured data. Another drawback is that material changes, such as microstructural changes due to plastic deformation, are currently not represented by analytical models (JAWAHIR ET AL. 2011). Analytical models have the advantage of a short computation time.

2.6.4 Numerical models

Parallel to the development of analytical models for determining residual stress generation in the sub-surface region during machining processes, considerable progress has been made in the further development of **numerical models** within the last decades (JAWAHIR ET AL. 2011). Using these, the chip formation during the cutting process is usually simulated by the finite element method (FEM) (MARKOPOULOS 2013). The method is applied for the orthogonal process in most cases. Here, the workpiece and the tool are discretized and the stresses and strains at the nodes of the elements are calculated. Compared to empirical and analytical models, this requires a high computational time. Additionally, FE chip formation simulations in numerical models require different input variables, such as a suitable material model and the modeling of the friction as well as the separation and chip breaking criterion in the Lagrange approach. The used input variables exert a significant influence on the resulting residual stresses. In this context, the empirical material model according to Johnson and Cook is most frequently implemented in the FE simulation for machining (JOHNSON & COOK 1983). In addition, according to FILICE ET AL. (2007), the simulated heat flow between the tool, the chip, and the workpiece is dependent on the friction modeling, which also exerts an influence on the residual stress calculation (LIU & GUO 2000). The separation criterion, which defines the material separation at the cutting edge, influences the prediction of the sub-surface properties (EE ET AL. 2005). In addition, the chip breaking criterion defines the tool wear and shear chip formation, which also influences the residual stress prediction (CHEN ET AL. 2004).

2.6.5 Hybrid models

Hybrid models combine the advantages of the previously mentioned approaches. LEÓN GARCÍA (2009), for example, used a semi-analytical model to predict the residual stresses. The incremental cutting force was used as a physical input variable and correlated with measured values of the residual stress curve. In addition, FE simulation without chip formation was combined with an analytical cutting force and temperature model for the orthogonal cut by OKUSHIMA & KAKINO (1972). They proved that tensile residual stresses are correlated with the angle of incidence of the mechanical ploughing forces. This approach was further developed by VALIORGUE ET AL. (2007) in terms of the analytical equations for the orthogonal machining of X2CrNiMo17-12-2 (1.4404, AISI 316L) steel and subsequently applied to external longitudinal turning (VALIORGUE ET AL. 2012). The method of GUILLEMOT ET AL. (2011) combines an analytical description and an FE machining simulation of bainitic steel 25MnCrSiVB6 (1.5233). In this work, ball-end milling was simplified as an oblique cut, and the thermo-mechanical workpiece load was calculated to determine the local residual stresses.

2.7 Concluding remarks

In this chapter, the fundamental principles underlying the machining of titanium alloys, particularly Ti-6Al-4V, were thoroughly presented. Section 2.2 discussed the classification and material microstructure of Ti-6Al-4V, emphasizing the material's unique properties, such as its high strength and low thermal conductivity, which pose significant challenges in terms of machinability. These material characteristics were analyzed in relation to their impact on tool wear and the machining performance. In Section 2.3, the basics of metal cutting were explored, focusing on the chip formation mechanisms, process forces, and the influence of the tool geometry on the cutting process. A detailed analysis of the engagement conditions and the thermo-mechanical interactions between the tool and the workpiece was provided, underscoring the importance of the cutting-edge geometry in achieving desired surface qualities and minimizing tool wear. Section 2.4 explained the process variables in machining, with particular attention to the thermal loads and process forces, and the influence of rounded cutting edges on these forces. Section 2.5 focused on the effects of machining on the sub-surface, discussing the microstructural changes, the deformations, and the residual stresses induced during the process. The chapter highlighted the importance of managing residual stresses to maintain the integrity and functional performance of the machined components. Finally, Section 2.6 reviewed the different modeling approaches used to calculate residual stresses, including empirical, analytical, numerical, and hybrid models, emphasizing their utility in optimizing machining processes. The fundamentals presented in Sections 2.2 to 2.6 provide a comprehensive understanding of the key factors that influence the machining process and the residual stress distribution during the milling of Ti-6Al-4V. These principles form the basis for the subsequent discussion in Chapter 3, where the state of the art regarding residual stress changes during machining of titanium and modeling of residual stresses in Ti-6Al-4V machining is explained.

3 State of the Art

3.1 Chapter overview

As described in Section 2.6, several experimental works and modeling methods have been dedicated to determining the effect of different metal-cutting processes on the machining-induced residual stress state in the sub-surface of Ti-6Al-4V. Chapter 3 offers an overview of the state of the art concerning the relationship between the machining process and the resulting residual stresses in the titanium alloy Ti-6Al-4V specifically. Section 3.2 focuses on the influence of the process parameters and the microgeometry of the tool. In Section 3.3, separate approaches for modeling the residual stress state are provided, whereas in Section 3.4, the state of the art is summarized, and the need for action is derived. Throughout Chapter 3, recent advances in the modeling of residual stresses in different metal-cutting processes are discussed, although the scope of this dissertation is confined to peripheral milling.

3.2 Residual stresses after machining titanium

3.2.1 General findings

Material-specific findings: During the machining process, a change in the residual stress state in the sub-surface can be caused by mechanical lattice deformations, thermal influences, or phase transformations (BRINKSMEIER 1982). Phase transformations caused by Ti-6Al-4V machining have been excluded for orthogonal grooving (VELÁSQUEZ ET AL. 2010) and end milling (SUN & GUO 2009) as a cause for the residual stress change. Furthermore, mechanical effects are primarily responsible for the residual stress change during the machining of Ti-6Al-4V (FRANZ 1979, GEY 2003, SUN & GUO 2009). The low thermal conductivity of titanium is considered to be the reason for this effect, which inhibits effective heat dissipation during machining. As a result, most of the energy from the cutting process is absorbed by mechanical deformation, leading to the development of mechanical residual stresses. This was experimentally confirmed by NESPOR (2015). As shown by laser experiments, he determined tensile stresses occur on the surface at a critical temperature of 480 °C. This temperature was not exceeded for any combination of the process parameters during the ball-end milling of Ti-6Al-4V, which led to the formation of compressive residual stresses. A negative residual stress state in the sub-surface was also demonstrated for other machining processes of Ti-6Al-4V (FRANZ 1979, NARUTAKI ET AL. 1983, M'SAOUBI ET AL. 2008, YANG ET AL. 2019, YANG ET AL. 2016, NESPOR 2015). The findings on the phase transformation by experimental investigations of the microstructure after machining and the occurrence of compressive residual stresses are the only correlations that can be comprehensively obtained from the literature.

Up- and down-milling: NESPOR (2015) demonstrated that the process strategy (up- and down-milling) has a minor influence on the resulting residual stresses in the ball-end milling of Ti-6Al-4V. On the contrary, WYEN ET AL. (2013) and FRANZ (1979) investigated face milling and peripheral milling and observed that the process strategy significantly influences the residual stress state.

Process kinematics and tool geometry: The change in the residual stress state due to the machining of Ti-6Al-4V was conducted for different metal-cutting processes and thus for various process kinematics. In this context, the studies on different turning processes of titanium, such as the investigations by ÖZEL & ULUTAN (2012) on facing turning, by NARUTAKI ET AL. (1983) on external longitudinal turning, by VELÁSQUEZ ET AL. (2010), and by ABBOUD (2015) on orthogonal grooving, demonstrate contradictory results. A direct comparison of the investigations on the residual stress variation is therefore not possible across different machining processes due to the varying process kinematics and the difference in the tool macro- and microgeometry as well as varying ranges of the process parameters. The contradictory results on machining-induced residual stresses were summarized by ULUTAN & ÖZEL (2011) in their keynote paper on the sub-surface properties of titanium and nickel-based alloys.

3.2.2 Effect of the process parameters on the residual stresses

Feed velocity: The influence of the process parameter feed velocity or feed per tooth f_z on the machining-induced residual stresses of the sub-surface has been qualitatively evaluated as the most important in the literature across all processes. The feed per tooth f_z defines the maximum chip thickness h_{max}, which has a direct effect on surface generation (TÖNSHOFF 1966). CAPELLO (2005), SASAHARA ET AL. (2004), TÖNSHOFF (1966), and M'SAOUBI ET AL. (1999) demonstrated that an increase in the chip thickness h or the feed per tooth f_z leads to a shift in the residual stresses in the tensile direction. YANG ET AL. (2019), MAIß ET AL. (2012), and YANG ET AL. (2016) confirmed this effect in their experimental studies on the peripheral milling of Ti-6Al-4V. NESPOR (2015) demonstrated a significant influence of the feed per tooth on the resulting residual stresses in the ball-end milling of Ti-6Al-4V. When the feed per tooth was changed in the range from 0.02 to 0.5 mm, the compressive residual stresses decreased by approximately 40 MPa.

ZANGER (2013) investigated the influence of the feed velocity during orthogonal turning of Ti-6Al-4V. The residual stress depth curves were all in the compressive residual stress range, which hardly varied with a change in the feed velocity. He observed an increase in the depth of residual stresses with increasing chip thickness, which he attributed to the higher mechanical load. MAIß ET AL. (2012) only observed a small change in residual stresses at the surface during face milling when the feed velocity was increased. They obtained the same results when considering the peripheral milling process.

RAO ET AL. (2011) observed an increase in compressive residual stresses at higher feeds per tooth during the face milling of Ti-6Al-4V. They attributed this to reduced friction between the tool and the material. Furthermore, ABBOUD (2015) observed a similar relationship, when the residual stresses for feed velocities in the range of 0.05–0.25 mm/rev during external longitudinal turning were investigated. YANG ET AL. (2019) investigated the peripheral milling of Ti-6Al-4V and found that when the feed per tooth was increased from 0.02 to 0.04 mm, the residual compressive stresses decreased.

Cutting speed: The residual stress change caused by the variation in the cutting speed during milling has been investigated by FRANZ (1979), GEY (2003), SUN & GUO (2009), and RAO ET AL. (2011), for example, but the results have been contradictory.

When the cutting speed v_c was increased, a shift of the surface residual stresses in the direction of tension was observed in most investigations, which is explained, among other things, by the increased heat input (GEY 2003, M'SAOUBI ET AL. 2008, OUTEIRO ET AL. 2006). In this context, ABBOUD (2015) observed a reduction in the surface compressive residual stresses during the external longitudinal turning of Ti-6Al-4V when the cutting speed was increased from 20 to 90 m/min. He attributed this to the temperature increase due to the change in the cutting speed. YANG & LIU (2018) and YANG ET AL. (2019) observed a decrease in compressive residual stresses when increasing the cutting speed v_c during the peripheral milling of Ti-6Al-4V. They investigated the 20–110 m/min range. This was confirmed by MADYIRA ET AL. (2013), who studied the turning process of Ti-6Al-4V. They found that the compressive residual stresses decreased significantly when the cutting speed was increased.

SUN & GUO (2009) reported contradictory results: they observed a shift in the residual stresses toward tensile stresses when the cutting speed v_c was reduced. During the face milling of Ti-6Al-4V, MAIß ET AL. (2012) observed an increase in compressive residual stresses with increasing cutting speed. Accordingly, the residual stress values at the surface varied only slightly, whereas the values deeper in the sub-surface exhibited significant differences.

They also investigated the peripheral milling process and found a reduction in the tensile residual stresses at higher cutting speeds.

RAO ET AL. (2011) did not observe any of these influences and attributed this to face milling by the secondary cutting edge, which significantly generated the surface and thus resulted in a lower heat input into the workpiece. YANG ET AL. (2012) investigated the high-speed milling of Ti-6Al-4V and found a small effect of the cutting speed in the range of 80–140 m/min on the machining-induced residual stresses. Even at high cutting speeds, high residual compressive stresses were observed. Furthermore, NESPOR (2015) reported no significant change in residual stresses for ball-end milling of Ti-6Al-4V when the cutting speed v_c was changed between 15 and 60 m/min. This is attributed to the low influence of thermal effects on the residual stresses when machining titanium alloys. In addition, he clarified that the forces generating the final surface are only slightly influenced by the cutting speed. Additionally, ÖZEL & ULUTAN (2012) investigated the influence of the cutting speed during the face turning of Ti-6Al-4V for differently coated tools. Independent of the coating, no significant change in residual stresses was found when the cutting speed v_c was changed between 55 and 90 m/min.

Depth of cut: In different investigations, the radial depth of cut a_e, respectively the axial depth of cut a_p, had no or only little influence on the residual stresses in the various processes including longitudinal turning, face turning, and milling. The explanatory approaches of LEÓN GARCÍA (2009) or SASAHARA ET AL. (2004), for example, are analogous to those of TÖNSHOFF (1966), as these parameters do not influence the generation of the final surface. This was confirmed by NESPOR (2015), who investigated the influence of the depth of cut on the residual stresses in the ball-end milling of Ti-6Al-4V and detected no significant influence. He attributed this to the final surface being indirectly influenced by the choice of the cutting depth. Furthermore, YANG ET AL. (2019) could not find any significant change in residual stresses during the peripheral milling of the titanium alloy Ti-6Al-4V at radial depths of cut ranging from 0.5 to 2.0 mm. Only MADYIRA ET AL. (2013) were able to detect a reduction in compressive residual stresses on the surface at lower depths of cut during turning.

3.2.3 Effect of the cutting-edge radius on the residual stresses

Cutting-edge radius: The cutting-edge rounding r_β significantly influences the residual stresses after machining both with respect to the material and the process (DENKENA ET AL. 2014). This has been demonstrated several times in the literature, among others, by LEÓN GARCÍA (2009) in the face milling of aluminum 7449, MATSUMOTO ET AL. (1999) in the external hard turning of 100Cr6, and JACOBUS ET AL. (2000) in the orthogonal turning of

40NiCrMo6. This is due to the so-called ploughing effect, where the material is not separated but quenched under the cutting-edge rounding. This leads to microstructural plastic deformations, which have been demonstrated by KACZMAREK (1966), for example, by hardness changes in the sub-surface. Consequently, the cutting-edge radius r_β has a significant influence on the resulting residual stresses across the processes including external turning (SASAHARA ET AL. 2004, CAPELLO 2005) and face milling (LEÓN GARCÍA 2009).

ULUTAN & ÖZEL (2011) observed that the influence of the tool microgeometry during the machining of titanium is still unexplored. In this regard, no studies have considered the influence of different cutting-edge roundings on the machining-induced residual stresses during the peripheral milling of Ti-6Al-4V yet. NESPOR (2015) investigated the influence of the cutting-edge radius on the resulting residual stress profiles in ball-end milling of Ti-6Al-4V. An increase in the cutting-edge radius between 5 and 60 µm resulted in an increase in the compressive residual stresses. ÖZEL & ULUTAN (2012) observed contrary results when face turning Ti-6Al-4V, where slightly higher compressive residual stresses were induced using larger cutting-edge radii. Notably, different coatings were used, making a comparison difficult.

ABBOUD (2015) observed contrary results when investigating the influence of the cutting-edge rounding during the external longitudinal turning of Ti-6Al-4V by varying the cutting-edge radius between 10 and 60 µm. His experiments showed that larger cutting-edge roundings resulted in lower compressive residual stresses at the surface of the component. In this case, the compressive residual stresses were reduced by 60 %.

WYEN ET AL. (2013) investigated the influence of cutting-edge rounding during the face milling of Ti-6Al-4V. They found that the residual compressive stresses on the surface parallel to the feed direction decreased for larger cutting-edge radii. The residual compressive stresses perpendicular to the feed direction increased using cutting-edge radii between 6 and 50 µm.

3.3 Modeling of residual stresses in Ti-6Al-4V machining

This section focuses specifically on Ti-6Al-4V, as its unique properties, including the low thermal conductivity and the high strength, result in distinct thermal and mechanical loads during machining. Direct comparison with residual stress models for other materials is impractical because the assumptions, input parameters, and boundary conditions are material-specific. The responses of Ti-6Al-4V to machining-induced deformation and heat differ significantly from those of other materials, requiring tailored modeling strategies to capture its unique behavior accurately. The modeling methods for residual stresses induced in the sub-surface by the machining process for Ti-6Al-4V can be divided into three categories: Numerical, empirical and analytical.

3.3.1 Numerical simulation of the machining process

In the last decades, significant progress has been made in the numerical modeling of surface integrity. This is due to the continuously increasing computing capabilities. A physically based (numerical) calculation of the resulting residual stresses includes the simulation of the entire chip-formation-process. In addition to a detailed description of the contact conditions, an appropriate formulation of the elastic-viscoplastic material behavior is required, in particular for the temperature- and strain rate-dependence. In this context, the use of more complex material-behavior-models that represent variations in the yield stress with the strain, the strain rate, and the temperature allow a comprehensive prediction of the surface integrity. In addition, numerical modeling approaches are capable of enabling the creation of specialized "user subroutines" that can include submodels to capture complex phenomena such as phase transformations and dynamic recrystallization in the sub-surface.

Thermo-mechanical finite element models, which are numerically complex, allow a detailed representation of numerous phenomena (e.g., the contact conditions, friction effects, and plastic instabilities in the form of shear bands), which influence the resulting residual stress distribution. The modeling approach requires numerous input parameters or variables with uncertainties, which lead to strong deviations of the simulation results. This was confirmed by JAWAHIR ET AL. (2011), where the finite element method was used to determine the residual stresses after an orthogonal cut of five different materials. A comparison of the simulated results with the measured residual stress profiles of Ti-6Al-4V in the cutting direction demonstrated a deviation of approximately 280 % at the surface. The models were then calibrated based on the cutting forces measured in the process and the morphology of the chip; however, this only slightly improved the simulation results.

ZANGER (2013) considered additional calibration coefficients in his work regarding the numerical simulation of the orthogonal turning of Ti-6Al-4V. He calibrated the FE simulation with the experimentally determined process forces, friction coefficients, chip temperature, and chip shape. The residual stress state was influenced by the cutting speed v_c and the chip thickness h. Different cutting-edge radii demonstrated no effect, which is contrary to the findings in the literature. The investigations conducted in this context were purely simulative.

Chip formation, the temperature in the sub-surface region, and the stress distributions during the machining of the titanium alloy Ti-6Al-4V have been investigated with numerical models (CHEN ET AL. 2004, ÖZEL ET AL. 2010, CALAMAZ ET AL. 2011, SIMA & ÖZEL 2010).

CHEN ET AL. (2004) performed residual stress predictions with the FE software ABAQUS using the Johnson–Cook model. They employed a damage model to represent the chip segmentation. This improved the prediction of residual stresses.

ÖZEL ET AL. (2010) investigated the use of a modified material model. A temperature-dependent yield softening model for the titanium alloy Ti-6Al-4V was implemented in the simulation. The investigations focused on the effects of tool coatings, the cutting forces, and the temperature field, stresses, and tool wear during segment chip formation using 2D elasto-viscoplastic and 3D viscoplastic simulation models.

ABBOUD ET AL. (2013) used a thermo-mechanically coupled FE model to predict the cutting forces, temperatures, and machining-induced residual stresses during the external longitudinal turning of Ti-6Al-4V. Higher prediction errors were observed at higher cutting speeds, which they attribute to the effect of chip segmentation.

3.3.2 Empirical models

Empirical models correlate the process parameters directly with the resulting residual stress distribution so that physical effects are not considered (ULUTAN ET AL. 2014). The residual stresses are determined experimentally using statistical methods for a specific parameter range and then summarized in an evaluation. Empirical equations or correlations are then derived based on the results of the experiments. The input parameters of the models are usually a combination of the cutting speed, feed rate, cutting depth, and tool geometry. This approach is suitable for efficiently estimating the residual stresses induced in the sub-surface or their characteristic parameters (e.g., the local maximum or the position of the maximum in the depth direction). However, the use of empirical models requires an extensive experimental data base and is only valid for the investigated tool–workpiece combination.

In the literature, different empirical models have been used to predict the residual stresses during metal cutting (CAPELLO 2005, SRIDHAR ET AL. 2003, JACOBUS ET AL. 2000, EL-AXIR 2002). The effects of the cutting speed, feed velocity, depth of cut, and workpiece properties have primarily been studied. The results of the investigations demonstrate that the cutting speed and the feed per tooth have the most significant influence on the residual stresses.

3.3.3 Analytical models

To determine the residual stresses, analytical models use physical input variables such as the temperatures and the cutting forces during the process. In the mostly two-dimensional models, the complete analytical solutions (of the heat conduction problem as well as of the mechanical problem) of the thermo-elastic half-plane are used under various simplifying assumptions and constraints (plane strain state and given distributions of the local heat flux and cutting force distribution at the cutting element). With the help of further hypotheses, the occurring plastic deformations as well as the resulting residual stress distributions can be estimated from the elastic solution. This approach was first proposed for rolling contact modeling and adopted for machining (MERWIN & JOHNSON 1963).

Despite the modeling complexity being considerably lower than that of the numerical simulation of the machining process, these approaches have recently been further developed and now represent a useful methodology in time-critical applications (ULUTAN ET AL. 2007, DA HUANG ET AL. 2018). In the literature, the tool is described using the Hertzian equations for mechanical loads or moving heat sources by, among others, JAEGER (1943) for the modeling of the residual stresses, where the respective input variables are derived from the cutting process. For this purpose, the residual stress depth curves were determined analytically by LAZOGLU ET AL. (2008), LIANG & SU (2007), and JACOBUS ET AL. (2000) for the orthogonal process of different materials.

Regarding the residual stress modeling during the milling process, the possibilities have been limited to date, as demonstrated by the approach of SU (2006) and SU ET AL. (2013) for flank and face milling of Ti-6Al-4V. The residual stress depth curves were predicted based on the analytically determined cutting forces and temperatures. However, the predicted residual stresses agreed only qualitatively with the measurement results.

WAN ET AL. (2017) developed a theoretical model to predict the residual stresses after peripheral milling. Their analytical model describes the internal stresses induced in the workpiece by the mechanical load based on Hertzian contact theory. They used a 3D contact model for the oblique cut to describe the contact conditions between the tool and the workpiece. They divided the load distribution into the force component acting in the shear zone and the ploughing force due to the rounded cutting edge. The coefficient of friction was determined purely analytically. The results of the analytical modeling were validated with the aid of an FEM simulation. The analytical model required four hours to calculate the residual stress curves, whereas the FEM model required two weeks. The theoretical simulation results demonstrate high tensile residual stresses on the surface, which is unusual for milling operations.

3.3.4 Hybrid models

NESPOR (2015) used a hybrid approach to calculate the residual stresses, incorporating an analytical as well as an empirical input from the ball-end milling of Ti-6Al-4V. He determined the depth and the corresponding residual stress value at the global minimum. By combining the empirical data with the analytical equation of the Herztian pressure, the residual stress curves were calculated in good agreement with the measured residual stress depth curves. However, this approach has not yet been applied to the peripheral milling of Ti-6Al-4V.

YANG ET AL. (2016) determined the residual stresses using a combination of FE modeling and statistical methods for peripheral milling of Ti-6Al-4V. A variable chip thickness was assumed in the FE simulation to represent the kinematics of the milling process. The simulated residual stress depth curve was calculated using an exponentially damped cosine function. The study showed a good agreement between the experimental data and the results generated by the hybrid model.

3.4 Conclusion and need for action

Influences of the machining process on the residual stress state

Building on the foundations in Chapter 2, Chapter 3 described the state of the art regarding the residual stresses after machining of Ti-6Al-4V. Section 3.2 provided a comprehensive overview of existing findings regarding the residual stress state after the machining of titanium alloys. Various publications have been issued in this area of research for different machining processes in recent years. During the machining process, a change in the residual stress state in the sub-surface can be caused by thermo-mechanical effects. In addition, it has been demonstrated that mechanical effects are mainly responsible for the residual stress change during the machining of Ti-6Al-4V. This was explained by the low thermal conductivity of the material, which limits the dissipation of heat during machining. Consequently, thermal effects generally have a minor influence. A large part of these research works deals with the influence of the process parameters on the residual stress state (cf. Sub-section 3.2.2). Due to the variation in the process kinematics, the different tool geometries, and the variety of the selected process parameters, the findings on the resulting residual stresses cannot directly be transferred to the peripheral milling process and are even to some extent contradictory. In addition, the effect of the microgeometry of the cutting edge has been studied (cf. Sub-section 3.2.3). The cutting-edge radius significantly influences the resulting residual stresses, independent of the process. The effect of the tool microgeometry on machining of titanium remains unexplored. In addition, there are only a few studies on the influence of the process parameters and the microgeometry, which consider the peripheral milling process.

The influences of the process parameters and the tool microgeometry in terms of the cutting-edge radius $r_β$ are qualitatively summarized in Figure 3-1.

The consensus on machining-induced residual stresses is that they become more tensile or change from compressive to tensile at the surface when the cutting speed v_c, the feed per tooth f_z or the uncut chip thickness h, and the depth or width of cut a_e or a_p are increased, although there is a non-negligible number of researchers claiming the opposite of these findings.

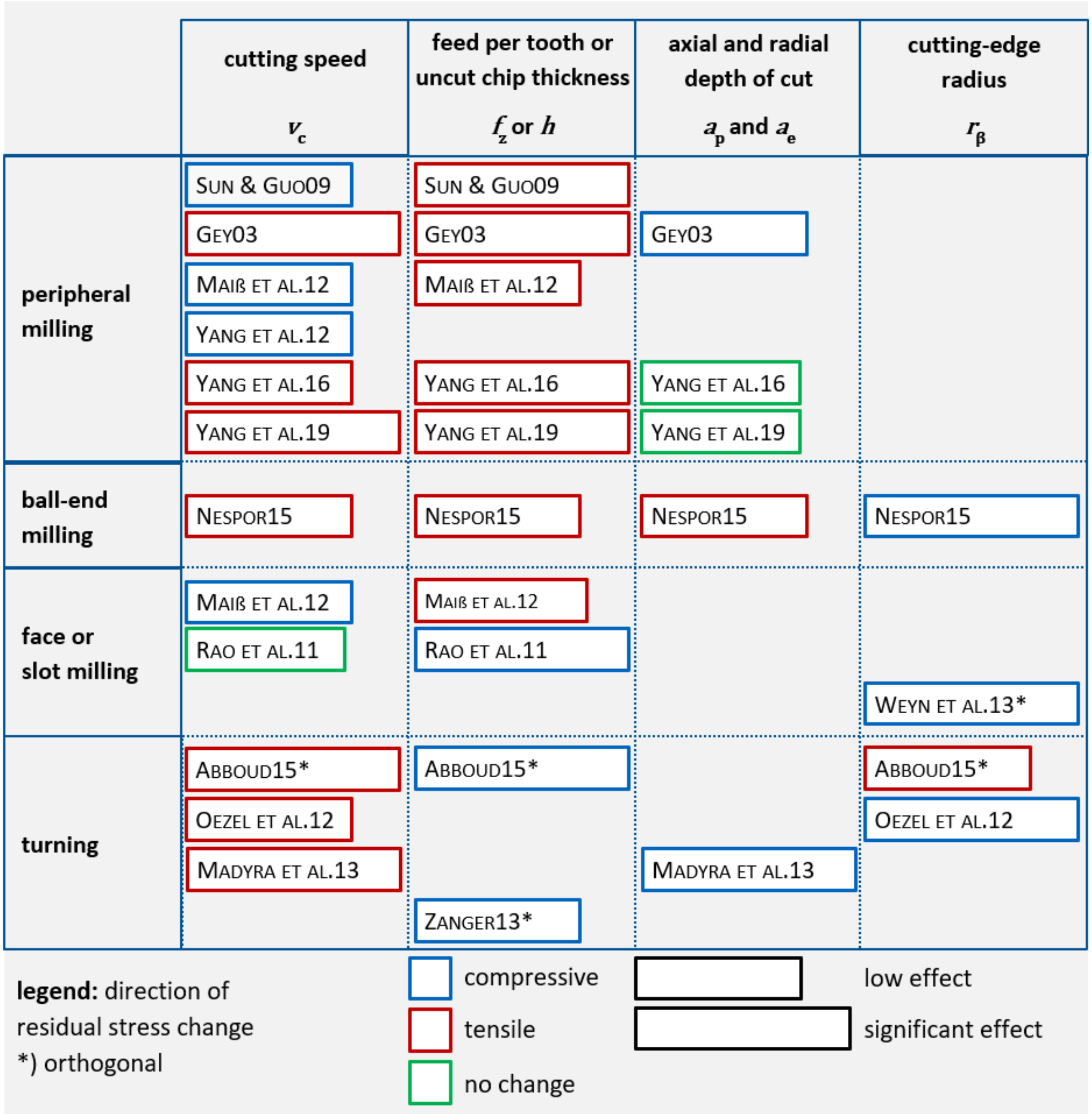

Figure 3-1: The relative influences of the process parameters and the cutting-edge radius on the residual stresses during the machining of Ti-6Al-4V

Residual Stress Modeling

The modeling and simulation of metal-cutting-operations has become very widespread today, with many researchers developing and/or using models to calculate the residual stresses during machining. The effectiveness of these models in predicting the relationship between the metal-cutting process and the resulting residual stress depends to a large extent on the accuracy of the models and the quality of the used input parameters. Section 3.3 focused on the methods of modeling the residual stresses in milling processes.

Empirical models generally offer the possibility of modeling relationships between the process parameters and the resulting residual stresses. In this context, investigations were conducted concerning the residual stress change as a function of the process parameters, the tool geometry, and the tool wear as well as the material properties. The models are suitable for quickly and reliably predicting effects in complex applications. However, the methods lack a physical basis for explaining the mechanisms occuring during machining. Furthermore, empirical models are only valid in the experimentally investigated parameter range and cannot be transferred to other processes or materials.

Numerical simulation approaches, which are mostly based on the finite element method, can be used to determine the resulting residual stresses without conducting experiments. However, FEM-based simulations usually require considerable time. The calculated results are generally close to the experimentally determined residual stresses. The quality of the results is strongly dependent on the material model used, which has to be calibrated experimentally. Therefore, FEM-based simulation models continuously focus on calibrating the parameters of the material constitutive model (commonly the Johnson–Cook material model) or the flow stress data using experimental and simulation results. Using improved material constitutive models and elasto-viscoplastic deformation, detailed simulations of the chip formation and other physical phenomena during machining can be achieved. The disadvantage of numerical modeling approaches is the high computational time required to simulate a short machining time under different machining conditions.

The use of analytical approaches usually requires a simplification of the process. Therefore, there is a risk of the modeling results deviating significantly from the effects that occur during the actual process. In addition, material changes, including microstructural changes due to plastic deformation, cannot be represented by analytical models (JAWAHIR ET AL. 2011). However, analytical models are based on physical principles and can thus reproduce many phenomena better than purely empirical methods. Another advantage of analytical modeling approaches is the computation time being lower than that of numerical simulations.

Hybrid approaches offer considerable potential for determining residual stresses in the peripheral milling of Ti-6Al-4V. They combine the advantages of the individual modeling methods. In this context, for example, the long computation time of numerical models can be considerably reduced. However, up to the writing of this dissertation, no experimentally supported or validated hybrid model existed to describe the residual stress variation due to the peripheral milling process of Ti-6Al-4V.

The prevalent research deficit is summarized below. The following remarks refer to the state of the art at the respective time of the publications issued according to the research findings described in Chapter 6 of this dissertation.

- Few studies describe the effects of the process parameters on the residual stress change for different machining processes. It is known that changes in the process parameters and the microgeometry affect the resulting residual stress state in the sub-surface. However, these influences have not yet been quantified comprehensively for the peripheral milling process.
- The change in residual stresses during machining is caused by thermo-mechanical effects. In the literature, compressive residual stresses in the sub-surface have been demonstrated for different processes after the machining of Ti-6Al-4V, which can be attributed to mechanical effects. For peripheral milling, there is no detailed experimental observation of the occurring forces and temperatures and their relationship with the machining-induced residual stresses.
- The influence of the cutting-edge microgeometry has been investigated by comparatively few studies. Here, the cutting-edge radius was identified as the most considerable variable concerning the residual stress change. However, no comprehensive study has investigated tool wear in the form of the increasing cutting-edge rounding during the peripheral milling of Ti-6Al-4V.
- Several works have considered the modeling of residual stresses for different machining processes. Hybrid method-based simulation models for predicting machining induced residual stress profiles seem to be the most promising research approach, considering the recent advances. No model has considered the influence of the process parameters that affect the resulting residual stresses in the sub-surface. In addition, a simplified 2D geometry of the manufacturing process is usually considered, which means that the peripheral milling process cannot be represented.
- Although some studies have been reported on the effects of the tool edge geometry during the machining of Ti-6Al-4V, the influence of the cutting-edge radius variation on obtaining favorable machining-induced residual stresses has not been explored well.

This dissertation aims to enable the determination of the residual stress state in the sub-surface of Ti-6Al-4V during peripheral milling using a model. The abovementioned unresolved issues define the need for action and provide the basis for the research approach, which is presented in the following chapter and was pursued over the course of this publication-based doctoral thesis.

4 Research Approach

4.1 Chapter Overview

This chapter outlines the scientific objectives of this thesis and the pursued research approach in Chapter 6. Chapter 3 serves as the foundation. In Section 4.2, the scientific objective is initially specified, leading to the derivation of sub-objectives (SO). These sub-objectives constitute the framework for the methodical approach presented in Section 4.3. The integration of the five publications, which form the research core of this work, into the methodology is also provided in this context.

4.2 Scientific objective

The overall objective of this work is to determine the relationship between the process parameters and the process variables affecting the resulting residual stress state during peripheral milling of Ti-6Al-4V. In this context, an optimized choice of the process parameters should lead to the highest possible compressive residual stress state, as the service life of the component can be consequently increased (cf. Section 2.5). In addition, the microgeometry of the cutting edge is expected to have a considerable effect on the machining-induced residual stresses (cf. Sub-section 3.2.3). Depending on the material, the thermo-mechanical workpiece loads that occur during machining and their effects on the sub-surface of Ti-6Al-4V will also be investigated. These interactions are to be experimentally validated and modeled to derive quantitative findings on the machining-induced residual stresses during the peripheral milling of Ti-6Al-4V.

Understanding the residual stress state induced during milling machining would allow effective component-specific design and machining, which would consistently improve part quality in terms of service life. Therefore, this work aims to determine the residual stresses generated during peripheral milling of Ti-6Al-4V workpieces. Four sub-objectives (SO) can be derived, which characterize the need for action identified in the preliminary stages of this work (cf. Section 3.4) and are listed below:

SO1: Identification of the significant influencing variables affecting the residual stress state in the sub-surface

The state of the art indicates that the influencing variables affecting the residual stress state in Ti-6Al-4V during machining are contradictory and not sufficiently known. The investigated values are the process parameters for the peripheral milling process as well as the cutting-edge radius.

SO2: Characterization of the thermo-mechanical load on the sub-surface during the peripheral milling process, considering the significant influencing variables

Measurements of the thermo-mechanical workpiece load during the peripheral milling process with variations in the significant influencing variables are required to predict the machining-induced residual stresses. Accordingly, the fundamental physical effects have to be explained. The aim was therefore to use a sensory tool holder for the in-process measurement of the process forces and temperatures during the milling process. These process variables subsequently serve as input variables for determining the thermo-mechanical workpiece load. The residual stresses can be calculated based on the thermal and mechanical stresses in the sub-surface.

SO3: Determination of the cause–effect relationships between the tool microgeometry and the residual stresses

The microgeometry of the cutting edge influences the resulting residual stress state. For this purpose, models had to be developed that also consider the cutting-edge radius. The microgeometry of the cutting edge has to be calculated to determine the exact contact conditions between the tool and the workpiece. A suitable method which can be used in parallel to the process, has to be identified.

SO4: Determination of the residual stresses in the sub-surface based on the significant process parameters and the tool microgeometry

The physical principles that determine the residual stresses due to the thermo-mechanical load on the workpiece have to be defined. Subsequently, suitable models should be established based on this knowledge and considering the tool microgeometry to reliably calculate the residual stress depth curves.

4.3 Methodology and integration of the publications

This section provides a classification of the publications written during the author's research activities based on their thematic focus with regard to the research objectives formulated in Section 4.2. The classification and the integration of the publications into the methodology are summarized in Figure 4-1, whereas a more detailed description of the core research findings is provided in Section 6.2. The section describes the need for action from a perspective as it existed prior to this research work.

SO1 Experimental study

First, process investigations for peripheral milling of Ti-6Al-4V are required. In this experimental study, the process parameters, which significantly affect the residual stress state, have to be identified. Subsequently, a sensitivity analysis has to be performed to quantify the influence of the individual process parameters. In addition, the effect of different cutting-edge radii on the residual stress state has to be analyzed. Furthermore, the microstructure of the Ti-6Al-4V samples has to be characterized. The results will provide the basis for further investigations. This experimental study is represented in Publication P1 and P2 as part of the methodical procedure shown in Figure 4-1 and addresses SO1, which was introduced in Section 4.2.

SO2 Experimental thermo-mechanical research

Subsequently, experimental investigations of the thermo-mechanical workpiece load during the peripheral milling process have to be conducted. A study using conventional measuring methods and a sensory tool holder to record the temperatures and cutting forces is to be provided. Here the process values are to be investigated by changing the identified significant process parameters. The aim is to determine the relationship between the occurring temperatures and forces and the resulting residual stress state. The relevance of the respective effect is investigated (cf. Subsection 6.2.3). These investigations are presented in the framework of Publication P3 and address SO2.

SO3 Determination of the cutting-edge radius

Publication P4 provides the results that contribute to SO3. The objective is the development of a model to determine the cutting-edge radius during the milling process. For this purpose, investigations regarding the change in the cutting-edge radius during the process have to be conducted. The parameter range of the significant process parameters identified in P1–P3 must be representable in the model. The modeling of the cutting-edge radius and the comparison of the results with experimental measurements have to be executed. The results can extend the knowledge about the change in the cutting-edge microgeometry and the influence on the machining-induced residual stresses during the peripheral milling process. The development of the model discussed above is presented in Publication P4.

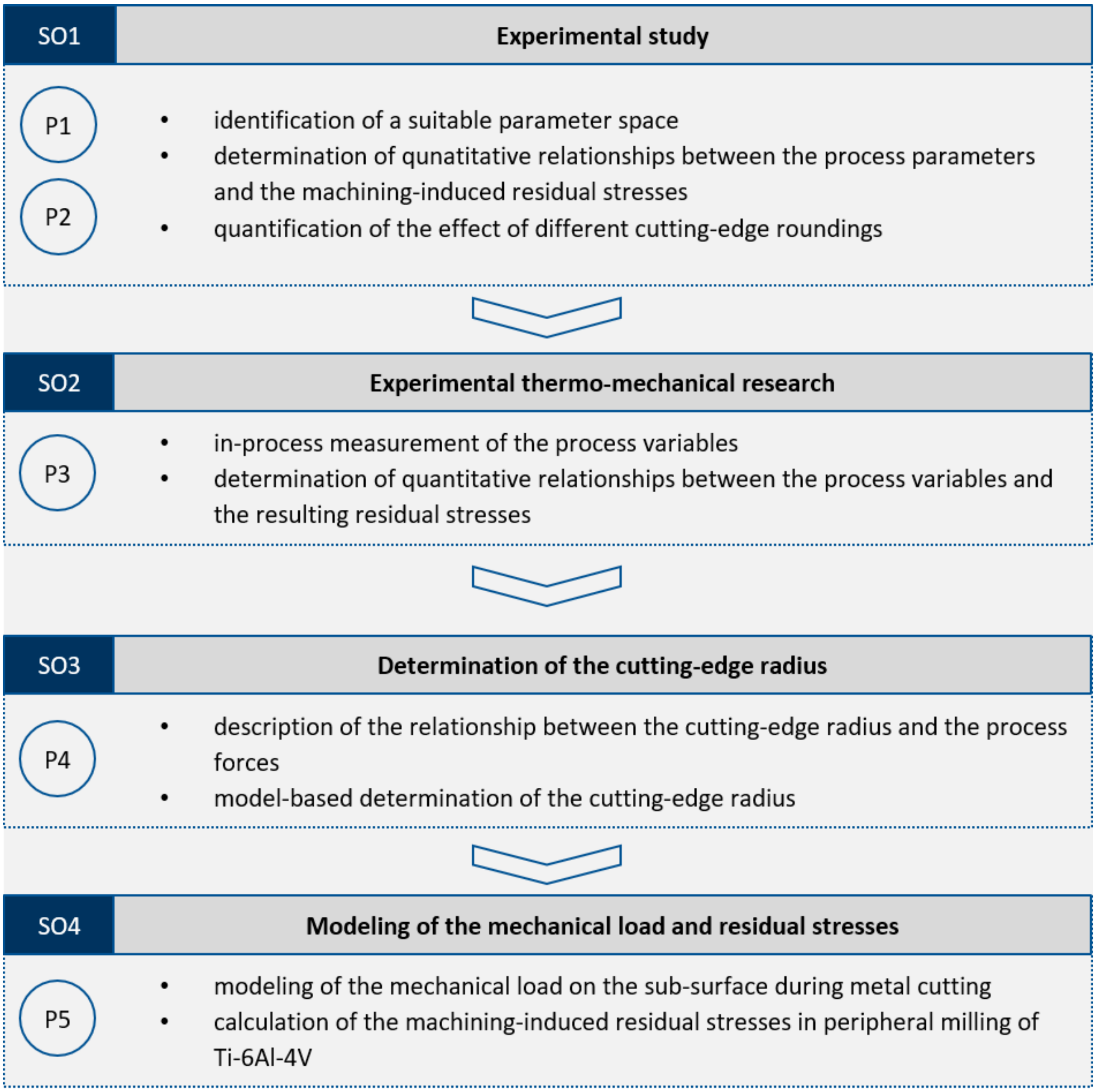

Figure 4-1: The methodical approach and the thematic classification of Publication P1–P5 regarding the sub-objectives (SO) defined in Section 4.2

SO4 Modeling of the mechanical load and the residual stresses

The modeling of the mechanical load on the sub-surface and the remaining residual stress state after peripheral milling is addressed in Publication P5 and contributes to SO4. In this context, an efficient and reliable modeling approach is required to determine the residual stresses. Currently employed empirical, analytical, and numerical modeling methods are usually inaccurate and require a high number of experiments for their calibration and validation (cf. Section 3.4). In addition, most modeling approaches consider only two-dimensional (2D) machining processes (e.g., orthogonal external longitudinal turning). Therefore, a hybrid modeling method must be implemented to calculate the residual stresses due to the 3D peripheral milling process, considering the process kinematics, size effects due to different cutting-edge radii, and the material properties of Ti-6Al-4V. For this purpose, the results from P4 serve as input variables. To calibrate the model, a 2D in-situ test setup is to be used to investigate the cause–effect relationships in the process zone. Digital image correlation (DIC) is to be used to determine the equivalent Hertzian contact length, the contact pressure, and the friction coefficients. The mechanical load on the workpiece is calculated based on these input variables. These measurements are subsequently utilized to determine the plastic deformation in the sub-surface. By geometrically converting the 2D modeling approach to the 3D peripheral milling process, the resulting residual stress state after the machining of Ti-6Al-4V can be determined.

5 Experimental procedure

Experimental machining tests were conducted to determine the significant parameters influencing the surface topography and the residual stresses. The description of the utilized machine technology, material, and tools, as well as the employed sensory tool holder, is provided in this chapter. If the test methods differ, for example in the case of analogy tests, that is described separately in the respective chapter.

5.1 Experimental Setup

Milling Machine

For the experimental milling tests, a five-axis machining center (Grob, type G350T, 2nd generation) was used. The specifications of the machining center are summarized in Figure 5-1.

G350T-5-axis universal mill-turn machining center

axes traverses:
x-/y-/z-axis = 600 x 855 x 750 mm³

motorized spindle:
n_{max} = 16,000 min^{-1}
P_{max} = 32 kW
M_{max} = 206 Nm

tool system:
HSK-A/T63
tool change for 117 tools

NC control:
Siemens 840d

Figure 5-1: Specifications of the 5-axis universal mill-turn machining center Grob G350T

Workpiece

Plates of semi-finished Ti-6Al-4V were used for the experiments. The material was hot rolled according to aerospace standards (Grade 5, material number 3.7164, according to ASM 4911 specified by the manufacturer), vacuum straightened, descaled, pickled, and subsequently stress-relieved to reduce residual stresses. The base material exhibits a purely bimodal α+β-microstructure.

Table 1 lists the chemical composition of the Ti-6Al-4V alloy used in this work according to SPIEß ET AL. (2009). The chemical compositions in Table 1 were verified using energy-dispersive X-ray spectroscopy (EDX) and it turned out that they were within the specified limits. The material properties of Ti-6Al-4V are listed in Table 2 and are based on the findings of SPIEß ET AL. (2009) and ROOS ET AL. (2017).

Table 1: *Chemical composition of Ti-6Al-4V in weight percent (SPIEß ET AL. 2009)*

Ti	Al	V	N	O_2	Fe	C	Rest
> 87.7	5.50 – 6.75	3.50 – 4.50	< 0.05	< 0.20	< 0.40	< 0.08	max. 0.40

Table 2: *Material properties of Ti-6Al-4V (SPIEß ET AL. 2009, ROOS ET AL. 2017)*

Description	Abbreviation	Value	Unit
Modulus of elasticity	E	108	GPa
Yield strength	$R_{p0.2}$	989	MPa
Tensile strength	R_m	1,016	MPa
Thermal conductivity	λ_{Ti}	6.30	W/(mK)
Mean specific heat capacity	c_{pm}	565.2	JK/kg
Mean coefficient of thermal expansion	$\alpha_{T,m}$	8.15	10^{-6}/K
Density	ρ	4,430	kg/m³

Tools

For the experimental investigations according to the incorporated publications in Chapter 6, end-milling tools were used. Their most important characteristics are summarized in Figure 5-2. The tools were mounted in a hydraulic expansion chuck, ensuring minimal runout and excellent clamping stability.

type	solid carbide end mill	number of teeth	$z = 4$
manufacturer	MAPAL	helix angle	$\beta = 40°$
designation	OptiMill-Titan-HPC	clearance angle	$\alpha = 6°$
diameter	$D = 12$ mm	rake angle	$\gamma = 11°$
total lenght	$L_1 = 83$ mm	cutting-edge radius	$r_\beta = 5$ µm
cutting length	$L_2 = 26$ mm	coating	none

Figure 5-2: Used solid carbide end mills

5.2 Test setup for the cutting force measurements

A variety of measuring methods for determining the residual stress state are available, which rely on different physical effects. Most of the measuring techniques cannot be effectively applied during the milling process due to a complex system-technology. Measurement principles based on the ferromagnetic behavior of the material are also unsuitable for Ti-6Al-4V due to its non-ferromagnetic nature.

Therefore, an alternative approach was employed for this work by implementing in-process measurements of the cutting forces using a sensory tool holder. Accordingly, this system was developed and integrated into the experimental setup, as shown in Figure 5-3.

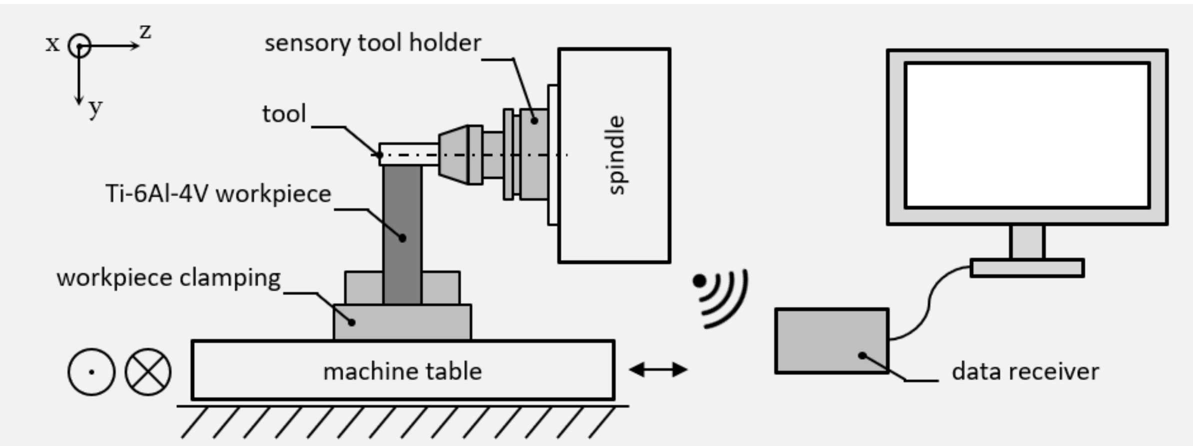

Figure 5-3: Experimental setup using the sensory tool holder for the in-process measurement of the cutting forces based on WIMMER ET AL. (2023)

The tool holder comprises a hydraulic expansion chuck, in which the sensors, the data transmission unit, and the power supply are integrated. Using two strain gauges attached to the tool holder, the applied bending moment on the tool can be measured at two positions.

These measured variables can be converted into the respective process forces during machining. In addition, a strain gauge on the chuck was used to measure the torsional moment applied to the tool shank. The strain gauges require a one-time calibration before measurement. The measured values can be recorded with a sampling rate of approximately 2 kHz and a resolution of up to 12 bits, ensuring high temporal and spatial accuracy for the recorded data.

6 Research Findings

6.1 Chapter overview

Building on the methodological approach presented in Section 4.3, this chapter provides the research findings obtained in the context of this work. The results are presented in the form of short recapitulations of the author's publications. After a summary of each publication, the respective contributions of the authors are briefly explicated. A classification of the core findings in relation to the state of the art is provided in Section 6.3.

6.2 Recapitulation of the embedded publications

6.2.1 P1: “Methodology for a model-based control of the boundary zone properties during milling of Ti-6Al-4V”

In Publication P1, "Methodology for a model-based control of the boundary zone properties during milling of Ti-6Al-4V" (WIMMER ET AL. 2019), the general approach for determining sub-surface properties during milling of Ti-6Al-4V was presented. Initially, the state of the art was analyzed, including the definition of the sub-surface properties and the importance of the residual stress state for the component’s service life. In addition, the mechanisms influencing the residual stresses in the sub-surface due to the machining process were analyzed and described. The influences of the individual process parameters, the microgeometry of the tool, and the thermo-mechanical load on the machining-induced residual stresses were discussed.

Experimental investigations of the peripheral milling process of Ti-6Al-4V were conducted based on the state of the art. The cutting speed v_c, the feed per tooth f_z, and the radial depth of cut a_e were varied in a statistically validated experimental plan. In addition, the influence of varying cutting-edge radii r_β on the residual stresses was analyzed. In the first step, the process variables occurring in the milling process, the cutting forces, and the process temperature were examined, and the employed measuring methods were described. The results indicated that the force component in the y-direction, which is directed perpendicular to the machined surface, possesses the highest value in the peripheral milling process. Furthermore, an analysis of the kinematics of the peripheral milling process revealed that a large portion of the surface generated in a tool revolution is over-milled in the subsequent cutter revolution. As a result, only a small part of the total force contributes to the formation of the final surface. It was found that an increase in the radial depth of cut a_e, the feed per tooth f_z, and the cutting-edge radius r_β led to an increase in the cutting forces. Conversely, lower cutting forces were observed at higher cutting speeds. A maximum temperature of 206 °C was measured using thermocouples positioned in the workpiece 0.01 mm below the machined surface. This occurred at high cutting speeds v_c of 70 m/min in combination with a high cutting-edge radius r_β.

Subsequently, a sensitivity analysis of residual stress measurements obtained via X-ray diffraction was presented. The results demonstrated that the cutting-edge radius r_β and the feed per tooth f_z had the most significant effect on the change in residual stresses in the sub-surface. For instance, increasing the cutting-edge radius r_β from 5.4 to 16.5 µm resulted in a significant increase in compressive residual stresses. Similarly, increasing the feed per tooth f_z from 0.04 to 0.08 mm caused a shift of the residual stresses towards the tensile residual stress range. In contrast, variations in the cutting speed v_c from 30 to 70 m/min and the radial depth of cut a_e from 3 to 6 mm exhibited only minor effects on the residual stress variation.

It was noted that the measured process forces and temperatures cannot be directly utilized to predict the residual stresses, as no explicit correlation between these variables was identified. To describe the relationship between the process variables and the resulting residual stresses, the thermo-mechanical effects within the sub-surface must be characterized. These effects should account for the specific conditions of peripheral milling of Ti-6Al-4V. Existing modeling methods were critically evaluated for this purpose. Different cutting force models were analyzed regarding their suitability for predicting residual stresses during the peripheral milling of Ti-6Al-4V. In addition, modeling approaches capable of representing the entire temperature field or heat flow within the material were reviewed, and the requirements were defined. Furthermore, the limitations of existing modeling strategies were identified.

In the context of Publication P1, the influences of the process parameters and the microgeometry of the cutting edge on the process variables and the resulting residual stresses was systematically analyzed. The process investigations established a foundation for understanding the interaction between the peripheral milling process and the resulting residual stresses in the titanium alloy Ti-6Al-4V. This paper also outlines the implementation of a sensory tool holder to measure the cutting forces and temperatures during the machining process. The measured values are intended for use as inputs in modeling the residual stress state of the sub-surface after machining. The sensory tool holder is described in more detail in Publication P2 and was applied for Publication P4.

Contributions of the authors

Matthias Wimmer, the author of this thesis, developed the idea for the paper concept. He planned the experiments and was responsible for the evaluation of the measurement data. The manuscript was written by Matthias Wimmer and edited by Phillip Rinck, Robin Kleinwort, and Michael F. Zaeh. All authors discussed and commented on the findings. Matthias Wimmer presented the results in a talk at the 15th International Conference on High Speed Machining (HSM) in Prague, Czech Republic, in 2019.

6.2.2 P2: "The influence of the process parameters on the surface integrity during peripheral milling of Ti-6Al-4V"

Publication P2 "The influence of the process parameters on the surface integrity during peripheral milling of Ti-6Al-4V" (WIMMER ET AL. 2020) builds upon the process investigations conducted for P1 to elucidate the modifications in sub-surface properties resulting from the peripheral milling of Ti-6Al-4V. The microstructure of the titanium alloy Ti-6Al-4V was examined and characterized, and the chemical composition of the material, determined through spectrometry, was presented. Furthermore, the changes in the residual stress state induced by thermo-mechanical loads during the milling process were analyzed in more detail. Thermal effects were found to increase tensile residual stresses, whereas mechanical effects primarily generated compressive residual stresses.

In this context, the principle underlying the X-ray diffraction method was thoroughly detailed, and the applied parameters were presented. Additionally, the measurement of residual stresses in the sub-surface was conducted using electrochemical layer-by-layer etching.

Throughout the main section of Publication 2, the process parameters – specifically, the feed per tooth f_z, and the cutting speed v_c – were varied at smaller increments compared to P1. The radial depth of cut a_e was kept constant, as it had no significant influence on the residual stresses, as shown in P1. The measured residual stress curves in the depth direction revealed that the compressive residual stresses in the feed direction were lower than those in the axial direction. The results confirmed the findings from P1, with the residual stresses at the surface in both directions exhibiting slightly higher tensile values. Moreover, the characteristic residual stress profiles showed a distinct zero-crossing point at a depth of approximately 250 µm. Maximum compressive residual stresses at the surface were achieved by combining a low cutting speed v_c with a small feed per tooth f_z.

Additionally, the design and function of the sensory tool holder presented in the approach according to P1 were described in detail. This tool holder, developed in collaboration with MAPAL Dr. Kress KG, Aalen, Germany, enables the in-process measurement of cutting forces and temperatures. It consists of a hydraulic expansion chuck for mounting the cutting tool, with strain gauges integrated at orthogonal orientations (90°) to measure strain, which is subsequently converted into the respective cutting force components. The temperature measurements were conducted using a thermocouple with a diameter of 5 mm, positioned in a centered hole in the rotating tool, with the tip extending to the tool-center-point. The energy supply for the sensory tool holder was provided by a rechargeable battery, and data were transmitted wirelessly at a sampling rate of 2 kHz via WiFi.

In the outlook of Publication P2, it was emphasized that determining the residual stresses during the peripheral milling of Ti-6Al-4V requires a detailed understanding of the thermo-mechanical loads applied to the workpiece. To model the resulting residual stresses, it is necessary to establish the relationships between the process parameters, the process variables, and the residual stress state.

Contributions of the authors

Matthias Wimmer planned, coordinated, and executed the experiments. Vanessa Weisbrodt assisted with the experiment execution as part of her master's thesis. Matthias Wimmer and Muhammed Zubair Shahul Hameed analyzed the experimental data and collaborated on discussing the findings. The manuscript was written by Matthias Wimmer, Muhammed Zubair Shahul Hameed, and Christoph Woelfle. Ewald Werner, Christian Krempaszky, Thomas Semm, and Michael F. Zaeh edited the publication. All authors commented on the results.

6.2.3 P3: "The influences of process parameters on the thermo-mechanical workpiece load and the sub-surface residual stresses during peripheral milling of Ti-6Al-4V"

Publication P3, "The influences of process parameters on the thermo-mechanical workpiece load and the sub-surface residual stresses during peripheral milling of Ti-6Al-4V" (WIMMER ET AL. 2021) addresses the effect of the process parameters on the process variables in terms of the cutting forces and the temperatures that occur during the peripheral milling of Ti-6Al-4V. The interactions between these process variables and the resulting residual stresses are analyzed.

The concept underlying the modeling method used for P5, which calculates the thermo-mechanical stresses based on the process variables, is introduced. Cutting forces generate mechanical stresses, while elevated process zone temperatures induce thermal stresses in the sub-surface. The total elastic stress results from the combined thermo-mechanical stresses, and the residual plastic deformation, along with the corresponding residual stresses, is derived from the sum of these thermo-mechanical stresses.

The sensory tool holder presented in P2 was employed to measure the cutting forces and temperatures at the tool's end during peripheral milling. Simultaneously, established methods were applied to measure process variables on the workpiece side. For this purpose, five thermocouples (diameter of 0.5 mm) were positioned 0.01 mm away from the machined surface. In addition, the cutting forces were recorded using a dynamometer of the type Kistler 92578.

For the temperature measurement, experiments involving different feeds per tooth f_z ranging from 0.04 to 0.08 mm and cutting speeds v_c ranging from 30 to 40 mm/min were performed. The radial depth of cut a_e was kept constant based on the findings from P1. The temperature measurements in the process zone revealed low values, not exceeding 140 °C. Comparing these temperature measurements with the residual stress data indicated no correlation between them, confirming the findings of NESPOR (2015), who demonstrated that tensile residual stresses only arise at a critical temperature exceeding 480 °C. The residual stress depth profiles predominantly exhibited compressive stresses, suggesting that mechanical effects dominate over thermal effects. In this context, the measured cutting forces were also compared to the residual stresses, but no correlation between the surface residual stresses and the process forces was identified. Consequently, the process forces are unsuitable for describing the residual stress evolution during the peripheral milling of Ti-6Al-4V.

The simulation of the cutting forces using the model according to ALTINTAS (2012) demonstrated that the cutting force can be calculated for various process parameter combinations.

However, changes in the cutting-edge radius r_β due to tool wear significantly affected the process forces. Conventional cutting force models are incapable of considering this effect. The process investigations from P1 confirmed that the cutting-edge rounding has the most significant effect on the resulting residual stresses. In this context, an increase in the cutting-edge radius r_β leads to higher ploughing forces F_{pl} during machining, emphasizing the importance of the microgeometry of the tool during peripheral milling. This aspect is further explored in P4.

Contributions of the authors

Matthias Wimmer planned, coordinated, and executed the experiments. He provided the input data and programmed the cutting force model. The data were analyzed by Matthias Wimmer and Christoph Woelfle, who also collaborated on drafting the manuscript and elaborated on the findings together. Christian Krempaszky and Michael F. Zaeh edited the manuscript. All authors discussed the findings and provided comments on the results. Matthias Wimmer presented the results in a talk at the 18th CIRP Conference on Modeling of Machining Operations (CIRP CMMO) in Ljubljana, Slovenia, in 2021.

6.2.4 P4: "Determination of the Cutting-Edge Microgeometry Based on Process Forces during Peripheral Milling of Ti-6Al-4V Using Machine Learning"

Publication P4, "Determination of the Cutting-Edge Microgeometry Based on Process Forces during Peripheral Milling of Ti-6Al-4V Using Machine Learning" (WIMMER ET AL. 2023), introduces a model for predicting the tool wear through in-process cutting force measurements. The influence of variations in the cutting-edge radius r_β on the force behavior and the machining-induced residual stresses was investigated experimentally. The resulting database was utilized to implement a machine learning (ML) algorithm for determining the hidden value of the tool wear. The predictions were validated through milling experiments using tools with specifically prepared cutting edges under different process parameters. The objective was to predict the cutting-edge radius r_β based on the measured cutting forces.

The paper introduces a novel artificial intelligence approach that leverages the relationships between the process parameters, the cutting-edge radius, and the measured cutting forces. Experiments were conducted with feed per tooth values f_z ranging from 0.04 to 0.08 mm to generate a dataset comprising the process parameters v_c, a_e, and f_z, the measured process forces in the Cartesian directions F_x, F_y, and F_z, and the measured cutting-edge radius r_β. A tool holder equipped with integrated sensors (described in P2) was employed to measure the forces during peripheral milling. Signal processing and data analysis were used to extract characteristic values such as average forces. The cutting-edge radii were determined using a laser scanning microscope (KEYENCE VK-X1050, Osaka, Japan) and extracted from the resulting profiles. The pre-processed force data and the process parameters were used as input variables, with the cutting-edge radius assigned as the output variable.

The experiments revealed that the average forces increased with higher f_z values, starting with an initial cutting-edge radius r_β of 5 μm (sharp tool). The cutting force components in the *x*- and *z*-direction showed slight increases with milling length, while the most significant impact of the tool wear on the force behavior was observed in the cutting force component F_y. Uniform wear behavior was noted among the individual cutting edges. The cutting-edge radius increased with the milling length for all tested feed per tooth values f_z (0.04 mm, 0.06 mm, and 0.08 mm). After 35 m of milling, the maximum cutting-edge radii were measured as 31 μm for a feed per tooth f_z of 0.04 mm, 43 μm for 0.06 mm, and 54 μm for 0.08 mm.

Machine learning algorithms were applied to the pre-processed data to identify the relationships between the cutting forces F_x, F_y, and F_z and the cutting-edge radius $r_β$ for different feed-per-tooth values. A multilayer perceptron (MLP) algorithm, based on the frameworks of MURPHY (2012) and BISHOP (2006), was utilized as a universal function approximator. Various architectures were tested, and the performance was assessed using the root mean square error (RMSE). The best results were achieved with an MLP employing an L-BFGS solver and a tanh activation function. The cutting-edge radius $r_β$ was predicted with an RMSE of 8.94 μm, with the F_y force component demonstrating the highest predictive capability.

To validate the prediction model, additional experiments with eight tools featuring cutting-edge radii ranging from 5 ± 1 μm (new tool) to 60 ± 1 μm were conducted. The cutting speed v_c and the radial depth of cut a_e were held constant, while the feed per tooth f_z was varied from 0.04 to 0.08 mm in steps of 0.2 mm. The residual stresses on the machined surface were measured using X-ray diffraction (Stresstech Xstress3000, Vaajakoski, Finland). The objective was to expand the experiments performed in P1 to determine the quantitative relationships between the cutting-edge rounding and the machining-induced residual stresses. Defined cutting-edge radii were prepared to investigate their effects systematically.

The residual stress measurements demonstrated compressive residual stresses on the machined surfaces. The magnitude of the compressive residual stresses perpendicular to the feed direction $σ_a$ and in the feed direction $σ_f$ increased with higher cutting-edge radii. For a feed per tooth of 0.04 mm, the residual compressive stresses perpendicular to the feed direction increased from 114 MPa with a cutting-edge radius of 5 μm to 289 MPa with a cutting-edge rounding of 60 μm. The resulting compressive residual stresses in the feed direction changed from 52 MPa to 253 MPa. Higher feed per tooth values reduced the maximum compressive stresses for the same cutting-edge microgeometry.

The developed prediction model, combined with the residual stress measurements, provides insights into the effects of cutting-edge microgeometry changes due to tool wear on the process forces and the residual stresses during peripheral milling of Ti-6Al-4V. The residual stresses in the sub-surface of the workpiece are influenced by the process parameters and the cutting-edge microgeometry. The predicted cutting-edge radii served as input variables for the model-based determination of the residual stress states later presented in P5.

Contributions of the authors

Matthias Wimmer developed the idea to predict the cutting-edge radius based on the measured process forces using ML methods. He was responsible for the experimental design and execution, prepared the milling tools with different cutting-edge radii, and conducted the peripheral milling tests. Matthias Wimmer evaluated the measured data. The manuscript was written by Matthias Wimmer and edited by Roman Hartl and Michael F. Zaeh. All authors discussed the data and commented on the results.

6.2.5 P5: "In-Situ Characterization and Modeling of Machining-Induced Residual Stresses in Peripheral Milling of Ti-6Al-4V with Rounded Cutting Edges"

Publication P5, "In-Situ Characterization and Modeling of Machining-Induced Residual Stresses in Peripheral Milling of Ti-6Al-4V with Rounded Cutting Edges" (WIMMER ET AL. 2024), presents a semi-analytical model for determining the resulting residual stresses after peripheral milling of Ti-6Al-4V. For this purpose, a hybrid approach based on physical principles is presented for the efficient calibration of a 2D model of the machining-induced residual stresses, utilizing the digital image correlation (DIC) analysis of in-situ-characterized displacement fields in the sub-surface (SCHOOP ET AL. 2022). Correlations between the two-dimensional process parameters, the cutting-edge radius, and the input variables of the model were determined analytically based on the experimental data.

First, the experimental characterization method was presented, in which the relevant input parameters were determined using an in-situ test setup. The high-speed in-situ images were analyzed using DIC. While most efforts focused on continuous flow (finite/large strain) through the primary and tertiary deformation zones, DIC was used to study nanometric subsurface deformations, which significantly influence the residual stress distribution. The principle underlying this specialized DIC technique is based on a two-step approach, which was first proposed by TAUSENDFREUND ET AL. (2015), for analyzing sub-surface deformation fields in milling.

The equivalent (quasi-elastic) Hertzian contact length $2a$, the friction coefficients μ_e, and the contact pressure p_0 for different feeds per tooth f_z and uncut chip thicknesses h were determined based on the shear angle and the cutting forces. The experimental setup with its linear axis was equipped with an ultrahigh-speed camera and ultrahigh-intensity LED lighting to capture the deformation of the sample microstructure due to the cutting process. This experimental setup was specifically developed to investigate the sub-surface during finishing processes and to analyze strain localization. A detailed characterization of the dynamic material behavior and the elasto-plastic deformation was performed using various cutting-edge radii (cf. P4). The experimentally determined variables and the material properties of Ti-6Al-4V (hardness, flow stress, Poisson's ratio, and Young's modulus) used to describe the elastic material behavior provided the input parameters for the semi-analytical model.

In the hybrid model, the 2D residual stresses were first calculated using the tractional sliding Hertzian contact model (MERWIN & JOHNSON 1963). These calculations were subsequently extended to the 3D peripheral milling process by incorporating the tool geometry and the kinematics. By considering the physical fundamentals of the process, Publication P5 demonstrates an experimentally calibrated approach validated against measured residual stresses. A correlation between the proposed 3D model and validation data was found to be within the margin of experimental error for most conditions. The proposed model adequately captures the overall behavior of 3D residual stress depth profiles with acceptable accuracy, particularly the key metrics of the near-surface stress, the peak stress magnitude and location, as well as the overall residual stress depth d_{RS}. The maximum RMSE was 29.87 MPa.

Contributions of the authors

Julius Schoop proposed the development of a semi-analytical model to evaluate the resulting residual stresses. Matthias Wimmer provided the experimental data, uncluding the cutting force measurement results, DIC images, and details regarding the milling process dimensions. Matthias Wimmer and Julius Schoop conducted the simulation studies and optimized the model parameters. Matthias Wimmer developed the 3D residual stress model, with support from Julius Schoop during the model's development. The data was analyzed by Matthias Wimmer and Julius Schoop, who also collaborated on drafting the manuscript. Michael F. Zaeh edited the manuscript. All authors discussed the findings and provided comments on the results.

6.3 Discussion of the findings

In this section, the results obtained and leading to Publication P1–P5 are briefly discussed, with a focus on their main contributions to the knowledge base when compared to the most relevant works from the state of the art. As shown in Figure 6-1, the publications can be categorized according to the values investigated during machining, the field in which they have contributed to knowledge and how the machining-induced residual stresses in the sub-surface of Ti-6Al-4V are determined. These investigated values are the process parameters, the microgeometry of the cutting edge, and the process variables. The publications in the field of residual stress modeling during the machining of Ti-6Al-4V can be sub-classified according to their modeling method. As described in Section 3.3, there are various approaches available to determine the residual stress state after machining. Furthermore, the effective interactions between machining and the resulting residual stresses in the sub-surface of Ti-6Al-4V were investigated for different machining processes. This is presented in Figure 6-1 using different background colors for the selected research contributions (gray for peripheral milling and blue for other processes).

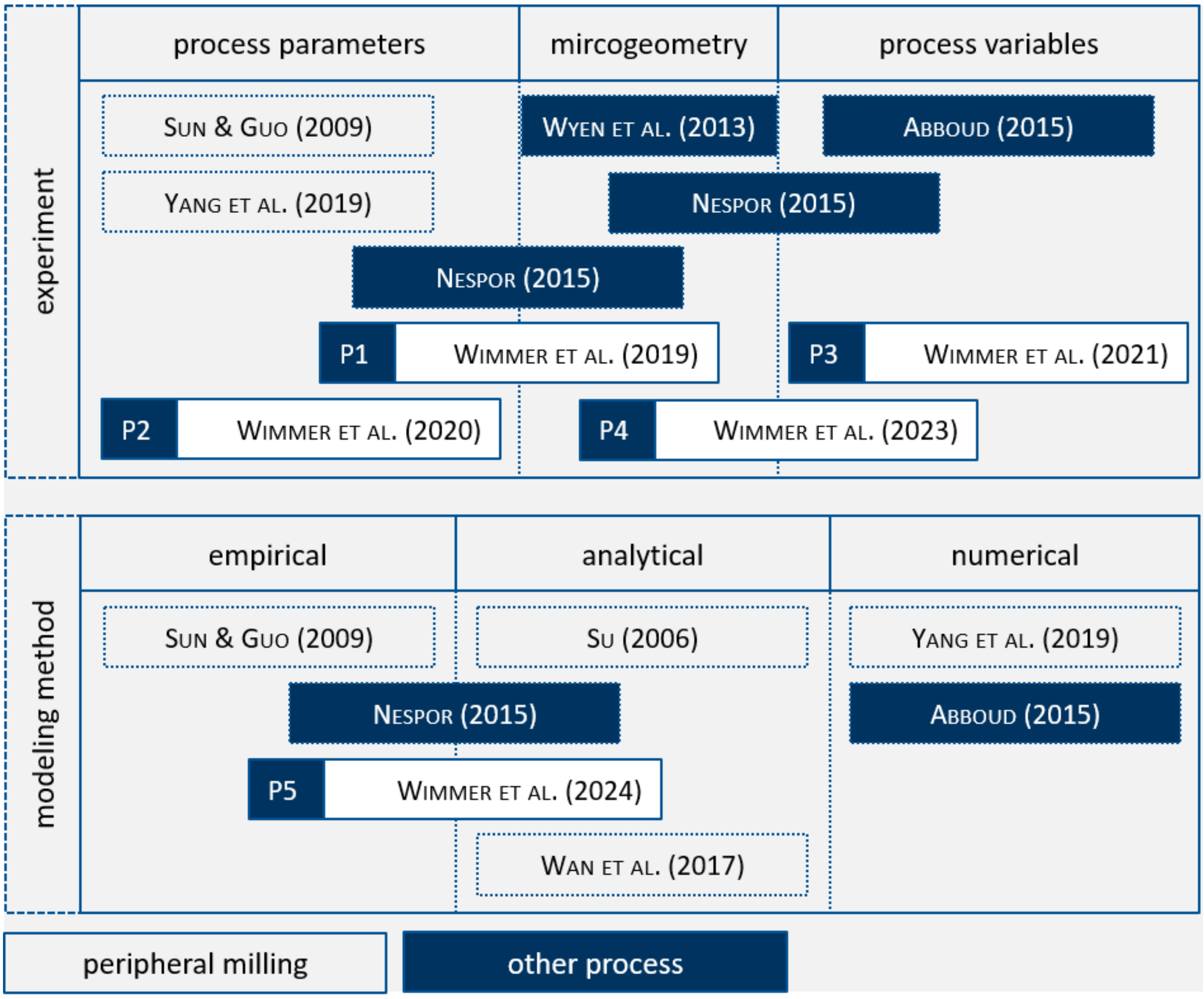

Figure 6-1: The classification of Publication P1–P5, arranged according to their respective investigated process parameters/values, and the modeling method, also considering the closest publications from the previous state of the art (cf. Chapter 3)

Publications P1 and P2 of this dissertation can be mainly assigned to the research field of residual stresses after titanium machining. Section 3.2 confirms that the state of the art incorporates studies on the influences of the process parameters on the machining-induced residual stress state of Ti-6Al-4V with contradictory findings. In this regard, it was experimentally demonstrated in P1 that the cutting-edge radius has the most significant influence on the change of residual stresses in peripheral milling. Previously, this effect was only studied for ball-end milling by NESPOR (2015) and orthogonal slot milling by WYEN ET AL. (2013). In P2, the influences of the cutting speed and the feed per tooth on the residual stresses were investigated, which led to different results in comparison to experimental studies by SUN & GUO (2009) and YANG ET AL. (2019). Specifically, the considerations of the influence of the microgeometry of the cutting edge on the residual stress state go beyond the state of the art (cf. Sub-section 3.2.3). Therefore, P1 and P2 fulfill the scientific subgoal SO1 defined in Section 4.2.

Publication P3 of this dissertation provided results that experimentally explain the thermo-mechanical effects during peripheral milling of Ti-6Al-4V on the residual stress state. In this context, the process variables were measured simultaneously with the process using a sensory tool holder and compared with the resulting residual stresses. No direct correlation between the thermal effects and the resulting residual stress state was detected in peripheral milling. In this respect, the findings of NESPOR (2015) for ball-end milling and ABBOUD (2015) for orthogonal external longitudinal turning were confirmed, which both independently proved that the temperatures occurring in the process zone are too low to cause phase transformations, respectively tensile residual stresses. The comparison of the process force measurements with the resulting residual stress data revealed that the cutting forces are not suitable for model-based descriptions of the resulting residual stresses and confirm the findings of NESPOR (2015) for ball-end milling. Thus, the main reason for the change in residual stresses during peripheral milling is to be seen in mechanical effects. These are strongly dependent on the relationship between the uncut chip thickness, the cutting-edge radius, and the resulting ploughing forces. Therefore, the scientific Sub-objective SO2 is fulfilled, which concerns the determination of the relationships between the process variables and the resulting residual stresses.

Publication P4 contributed to a more profound understanding of the change in the cutting-edge radius due to tool wear during the peripheral milling process and the effect on the machining induced residual stresses. Thematically related research includes that by NESPOR (2015) and WYEN ET AL. (2013), who empirically determined the effect of the cutting-edge radius on the residual stresses. However, P4 differs from that by combining the measurement of process forces by applying a data-driven approach to determine the current cutting-edge radius existent during the process. In this context, an in-process modeling approach that uses a sensory tool holder was presented. Therefore, the formulated requirements of the scientific Sub-objective SO3 were fulfilled in P4.

Publication P5 provides a model for determining the resulting residual stresses during peripheral milling of Ti-6Al-4V with different cutting-edge radii. A semi-analytical approach was chosen, which is based on the basic idea of NESPOR (2015). However, he investigated the ball-end milling process, and the body responsible for the Hertzian pressure was considered as a sphere. The contact between the tool cutting edge and the workpiece is assumed to be a cylinder in the model presented in Publication P5. Orthogonal cutting experiments were performed to enable the in-situ determination of the characteristic chip formation parameters and the process forces. The uncut chip thickness and the shear angle were measured using high-speed imaging combined with subsequent image analysis. The cutting forces were recorded using integrated force sensors under identical boundary conditions.

For the first time, the influence of varying cutting-edge radii on the chip formation parameters and the process forces was systematically investigated, enabling a detailed analysis of geometric effects on the cutting process. The experimentally determined data served as input parameters for the subsequent development of a semi-analytical model to describe the residual stress state after peripheral milling. As a result, the mechanical contact length, the friction, and the Hertzian pressure were determined analytically. The approach of the orthogonal model was then applied to the peripheral milling process. In this context, the residual stress state of the sub-surface of Ti-6Al-4V was calculated as a function of the process parameters, the cutting-edge radius, and the process variables. The hybrid modeling method combines the advantages of analytical (WAN ET AL. 2017; SU 2006) and empirical (SUN & GUO 2009) approaches. Sub-objective SO4 (cf. Section 4.2) regarding the modeling of the mechanical load and the residual stresses was thereby fulfilled.

7 Summary and Outlook

7.1 Summary

The titanium alloy Ti-6Al-4V is becoming increasingly popular due to its superior material properties compared to other lightweight alloys, such as low density, high strength at elevated temperatures, high corrosion resistance, high creep resistance, high toughness and durability, and high biological compatibility (cf. Sub-section 2.2). The quality and lifetime performance of a product are directly related to the surface integrity achieved by the final manufacturing process (cf. Sub-section 2.3). The peripheral milling of Ti-6Al-4V alters the residual stress state of the sub-surface due to the thermo-mechanical loading (cf. Sub-sections 2.4 and 2.5). The residual stress profile is a critical characteristic of the component's surface integrity and, therefore, significantly influences the functional performance and the service life. Compressive residual stresses have a positive influence on the mechanical properties and are therefore in some cases deliberately induced in industrial settings via post-treatment processes such as shot peening (cf. Sub-section 2.5.3). Complex measurement techniques, such as X-ray diffraction, are required to evaluate the residual stresses. Using models to calculate the residual stress state of the sub-surface (cf. Section 2.6) prior to peripheral milling would allow effective, component-specific design and process optimization while maintaining high component quality.

The objective of this dissertation was to enable the model-based determination of the residual stress state in the sub-surface of Ti-6Al-4V during and after peripheral milling. Chapter 3 in this thesis examines existing approaches in the field of residual stresses after titanium machining, with a detailed discussion of the influence of the process parameters (cf. Sub-section 3.2.2) and the cutting-edge radius (cf. Sub-section 3.2.3). In addition, the residual stress modeling during milling processes (cf. Section 3.3) was discussed. The identified need for action can be summarized as follows:

- The interdependencies between the process parameters, the process variables, and the resulting residual stresses during peripheral milling had to be quantified. The significance of the individual influencing factors had to be determined.

- A change in the microgeometry of the cutting edge due to tool wear, especially the cutting-edge radius, is a key factor affecting the resulting residual stress state in the sub-surface of the machined surface. Therefore, these influences had to be considered and quantified comprehensively for the peripheral milling process. A prediction of the actual cutting-edge microgeometry based on values measured during the process was required.

- The change in the residual stresses is caused by thermo-mechanical effects. For the peripheral milling of Ti-6Al-4V, a detailed experimental investigation of the forces and temperatures occurring during machining and their correlation with the machining-induced residual stresses had to be conducted.
- Various modeling methods exist for the calculation of residual stresses. A hybrid simulation model for the prediction of machining-induced residual stress profiles had to be established. The influence of varying cutting-edge radii on the resulting residual stresses had to be considered.
- In literature, the resulting residual stress state of the sub-surface has only been determined for kinematically simple cutting processes. A model that represents the complex 3D geometry of the peripheral milling process is required.

The scientific approach of this work includes the development of a foundational methodology for determining the residual stress state after the peripheral milling of Ti-6Al-4V. The influence of the individual process parameters and the microgeometry of the tool on the resulting residual stresses was investigated (cf. Sub-section 6.2.1). The experiments were subsequently extended to elucidate the change in the sub-surface properties due to the peripheral milling of Ti-6Al-4V. The most significant variables affecting the residual stress state were identified. The results showed that the cutting-edge radius r_β of the milling tool has a substantial influence on the residual stresses (cf. Sub-section 6.2.2). Furthermore, the interactions between the process parameters and the process variables in terms of the cutting forces and the temperatures were analyzed. The focus was placed on describing effective relationships between the process variables and the resulting residual stresses. Moreover, it was demonstrated that, in the milling of the titanium alloy Ti-6Al-4V, the thermal load on the sub-surface has no significant influence on the resulting residual stresses. Instead, they are predominantly affected by mechanical effects (cf. Sub-section 6.2.3). With respect to the significant influence of the cutting-edge radius on the residual stress state, a model for the prediction of tool wear was developed. The aim was to predict the cutting-edge rounding based on the measured cutting forces. The effects of changes in the cutting-edge microgeometry on the force behavior and the machining-induced residual stresses were experimentally investigated. The resulting database was used to implement a Machine Learning algorithm for calculating the actual cutting-edge radius (cf. Sub-section 6.2.4).

Subsequently, a semi-analytical model was established to calculate the resulting residual stresses during peripheral milling (cf. Sub-section 6.2.5). In this regard, a data-driven approach based on physical principles was presented to efficiently calibrate a 2D model of the machining-induced residual stresses by DIC analysis of in-situ characterized displacement fields in the sub-surface. Based on the experimental data, correlations between the 2D process parameters, the cutting-edge rounding, and the input variables of the model were analytically determined. Additionally, the 2D modeling approach was adapted to the complex geometry and the 3D kinematics of the peripheral milling process in a final step. By considering the physical fundamentals of the cutting process, the residual stresses were calculated for different process parameters and cutting-edge radii. The model results were validated based on measured residual stresses. The correlation between the proposed 3D model and validation data was found to be within the margin of experimental error for most conditions. The proposed model appears to capture the overall behavior of 3D residual stress depth profiles with acceptable accuracy, particularly the key metrics of the near-surface stress, the peak stress magnitude and the location, as well as the overall stress profile depth. For each considered aspect, an enhancement compared to the state of the art was achieved (cf. Section 6.3)

7.2 Outlook

Potential for advances can be identified based on the findings within the framework of this thesis to translate the primary findings into practice. These are described in the following.

Process- and material-dependent thermal effects

In Publication P5 (cf. Sub-section 6.2.5), an important assumption is made: the exclusion of thermal effects in the prediction of residual stresses. This simplification affects the interaction between the material properties of Ti-6Al-4V and the process-specific variables of peripheral milling (cf. Sub-section 6.2.1 to 6.2.5). The extent to which these simplifications can be applied to other materials and machining processes remains unclear. Presumably, this simplification does not apply to high-speed milling, which means that the hybrid residual stress model developed in this work would no longer be applicable and would have to be extended by thermal influences. Future research should focus on developing an approach that integrates the coupled thermal-mechanical workpiece load, thereby enabling the generalization of residual stress predictions. The interdependencies of the workpiece load and deformation morphology need to be examined independently and in more detail with a specific consideration of material- and process-specific factors.

Rigid Workpiece

Another notable simplification in this work is the assumption of a rigid workpiece, which is not the case for thin structures such as compressor blades or blisks. In practice, clamping systems are designed to minimize workpiece compliance and vibration by means of adaptive fixtures. However, these systems are not always comparable to a rigid workpiece. To adress this limitation, the workpiece compliance, as well as the tool and the workpiece vibrations, along with their interactions should be considered for the calculation of the residual stresses to improve accuracy and applicability.

Implications for industrial usage

The experiments described in Publication P1 (cf. Sub-section 6.2.1), Publication P4 (cf. Sub-section 6.2.4), and Publication P5 (cf. Sub-section 6.2.5) demonstrate that the residual stresses during peripheral milling of Ti-6Al-4V are significantly affected by the cutting-edge radius r_β. This insight presents an opportunity for tool manufacturers to design tools with specially prepared cutting edges. Therefore, tools with large cutting-edge radii should be used for applying high compressive residual stresses near the workpiece surface while maintaining the desired surface quality (e.g., roughness). Additionally, the rake and clearance angles should be optimized to extend the tool life. Productivity can be improved by increasing the cutting speed and the radial depth of cut, which only slightly influences the resulting residual stresses.

Control of the machining process

Publication P4 (cf. Sub-section 6.2.4) provides a model for determining the cutting-edge radius during peripheral milling of Ti-6Al-4V in parallel (simultaneously) to the machining process. Building upon these results, the mechanical load and the resulting residual stress state in the component sub-surface during machining were modeled in Publication P5 (cf. Sub-section 6.2.5). The models could be used for a process control concerning the residual stress state. In this context, tool wear can be considered as a disturbance variable. This requires the development and implementation of a suitable control concept and the verification of the control for robustness against disturbances. Furthermore, the model and the control strategies can be extended by incorporationg additional variables. For instance, beyond the conventional process parameters already considered, the influence of the tool inclination angle could be investigated and integrated into the control system.

8 References

Please note that wherever no bibliographic indices are given, the information is not available or not known to the author.

ABBOUD ET AL. 2013
Abboud, E.; Shi, B.; Attia, H.; Thomson, V.; Mebrahtu, Y.: Finite element based modeling of machining-induced residual stresses in Ti-6Al-4V under finish turning conditions. 14th CIRP Conference on Modeling of Machining Operations (CIRP CMMO) (2013) 8, pp. 63-68.

ABBOUD 2015
Abboud, E.: Characterization of machining-induced residual stresses in titanium-based alloys. (Dissertation). Department of Mechanical Engineering, McGill University. Montreal, Quebec (2015).

ABELE & FRÖHLICH 2008
Abele, E.; Fröhlich, B.: High speed milling of titanium alloys. Advances in production engineering & management 3 (2008) 3, pp. 131-140.

ADENSTEDT & WHITMORE 1955
Adenstedt, H. K.; Whitmore, M. R.: Handbook on titanium. US Department of Commerce, Office of Technical Services. 2. Edition. 1955.

ALBRECHT 1960
Albrecht, P.: New developments in the theory of the metal-cutting process: Part I. The ploughing process in metal cutting. Journal of Engineering for Industry 82 (1960) 4, pp. 348-357.

ALTINTAS 2012
Altintas, Y.: Manufacturing automation. Metal cutting mechanics, machine tool vibrations, and CNC design. 2. Edition. Cambridge, New York: Cambridge University Press 2012. ISBN: 978-1-139-22411-6.

ALTMÜLLER 2001
Altmüller, S.: Simultanes fünfachsiges Fräsen von Freiformflächen aus Titan [Simultaneous five-axis milling of free-form surfaces made of titanium, own translation]. (Dissertation). Institut für Produktionstechnologien, Rheinisch-Westfälische Technische Hochschule. Aachen (2001).

ARAMCHAROEN & MATIVENGA 2009
Aramcharoen, A.; Mativenga, P. T.: Size effect and tool geometry in micromilling of tool steel. Precision Engineering 33 (2009) 4, pp. 402-407.

ARMENDIA ET AL. 2010
Armendia, M.; Garay, A.; Villar, A.; Davies, M.; Arrazola, P.: High bandwidth temperature measurement in interrupted cutting of difficult to machine materials. CIRP Annals - Manufacturing Technology 59 (2010) 1, pp. 97-100.

ARRAZOLA ET AL. 2009
Arrazola, P. J.; Garay, A.; Iriarte, L. M.; Armendia, M.; Marya, S.; Le Maître, F.: Machinability of titanium alloys (Ti6Al4V and Ti555.3). Journal of Materials Processing Technology 209 (2009) 5, pp. 2223-2230.

ASM 4911
AMS G Titanium and Refractory Metals Committee 4911: Titanium Alloy, Sheet, Strip, and Plate, 6Al - 4V, Annealed. 400 Commonwealth Drive, Warrendale, PA, United States: SAE International.

AWISZUS 2002
Awiszus, B. (Ed.): Grundlagen der Fertigungstechnik [Fundamentals of manufacturing technology, own translation]. München, Wien: Fachbuchverlag Leipzig im Hanser-Verlag 2002. ISBN: 34462-20577.

AXINTE & DEWES 2002
Axinte, D.; Dewes, R.: Surface integrity of hot work tool steel after high speed milling-experimental data and empirical models. Journal of Materials Processing Technology 127 (2002) 3, pp. 325-335.

BISHOP 2006
Bishop, C. M.: Pattern recognition and machine learning. New York, NY: Springer Science + Business Media LLC 2006. (Information Science and Statistics).

BMU – BUNDESMINISTERIUM FÜR UMWELT, NATURSCHUTZ UND NUKLEARE SICHERHEIT (FEDERAL MINISTRY FOR THE ENVIRONMENT, NATURE CONSERVATION AND NUCLEAR SAFETY). (2019, 12. NOVEMBER). KLIMASCHUTZPLAN 2050 [CLIMATE ACTION PLAN 2050]. HTTPS://WWW.BMU.DE/FILEADMIN/DATEN_BMU/DOWNLOAD_PDF/KLIMASCHUTZ/KLIMASCHUTZPLAN_2050_BF.PDF.

BREIDENSTEIN 2011
Breidenstein, B.: Oberflächen und Randzonen hoch belasteter Bauteile [Surfaces and subsurfaces of highly loaded components, own translation]. (Dissertation). Institut für Fertigungstechnik und Werzeugmaschinen, Leibniz Universität Hannover. Garbsen (2011).

BREIDENSTEIN ET AL. 2020
Breidenstein, B.; Denkena, B.; Krödel, A.; Prasanthan, V.; Poll, G.; Pape, F.; Coors, T.: Production-related surface and subsurface properties and fatigue life of hybrid roller bearing components. Metals 10 (2020) 10, p. 1339.

BRINKSMEIER 1982
Brinksmeier, E.: Randzonenanalyse geschliffener Werkstücke [Analysis of surface layers of ground workpieces, own translation]. (Dissertation). Institut für Fertigungstechnik und Werkzeugmaschinen, Leibniz Universität Hannover. Garbsen (1982).

BRINKSMEIER ET AL. 1982
Brinksmeier, E.; Cammett, J. T.; König, W.; Leskovar, P.; Peters, J.; Tönshoff, H. K.: Residual stresses - measurement and causes in machining processes. CIRP Annals 31 (1982) 2, pp. 491-510.

CALAMAZ ET AL. 2011
Calamaz, M.; Coupard, D.; Nouari, M.; Girot, F.: Numerical analysis of chip formation and shear localisation processes in machining the Ti-6Al-4V titanium alloy. The International Journal of Advanced Manufacturing Technology 52 (2011) 9, pp. 887-895.

CAPELLO 2005
Capello, E.: Residual stresses in turning. Journal of Materials Processing Technology 160 (2005) 2, pp. 221-228.

CHEN ET AL. 2004
Chen, L.; El-Wardany, T. I.; Harris, W. C.: Modelling the effects of flank wear land and chip formation on residual stresses. CIRP Annals 53 (2004) 1, pp. 95-98.

DA HUANG ET AL. 2018
Da Huang, X.; Zhang, X. M.; Leopold, J.; Ding, H.: Analytical model for prediction of residual stress in dynamic orthogonal cutting process. Journal of Manufacturing Science and Engineering 140 (2018) 1.

DENKENA ET AL. 2014
Denkena, B.; Vehmeyer, J.; Niederwestberg, D.; Maaß, P.: Identification of the specific cutting force for geometrically defined cutting edges and varying cutting conditions. International Journal of Machine Tools and Manufacture 82-83 (2014), pp. 42-49.

DENKENA & TÖNSHOFF 2011
Denkena, B.; Tönshoff, H. K.: Spanen. Grundlagen [Cutting. Fundamentals, own translation]. Wiesbaden: Springer Fachmedien 2011. ISBN: 978-3-642-19771-0.

DIN 6528
DIN 6528: Solid hardmetal end mills with continuous parallel shank - Dimensions. Berlin: Beuth Verlag GmbH 2002-01.

DIN 6580
DIN 6580: Terminology of chip removing; movements and geometry of the chip removing process. Berlin: Beuth Verlag GmbH 1985-10.

DIN 6581
DIN 6581: Terminology of chip removing; reference systems and angles on the cutting part of the tool. Berlin: Beuth Verlag GmbH 1985-10.

DIN 6582
DIN 6582: Terminology of cutting; additional terms for the tool, wedge and the cutting edge. Berlin: Beuth Verlag GmbH 1988-02.

DIN 6583
DIN 6583: Terms of cutting procedures; tool life criteria. Berlin: Beuth Verlag GmbH 1981-09.

DIN 6584
DIN 6584: Terms of the cutting technique; forces, energy, work, power. Berlin: Beuth Verlag GmbH 1982-10.

DIN 8589-3
DIN 8589-3: Manufacturing processes chip removal - Part 3: Milling; Classification, subdivision, terms and definitions. Berlin: Beuth Verlag GmbH 2003-09.

DONACHIE 2000
Donachie, M. J.: Titanium: A Technical Guide. ASM International, 2. Edition. (2000).

EE ET AL. 2005
Ee, K. C.; Dillon, O. W.; Jawahir, I. S.: Finite element modeling of residual stresses in machining induced by cutting using a tool with finite edge radius. International Journal of Mechanical Sciences 47 (2005) 10, pp. 1611-1628.

EL-AXIR 2002
El-Axir, M.: A method of modeling residual stress distribution in turning for different materials. International Journal of Machine Tools and Manufacture 42 (2002) 9, pp. 1055-1063.

EL-KHABEERY & FATTOUH 1989
El-Khabeery, M.; Fattouh, M.: Residual stress distribution caused by milling. International Journal of Machine Tools and Manufacture 29 (1989) 3, pp. 391-401.

EZUGWU & WANG 1997
Ezugwu, E.; Wang, Z.: Titanium alloys and their machinability - a review. Journal of Materials Processing Technology 68 (1997) 3, pp. 262-274.

FIELD & KAHLES 1964
Field, M.; Kahles, J. F.: The surface integrity of machined and ground high-strength steels. DMIC Report 210 (1964), pp. 54-77.

FIELD & KAHLES 1971
Field, M.; Kahles, J. F.: Review of surface integrity of machined components. Defense Technical Information Center. 1971.

FILICE ET AL. 2007
Filice, L.; Umbrello, D.; Micari, F.; Settineri, L.: On the finite element simulation of thermal phenomena in machining processes. (Eds.): Advanced Methods in Material Forming. Berlin, Heidelberg: Scholars Portal 2007, pp. 263-278. ISBN: 978-3-540-69844-9.

FRANZ 1979
Franz, H.: Bestimmung der Eigenspannung an definiert bearbeiteten Oberflächen der Werkstoffe TiAl6V4 [Determination of the residual stresses on specifically machined surfaces of TiAl6V4 materials, own translation].. HTM - Härterei-Technische-Mitteilungen 34 (1979) 1, pp. 24-37.

FRIEDRICH 2017
Friedrich, H. E.: Leichtbau in der Fahrzeugtechnik [Lightweight construction in automotive engineering, own translation]. 2. Edition. Wiesbaden: Springer Vieweg 2017. ISBN: 978-3-658-12294-2.

FRITZ & SCHULZE 2015
Fritz, A. H.; Schulze, G.: Fertigungstechnik [Manufacturing technology, own translation]. Berlin, Heidelberg: Springer Vieweg 2015. ISBN: 978-3-662-46555-4.

FROES 2015
Froes, F. H.: Titanium: ASM International 2015. ISBN: 978-1-62708-318-8.

GEY 2003
Gey, C.: Prozessauslegung für das Flankenfräsen von Titan [Process design for flank milling of titanium, own translation]. (Dissertation). Institut für Fertigungstechnik und Werkzeugmaschinen, Universität Hannover. Garbsen (2003).

GRIEST & FROST 1957
Griest, A. J.; Frost, P. D.: Principles and application of heat treatment for titanium alloys. Battelle Memorial Institute. Titanium Metallurgical Laboratory, Columbus, Ohio. (1957).

GROVE 2015
Grove, T.: Hochleistungszerspanung von Titan [High-performance machining of titanium, own translation]. (Dissertation). Institut für Fertigungstechnik und Werkzeugmaschinen, Universität Hannover. Garbsen (2015).

GUILLEMOT ET AL. 2011
Guillemot, N.; Beaubier, B.; Braham, T.; Lartigue, C.; Billardon, R.: A hybrid approach to predict residual stresses induced by ball-end tool finishing milling of a bainitic steel. Advanced Materials Research 223 (2011), pp. 391-400.

HEISEL ET AL. 2014
Heisel, U.; Klocke, F.; Uhlmann, E.; Spur, G.: Handbuch Spanen [Handbook of machining, own translation]. 2. Edition. München: Hanser 2014. ISBN: 978-3-446-42826-3.

HOPPE 2003
Hoppe, S.: Experimental and numerical analysis of chip formation in metal cutting. (Dissertation). Werkzeugmaschinenlabor WZL, Rheinisch-Westfälische Technische Hochschule. Aachen (2003).

IMBROGNO ET AL. 2018
Imbrogno, S.; Rinaldi, S.; Umbrello, D.; Filice, L.; Franchi, R.; Del Prete, A.: A physically based constitutive model for predicting the surface integrity in machining of Waspaloy. Materials & Design 152 (2018), pp. 140-155.

ISO 3002
ISO 3002: Basic quantities in cutting and grinding; part 1: geometry of the active part of cutting tools; general terms, reference systems, tool and working angles, chip breakers; amendment 1: 1992-12.

JACOBUS ET AL. 2000
Jacobus, K.; DeVor, R. E.; Kapoor, S. G.: Machining-induced residual stress: Experimentation and modeling. Transactions of the ASME (2000) 122, pp. 20-31.

JAEGER 1943
Jaeger, J. C.: Moving sources of heat and the temperature at sliding contacts. Journal and proceedings of the Royal Society of New South Wales (1943).

JAWAHIR ET AL. 2011
Jawahir, I. S.; Brinksmeier, E.; M'Saoubi, R.; Aspinwall, D. K.; Outeiro, J. C.; Meyer, D.; Umbrello, D.; Jayal, A. D.: Surface integrity in material removal processes: Recent advances. CIRP Annals 60 (2011) 2, pp. 603-626.

JOHNSON & COOK 1983
Johnson, G. R.; Cook, W. H.: A constitutive model and data for metals subjected to large strains, high strain rates and high temperatures. Proceedings of the Seventh International Symposium on Ballistics, The Hague (1983), pp. 541-547.

KACZMAREK 1966
Kaczmarek, J.: Untersuchung des Einflusses der Schneidenabrundung auf die Verfestigung der Oberflächenschicht [Investigation of the influence of cutting-edge rounding on the hardening of the surface layer, own translation]. Annals of the CIRP XIII (1966), pp. 139-145.

KLEIN & EIFLER 2010
Klein, M.; Eifler, D.: Influences of the manufacturing processes on the surface integrity and the resulting fatigue behavior of quenched and tempered SAE 4140. Procedia Engineering 2 (2010) 1, pp. 2239-2247.

KLOCKE & KÖNIG 2008
Klocke, F.; König, W.: Fertigungsverfahren Band 1 - Drehen, Fräsen, Bohren [Manufacturing processes Volume 1 – Turning, milling, drilling, own translation]. 8. Edition. Berlin Heidelberg: Springer-Verlag 2008.

KLOCKE & KÖNIG 2018
Klocke, F.; König, W.: Zerspanung mit geometrisch bestimmter Schneide [Machining with geometrically defined cutting edges, own translation]. 9. Edition. Berlin: Springer Vieweg 2018. ISBN: 978-3-662-54207-1.

KOMANDURI 1982
Komanduri, R.: Some clarifications on the mechanics of chip formation when machining titanium alloys. Wear 76 (1982) 1, pp. 15-34.

KOMANDURI & HOU 2000
Komanduri, R.; Hou, Z.: Thermal modeling of the metal cutting process: Part I - Temperature rise distribution due to shear plane heat source. International Journal of Mechanical Sciences 42 (2000) 9, pp. 1715-1752.

KOMANDURI & HOU 2001a
Komanduri, R.; Hou, Z. B.: Thermal modeling of the metal cutting process - Part II: temperature rise distribution due to frictional heat source at the tool–chip interface. International Journal of Mechanical Sciences 43 (2001) 1, pp. 57-88.

KOMANDURI & HOU 2001b
Komanduri, R.; Hou, Z. B.: Thermal modeling of the metal cutting process - Part III: temperature rise distribution due to the combined effects of shear plane heat source and the tool-chip interface frictional heat source. International Journal of Mechanical Sciences 43 (2001) 1, pp. 89-107.

KÖNIG ET AL. 1982
König, W.; Essel, K.; Witte, L.; Verein Deutscher Eisenhüttenleute: Spezifische Schnittkraftwerte für die Zerspanung metallischer Werkstoffe [Specific cutting force values for machining metallic materials, own translation]. Düsseldorf: Verlag Stahleisen Düsseldorf 1982. ISBN: 35140-01294.

KORNILOV & BORSIKINA 1965
Kornilov, I. I.; Borsikina, N.: Mechanical and engineering Properties of titanium alloy. Research & microfilm Publications (1965).

KOSTER ET AL. 1970
Koster, W. P.; Field, M.; Fritz, L. J.; Luciano, R. G.; Kahles, J. F.: Surface integrity of machined structural components. Technical Report (1970).

KREIS 1973
Kreis, W.: Verschleißursachen beim Drehen von Titanwerkstoffen [Causes of tool wear during turning of titanium materials, own translation]. (Dissertation). Rheinisch-Westfälische Technische Hochschule. Aachen (1973).

KROLL 2019
Kroll, L.: Technologiefusion für multifunktionale Leichtbaustrukturen [Technology fusion for multifunctional lightweight structures, own translation]. Springer Berlin Heidelberg 2019. ISBN: 978-3-662-54733-5.

KRONENBERG 1969
Kronenberg, M.: Grundzüge der Zerspanungslehre. Theorie und Praxis der Zerspanung für Bau und Betrieb von Werkzeugmaschinen Dritter Band Mehrschneidige Zerspanung (Umfangsfräsen, Räumen) [Fundamentals of machining science. Theory and practice of machining for the design and operation of machine tools: Volume 3, Multi-cutting machining (Peripheral milling, shaping), own translation]. 2. Edition. Berlin, Heidelberg: Springer 1969. ISBN: 978-3-642-92980-9.

KRYZHANIVSKYY ET AL. 2019
Kryzhanivskyy, V.; M'Saoubi, R.; Ståhl, J. E.; Bushlya, V.: Tool–chip thermal conductance coefficient and heat flux in machining: Theory, model and experiment. International Journal of Machine Tools and Manufacture 147 (2019) 2, pp. 1034-1068.

KUMAR & AJAY 2012
Kumar, L. D.; Ajay, V.: Modelling of temperature profile in metal cutting process. International Journal of Innovative Research and Development 1 (2012) 8, pp. 216-227.

LAZOGLU ET AL. 2008
Lazoglu, I.; Ulutan, D.; Alaca, B. E.; Engin, S.; Kaftanoglu, B.: An enhanced analytical model for residual stress prediction in machining. CIRP Annals 57 (2008) 1, pp. 81-84.

LEÓN GARCÍA 2009
León García, L. R. de: Residual stress and part distortion in milled aerospace aluminium. (Dissertation). Institut für Fertigungstechnik und Werkzeugmaschinen, Leibniz Universität Hannover. Garbsen (1982).

LIANG & SU 2007
Liang, S. Y.; Su, J. C.: Residual stress modeling in orthogonal machining. CIRP Annals 56 (2007) 1, pp. 65-68.

LIAO ET AL. 2019
Liao, Z.; Axinte, D.; Gao, D.: On modelling of cutting force and temperature in bone milling. Journal of Materials Processing Technology 266 (2019), pp. 627-638.

LINSLER ET AL. 2016
Linsler, D.; Schröckert, F.; Scherge, M.: Influence of subsurface plastic deformation on the running-in behavior of a hypoeutectic AlSi alloy. Tribology International 100 (2016) C, pp. 224-230.

LIU & GUO 2000
Liu, C. R.; Guo, Y. B.: Finite element analysis of the effect of sequential cuts and tool–chip friction on residual stresses in a machined layer. International Journal of Mechanical Sciences 42 (2000) 6, pp. 1069-1086.

LIU & MITTAL 1998
Liu, C. R.; Mittal, S.: Optimal pre-stressing the surface of a component by superfinish hard turning for maximum fatigue life in rolling contact. Wear 219 (1998) 1, pp. 128-140.

LOEWEN & SHAW 1954
Loewen, E.; Shaw, M.: On the analysis of cutting tool temperature. ASME Transactions Journal of Engineering for Industry 76 (1954), pp. 217-231.

LÜTJERING & WILLIAMS 2007
Lütjering, G.; Williams, J. C.: Titanium. 2. Edition. Heidelberg: Springer 2007. ISBN: 978-3-540-71397-5. (Engineering Materials and Processes).

M. KLEIN ET AL. 2011
M. Klein; P. Starke; D. Eifler: Manufacturing influences on the fatigue properties of quenched and tempered SAE 4140 specimens. Procedia Engineering 10 (2011), pp. 1184-1189.

M'SAOUBI ET AL. 1999
M'Saoubi, R.; Outeiro, J. C.; Changeux, B.; Lebrun, J. L.; Morão Dias, A.: Residual stress analysis in orthogonal machining of standard and resulfurized AISI 316L steels. Journal of Materials Processing Technology 96 (1999) 1, pp. 225-233.

MACHADO & WALLBANK 1990
Machado, A. R.; Wallbank, J.: Machining of titanium and its alloys - a review. Proceedings of the Institution of Mechanical Engineers, Part B: Journal of Engineering Manufacture 204 (1990) 1, pp. 53-60.

MACHERAUCH ET AL. 1973
Macherauch, E.; Wohlfahrt, H.; Wolfstieg, U.: Zur zweckmäßigen Definition von Eigenspannungen [On the appropriate definition of residual stresses, own translation]. HTM - Härterei-Technische-Mitteilungen 28 (1973) 3, pp. 201-211.

MADYIRA ET AL. 2013
Madyira, D. M.; Laubscher, R. F.; van Rensburg, N. J.; Henning, P.: High speed machining induced residual stresses in Grade 5 titanium alloy. Proceedings of the Institution of Mechanical Engineers, Part L: Journal of Materials: Design and Applications 227 (2013) 3, pp. 208-215.

MAIß ET AL. 2012
Maiß, O.; Köhler, J.; T. Grove; B. Denkena: Residual stresses in milled titanium parts. Procedia CIRP 2 (2012), pp. 79-82.

MARKOPOULOS 2013
Markopoulos, A. P.: Finite element method in machining processes. London, New York: Springer 2013. ISBN: 978-1-4471-4329-1.

MARTELOTTI 1941
Martelotti, M. E.: An analysis of the milling process. Transactions of the American Society of Mechanical Engineers 63 (1941), pp. 677–700.

MASUKO 1953
Masuko, M.: Fundamental research on metal cutting (1st report): A new analysis of cutting forces. Transactions of the Japan Society of Mechanical Engineers 19 (1953), pp. 32-39.

MATSUMOTO ET AL. 1991
Matsumoto, Y.; Magda, D.; Hoeppner, D. W.; Kim, T. Y.: Effect of machining processes on the fatigue strength of hardened AISI 4340 steel. Journal of Engineering for Industry 113 (1991) 2, pp. 154-159.

MATSUMOTO ET AL. 1999
Matsumoto, Y.; Hashimoto, F.; Lahoti, G.: Surface integrity generated by precision hard turning. CIRP Annals - Manufacturing Technology 48 (1999) 1, pp. 59-62.

MCQUILLAN ET AL. 1956
McQuillan, A. D.; McQuillan, M. K.; Green, R. B.: Titanium. Metallurgy of the Rarer Metals, Volume 4. Butterworths Scientific Publications, London (1956).

MEINECKE 2009
Meinecke, M.: Prozessauslegung zum fünfachsigen zirkularen Schruppfräsen von Titanlegierungen [Process design for five-axis circular rough milling of titanium alloys, own translation]. Rheinisch-Westfälische Technische Hochschule. Aachen (2009).

MERCHANT 1945
Merchant, M. E.: Mechanics of the Metal Cutting Process. II. Plasticity conditions in orthogonal cutting. Journal of Applied Physics 16 (1945) 6, pp. 318-324.

MERWIN & JOHNSON 1963
Merwin, J. E.; Johnson, K. L.: An analysis of plastic deformation in rolling contact. Proceedings of the Institution of Mechanical Engineers 177 (1963) 1, pp. 676-690.

MEYER 2009
Meyer, S.: Zirkulare Fräsbearbeitung von Titanlegierungen für die Blisk-Herstellung in der Luftfahrtindustrie [Circular milling of titanium alloys for blisk manufacturing in the aerospace industry, own translation]. (Dissertation). Rheinisch-Westfälische Technische Hochschule. Aachen (2009).

MILBERG 1992
Milberg, J.: Werkzeugmaschinen - Grundlagen [Machine tools – Fundamentals, own translation]. Berlin, Heidelberg: Springer 1992. ISBN: 978-3-540-54538-5.

MOHAMMADPOUR ET AL. 2010
Mohammadpour, M.; Razfar, M. R.; Jalili Saffar, R.: Numerical investigating the effect of machining parameters on residual stresses in orthogonal cutting. Simulation Modelling Practice and Theory 18 (2010) 3, pp. 378-389.

M'SAOUBI ET AL. 2008
M'Saoubi; R; Outeiro, J. C.; Chandrasekaran, H.; Jr., O. D.; Jawahir, I. S.: A review of surface integrity in machining and its impact on functional performance and life of machined products. International Journal of Sustainable Manufacturing 1 (2008) 1/2, p. 203.

MÜLLER 2004
Müller, B.: Thermische Analyse des Zerspanens metallischer Werkstoffe bei hohen Schnittgeschwindigkeiten [Thermal analysis of machining metallic materials at high cutting speeds, own translation]. (Dissertation). Rheinisch-Westfälische Technische Hochschule. Aachen (2004).

MURPHY 2012
Murphy, K. P.: Machine learning. A probabilistic perspective. Cambridge, Mass.: MIT Press 2012. ISBN: 978-0-262-30432-0. (Adaptive computation and machine learning series).

NARUTAKI ET AL. 1983
Narutaki, N.; Murakoshi, A.; Motonishi, S.; Takeyama, H.: Study on Machining of Titanium Alloys. CIRP Annals 32 (1983) 1, pp. 65-69.

NESPOR 2015
Nespor, D.: Randzonenbeeinflussung durch die Rekonturierung komplexer Investitionsgüter aus Ti-6Al-4V [Influence on the surface layer due to the re-contouring of complex capital goods made of Ti-6Al-4V, own translation]. (Dissertation). Gottfried Wilhelm Leibniz Universität. Hannover (2015).

NIKNAM ET AL. 2014
Niknam, S. A.; Khettabi, R.; Songmene, V.: Machinability and machining of titanium alloys: A review. (Eds.): Machining of Titanium Alloys: Springer, Berlin, Heidelberg 2014, pp. 1-30.

OKUSHIMA & KAKINO 1972
Okushima, K.; Kakino, Y.: A study of residual stress produced by metal cutting. Memoirs of the Faculty of Engineering, Kyoto University 34 (1972), pp. 234-248.

OUTEIRO ET AL. 2006
Outeiro, J.; Umbrello, D.; M'Saoubi, R.: Experimental and numerical modelling of the residual stresses induced in orthogonal cuttingof AISI 316L steel. International Journal of Machine Tools & Manufacture 46 (2006) 14, pp. 1786-1794.

ÖZEL ET AL. 2010
Özel, T.; Sima, M.; Srivastava, A. K.; Kaftanoglu, B.: Investigations on the effects of multi-layered coated inserts in machining Ti–6Al–4V alloy with experiments and finite element simulations. CIRP Annals 59 (2010) 1, pp. 77-82.

ÖZEL & ULUTAN 2012
Özel, T.; Ulutan, D.: Prediction of machining induced residual stresses in turning of titanium and nickel based alloys with experiments and finite element simulations. CIRP Annals - Manufacturing Technology 61 (2012) 1, pp. 547-550.

PABST 2008
Pabst, R.: Mathematische Modellierung der Wärmestromdichte zur Simulation des thermischen Bauteilverhaltens bei der Trockenbearbeitung [Mathematical modeling of heat flux density for simulating the thermal behavior of the workpiece during dry machining, own translation]. (Dissertation). Institut für Produktionstechnik, Karlsruhe Institute of Technology. Karlsruhe (2008).

PEKELHARING 1978
Pekelharing, A. J.: The exit failure in interrupted cutting. CIRP Annals 27 (1978) 1, pp. 5-10.

PETERS & CLEMENS 2010
Peters, M.; Clemens, H.: Titan, Titanlegierungen und Titanaluminide – Basis für innovative Anwendungen [Titan, titanium alloys, and titanium aluminides – Basis for innovative applications, own translation]. BHM Berg- und Hüttenmännische Monatshefte 155 (2010) 5, pp. 402-408.

PETERS & LEYENS 2002
Peters, M.; Leyens, C.: Titan und Titanlegierungen [Titanium and titanium alloys, own translation]. 3. Edition. Weinheim: WILEY-VCH Verlag GmbH & Co. 2002. ISBN: 978-3-527-30539-1.

PUERTA VELÁSQUEZ 2007
Puerta Velásquez, J. D.: Etude des copeaux et de l'intégrité de surface en usinage à grande vitesse de l'alliage de titane TiAl6V4 [Study of chips and surface integrity in high-speed machining of the titanium alloy TiAl6V4, own translation]. (Dissertation). Université Paul Verlaine. Metz (2007).

RAO ET AL. 2011
Rao, B.; Dandekar, C. R.; Shin, Y. C.: An experimental and numerical An experimental and numerical study on the face milling of Ti-6Al-4V alloy: Tool performance and surface integrity. Journal of Materials Processing Technology 211 (2011) 2, pp. 294-304.

REIßNER 1931
Reißner, H.: Eigenspannungen und Eigenspannungsquellen [Residual stresses and sources of residual stresses, own translation]. Zeitschrift für angewandte Mathematik und Mechanik 11 (1931), pp. 1-8.

ROOS ET AL. 2017
Roos, E.; Maile, K.; Seidenfuß, M.: Werkstoffkunde für Ingenieure. Grundlagen, Anwendung, Prüfung [Materials science for engineers. Fundamentals, applications, testing, own translation]. 6. Edition. Berlin, Heidelberg: Springer-Verlag 2017. ISBN: 978-3-662-49532-2.

RÖSCH 2015
Rösch, O.: Steigerung der Arbeitsgenauigkeit bei der Fräsbearbeitung metallischer Werkstoffe mit Industrierobotern [Improvement of the work accuracy in milling of metallic materials with industrial robots, own translation]. (Dissertation). Institut für Werkzeugmaschinen und Betriebswissenschaften, Technische Universität. München (2015).

ROTELLA ET AL. 2014
Rotella, G.; Dillon, O. W.; Umbrello, D.; Settineri, L.; Jawahir, I. S.: The effects of cooling conditions on surface integrity in machining of Ti6Al4V alloy. The International Journal of Advanced Manufacturing Technology 71 (2014) 1-4, pp. 47-55.

SALOMON 1924
Salomon, C.: Einfluss der Veränderlichkeit des spezifischen Schnittwiderstandes beim Fräsen unter besonderer Berücksichtigung der Wirkung der Spirale [Influence of the variability of the specific cutting resistance in milling with special consideration of the effect of the spiral, own translation]. (Dissertation). Technische Hochschule. München (1924).

SASAHARA ET AL. 2004
Sasahara, H.; Obikawa, T.; Shirakashi, T.: Prediction model of surface residual stress within a machined surface by combining two orthogonal plane models. International Journal of Machine Tools and Manufacture 44 (2004) 7-8, pp. 815-822.

SCHLENKER 2014
Schlenker, J.: Spanende Mikrobearbeitung von Titan und Titanlegierungen [Micro-machining of titanium and titanium alloys, own translation]. (Dissertation). Institut für Spanende Fertigung, Technische Universität. Dortmund (2014).

SCHMIDT 1949
Schmidt, A.: Heat in metal cutting. In: Proceedings of the American Society of Mechanical Engineers (1949).

SCHOLTES 1991
Scholtes, B.: Eigenspannungen in mechanisch randschichtverformten Werkstoffzuständen [Residual stresses in mechanically surface-layer deformed material states, own translation]. (Dissertation). Institut für Werkstoffkunde, Karlsruher Insitut für Technologie. Karlsruhe (1991).

SCHOOP ET AL. 2022
Schoop, J.; Hasan, M. M.; Zannoun, H.: Physics-informed and data-driven prediction of residual stress in three-dimensional machining. Experimental Mechanics 62 (2022) 8, pp. 1461-1474.

SCHULZE 2003
Schulze, V.: Characteristics of surface layers produced by shot peening. In: Wagner, L. (Eds.): Shot peening. Weinheim, Cambridge: Wiley-VCH 2003, pp. 143-160. ISBN: 978-3-527-60658-0.

SCHWARZ 2010
Schwarz, F.: Simulation der Wechselwirkungen zwischen Prozess und Struktur bei der Drehbearbeitung [Simulation of the interactions between the process and the structure in turning, own translation]. (Dissertation). Institut für Werkzeugmaschinen und Betriebswissenschaften, Technische Universität. München (2010).

SHAW 1996
Shaw, M. C.: Energy conversion in cutting and grinding. CIRP Annals - Manufacturing Technology 45 (1996) 1, pp. 101-104.

SIMA & ÖZEL 2010
Sima, M.; Özel, T.: Modified material constitutive models for serrated chip formation simulations and experimental validation in machining of titanium alloy Ti–6Al–4V. International Journal of Machine Tools and Manufacture 50 (2010) 11, pp. 943-960.

SPIEß ET AL. 2009
Spieß, L.; Teichert, G.; Schwarzer, R.; Behnken, H.; Genzel, C.: Moderne Röntgenbeugung. Röntgendiffraktometrie für Materialwissenschaftler, Physiker und Chemiker [Modern X-ray diffraction. X-ray diffractometry for materials scientists, physicists, and chemists, own translation]. 2. Edition, Wiesbaden: Vieweg + Teubner 2009. ISBN: 978-3-8351-0166-1.

SRIDHAR ET AL. 2003
Sridhar, B. R.; Devananda, G.; Ramachandra, K.; Bhat, R.: Effect of machining parameters and heat treatment on the residual stress distribution in titanium alloy IMI-834. Journal of Materials Processing Technology 139 (2003) 1-3, pp. 628-634.

SU 2006
Su, J.-C.: Residual stress modeling in maching processes. (Dissertation). Georgia Institute of Technology, George W. Woodruff School of Mechanical Engineering. Atlanta (2006).

SU ET AL. 2013
Su, J.-C.; Young, K. A.; Ma, K.; Srivatsa, S.; Morehouse, J. B.; Liang, S. Y.: Modeling of residual stresses in milling. The International Journal of Advanced Manufacturing Technology 65 (2013) 5-8, pp. 717-733.

SUN & GUO 2009
Sun, J.; Guo, Y. B.: A comprehensive experimental study on surface integrity by end milling Ti–6Al–4V. Journal of Materials Processing Technology 209 (2009) 8, pp. 4036-4042.

TAUSENDFREUND ET AL. 2015
Tausendfreund, A.; Stöbener, D.; Dumstorff, G.; Sarma, M.; Heinzel, C.; Lang, W.; Goch, G.: Systems for locally resolved measurements of physical loads in manufacturing processes. CIRP Annals 64 (2015) 1, pp. 495-498.

TAYLOR 1907
Taylor, F. W.: On the art of cutting metals. Transactions of the American Society of Mechanical Engineers, Volume 28, 1907, pp. 31–279.

TÖNSHOFF 1966
Tönshoff, H. K.: Eigenspannung und plastische Verformungen im Werkstück durch spanende Bearbeitung [Residual stresses and plastic deformations in the workpiece caused by machining, own translation]. (Dissertation). Technische Hochschule. Hannover (1966).

ULUTAN ET AL. 2007
Ulutan, D.; Erdem Alaca, B.; Lazoglu, I.: Analytical modelling of residual stresses in machining. Journal of Materials Processing Technology 183 (2007) 1, pp. 77-87.

ULUTAN ET AL. 2014
Ulutan, D.; Arisoy, Y. M.; Özel, T.; Mears, L.: Empirical modeling of residual stress profile in machining nickel-based superalloys using the sinusoidal decay function. Procedia CIRP 13 (2014), pp. 365-370.

ULUTAN & ÖZEL 2011
Ulutan, D.; Özel, T.: Machining induced surface integrity in titanium and nickel alloys: A review. International Journal of Machine Tools & Manufacture 51 (2011) 3, pp. 250–280.

VALIORGUE ET AL. 2007
Valiorgue, F.; Rech, J.; Hamdi, H.; Gilles, P.; Bergheau, J. M.: A new approach for the modelling of residual stresses induced by turning of 316L. Journal of Materials Processing Technology 191 (2007) 1, pp. 270-273.

VALIORGUE ET AL. 2012
Valiorgue, F.; Rech, J.; Hamdi, H.; Gilles, P.; Bergheau, J. M.: 3D modeling of residual stresses induced in finish turning of an AISI304L stainless steel. International Journal of Machine Tools and Manufacture 53 (2012) 1, pp. 77-90.

VELÁSQUEZ ET AL. 2010
Velásquez, J. P.; Tidu, A.; Bolle, B.; Chevrier, P.; Fundenberger, J.-J.: Subsurface and surface analysis of high speed machined Ti-6Al-4V alloy. Materials Science and Engineering A 527 (2010) 10-11, pp. 2572-2578.

VICTOR ET AL. 1983
Victor, H.; Müller, M.; Opferkuch, R.: Zerspantechnik. Teil II Drehen, Hobeln und Stoßen, Räumen, Bohren, Fräsen [Machining technology. Part II: Turning, planing and shaping, broaching, drilling, milling, own translation]. Berlin, Heidelberg: Springer 1983. ISBN: 978-3-540-11861-9.

VIEREGGE 1953
Vieregge, G.: Die Energieverteilung und die Temperatur bei der Zerspanung [Energy distribution and temperature in machining, own translation]. Werkstatt und Betrieb 86 (1953) 11, pp. 691-703.

WAGNER & GREGORY 1994
Wagner, L.; Gregory, J. K.: Thermomechanical surface treatment of titanium alloys. Materials Science Forum 163-165 (1994), pp. 159-172.

WALDORF ET AL. 1998
Waldorf, D. J.; DeVor, R. E.; Kapoor, S. G.: A slip-line field for ploughing during orthogonal cutting. Journal of Manufacturing Science and Engineering 120 (1998) 4, pp. 693-699.

WAN ET AL. 2017
Wan, M.; Ye, X.-Y.; Yang, Y.; Zhang, W.-H.: Theoretical prediction of machining-induced residual stresses in three-dimensional oblique milling processes. International Journal of Mechanical Sciences 133 (2017), pp. 426-437.

WAN ET AL. 2019
Wan, M.; Wen, D.-Y.; Ma, Y.-C.; Zhang, W.-H.: On material separation and cutting force prediction in micro milling through involving the effect of dead metal zone. International Journal of Machine Tools and Manufacture 146 (2019), pp. 103452.

WARNECKE 1974
Warnecke, G.: Spanbildung bei metallischen Werkstoffen [Chip formation in metallic materials, own translation]. Gräfelfing: Technischer Verlag Resch 1974.

WESSELS 2007
Wessels, T.: Bohren in Titan- und Nickelbasislegierungen [Drilling in titanium and nickel-based alloys, own translation]. (Dissertation). Instituts für Werkzeugmaschinen und Fertigungstechnik, Technische Universität. Braunschweig (2007).

WIMMER ET AL. 2019
Wimmer, M.; Rinck, P.; Kleinwort, R.; Zaeh, M. F.: Methodology for a model-based control of the boundary zone properties during milling of Ti-6Al-4V. MM Science Journal 2019 (2019) 4, pp. 3214-3219.

WIMMER ET AL. 2020
Wimmer, M.; S. Hameed, M. Z.; Wölfle, C.; Weisbrodt, V.; Zaeh, M.; Werner, E.; Krempaszky, C.; Semm, T.: The influence of the process parameters on the surface integrity during peripheral milling of Ti-6Al-4V. tm - Technisches Messen 87 (2020), pp. 721-731.

WIMMER ET AL. 2021
Wimmer, M.; Woelfle, C. H.; Krempaszky, C.; Zaeh, M. F.: The influences of process parameters on the thermo-mechanical workpiece load and the sub-surface residual stresses during peripheral milling of Ti-6Al-4V. Procedia CIRP 102 (2021), pp. 471-476.

WIMMER ET AL. 2023
Wimmer, M.; Hartl, R.; Zaeh, M. F.: Determination of the Cutting-Edge Microgeometry Based on Process Forces during Peripheral Milling of Ti-6Al-4V Using Machine Learning. Journal of Manufacturing and Materials Processing 7 (2023) 3: 100.

WIMMER ET AL. 2024

Wimmer, M.; Schoop, J.; Zaeh, M. F.: In-situ characterization and modeling of machining-induced residual stresses in peripheral milling of Ti–6Al–4V with rounded cutting edges. Production Engineering Research and Development (2024).

WITTY 2014
Witty, M.: Prozessauslegung für das Tauchfräsen tiefer Kavitäten [Process design for plunge milling of deep cavities, own translation]. (Dissertation). Fraunhofer Institut für Produktionstechnologie, Rheinisch-Westfälische Technische Hochschule. Aachen (2014).

WYEN 2011
Wyen, C.-F.: Rounded cutting edges and their influence in machining titanium. (Dissertation). Department of Mechanical and Process Engineering, Eidgenössische Technische Hochschule. Zürich (2011).

WYEN ET AL. 2012
Wyen, C.-F.; Knapp, W.; Wegener, K.: A new method for the characterisation of rounded cutting edges. The International Journal of Advanced Manufacturing Technology 59 (2012) 9-12, pp. 899-914.

WYEN ET AL. 2013
Wyen, C.-F.; Jaeger, D.; Wegener, K.: Influence of cutting edge radius on surface integrity and burr formation in milling titanium. The International Journal of Advanced Manufacturing Technology 67 (2013) 1-4, pp. 589-599.

YANG ET AL. 2002
Yang, X.; Richard Liu, C.; Grandt, A. F.: An Experimental study on fatigue life variance, residual stress variance, and their correlation of face-turned and ground Ti-6Al-4V samples. Journal of Manufacturing Science and Engineering 124 (2002) 4, pp. 809-819.

YANG ET AL. 2012
Yang, X.; Ren, C.; Wang, Y.; Chen, G.: Experimental study on surface integrity of Ti-6Al-4V in high speed side milling. Transactions of Tianjin University 18 (2012) 3, pp. 206-212.

YANG ET AL. 2016
Yang, D.; Liu, Z.; Ren, X.; Zhuang, P.: Hybrid modeling with finite element and statistical methods for residual stress prediction in peripheral milling of titanium alloy Ti-6Al-4V. International Journal of Mechanical Sciences 108-109 (2016), pp. 29-38.

YANG ET AL. 2019
Yang, D.; Xiao, X.; Liu, Y.; Sun, J.: Peripheral milling-induced residual stress and its effect on tensile–tensile fatigue life of aeronautic titanium alloy Ti–6Al–4V. The Aeronautical Journal 123 (2019) 1260, pp. 212-229.

YANG & LIU 2002a
Yang, X.; Liu, C. R.: A Methodology for Predicting the Variance of Fatigue Life Incorporating the Effects of Manufacturing Processes. Journal of Manufacturing Science and Engineering 124 (2002) 3, pp. 745-753.

YANG & LIU 2002b
Yang, X.; Liu, C. R.: A new stress-based model of friction behavior in machining and its significant impact on residual stresses computed by finite element method. International Journal of Mechanical Sciences 44 (2002) 4, pp. 703-723.

YANG & LIU 2018
Yang, D.; Liu, Z.: Surface integrity generated with peripheral milling and the effect on low-cycle fatigue performance of aeronautic titanium alloy Ti-6Al-4V. The Aeronautical Journal 122 (2018) 1248, pp. 316-332.

ZABEL 2010
Zabel, A.: Prozesssimulation in der Zerspanung [Process simulation in machining, own translation]. (Dissertation). Institut für Spanende Fertigung, Technische Universität. Dortmund (2010).

ZANGER 2013
Zanger, F.: Segmentspanbildung, Werkzeugverschleiß, Randschichtzustand und Bauteileigenschaften [Segmental chip formation, tool wear, surface layer condition and component properties, own translation]. (Dissertation). Institut für Produktionstechnik, Karlsruhe Institute of Technology. Karlsruhe (2013).

9 Appendix

A1 List of supervised student-research projects

In the context of this work, several student-research-projects were supervised in terms of content and organization. The supervision was performed at the Institute for Machine Tools and Industrial Management (*iwb*) of the Technical University of Munich. Some of the jointly gained insights have been incorporated in this dissertation and the publications described in Section 6.2. The author of this dissertation would like to sincerely thank the students for the valuable discussions and the ideas that have been developed during the collaboration.

Name of Student	**Title and date of student research project**
Schuhbeck, M.	Experimental Investigation and Influence Analysis of Process Parameters on the Residual Stress State during Milling of Ti-6Al-4V, submitted in August 2019
Liang, W.	Analytical modeling of the cutting forces for peripheral milling of Ti-6Al-4V, submitted in March 2020
Weisbrodt, V.	Investigation of the Influence of Peripheral Milling on the Surface Integrity of Ti-6Al-4V Components, submitted in January 2021
Geissinger, A.M.	Determination of the Cutting-Edge Rounding Based on the Cutting Forces Using Machine Learning Algorithms, submitted in September 2021
Widmann, R.	Simulation of the Cutting and the Ploughing Forces during Peripheral Milling of Ti-6Al-4V, submitted in July 2021
Güray, A.	Modeling of Residual Stresses for Peripheral Milling of Ti-6Al-4V, submitted in December 2021
Freimoser, A.	Determination of the Thermal Workpiece Loading during Peripheral Milling of Ti-6Al-4V, submitted in July 2022

A2 Publications of the Author

The author's publications, which were elaborated in the course of writing this dissertation, are listed below in chronological order.

- **Wimmer, M.; Rinck, P.; Kleinwort, R.; Zaeh, M. F.:** Methodology for a model-based control of the boundary zone properties during milling of Ti-6Al-4V. 15th International Conference on High Speed Machining, MM Science Journal (2019), pp. 3214-3219. **Publication P1 of this dissertation.**

- **Wimmer, M.; S. Hameed, M. Z.; Woelfle, C.; Weisbrodt, V.; Zaeh, M. F.; Werner, E.; Krempaszky, C.; Semm, T.:** The influence of the process parameters on the surface integrity during peripheral milling of Ti-6Al-4V. tm - Technisches Messen 87, no. 11 (2020), pp. 721-731. **Publication P2 of this dissertation.**

- **Woelfle, C.; Wimmer, M.; S. Hameed, M. Z.; Krempaszky, C.; Zaeh, M.; Werner, E.:** Towards real-time prediction of residual stresses induced by peripheral milling of Ti–6Al–4V. Continuum Mechanics and Thermodynamics 33 (2020), pp. 1023 - 1039.

- **Wimmer, M.; Woelfle, C. H.; Krempaszky, C.; Zaeh, M. F:** The influences of process parameters on the thermo-mechanical workpiece load and the sub-surface residual stresses during peripheral milling of Ti-6Al-4V. 18th CIRP Conference on Modeling of Machining Operations. Procedia CIRP 102 (2021), pp. 471–476. **Publication P3 of this dissertation.**

- **Wimmer, M.; Hartl, R.; Zaeh, M. F.:** Determination of the Cutting-Edge Microgeometry Based on Process Forces during Peripheral Milling of Ti-6Al-4V Using Machine Learning. Journal of Manufacturing and Materials Processing 7 (2023), no. 3: 100. **Publication P4 of this dissertation.**

- **Mayer, M. M.; Ott, M.; Wimmer, M.; Hartl, R.; Volk, W.; Zaeh, M. F.:** Machining-Induced Distortion during Peripheral Milling of High Strength Aluminum Parts. 17th CIRP Conference on Intelligent Computation in Manufacturing Engineering (CIRP ICME ‘23). Procedia CIRP 126 (2024), pp. 312-317.

- **Wimmer, M.; Schoop, J.; Zaeh, M. F.:** In-Situ Characterization and Modeling of Machining-Induced Residual Stresses in Peripheral Milling of Ti-6Al-4V with

Rounded Cutting Edges. Production Engineering Research and Development (2024). **Publication P5 of this dissertation.**